Final Report

Studying Arsenic Genesis and Developing Alternate Water Supply Management Strategies in the Ganga Basin

(NIH/GWH/NIH/22-25)




NATIONAL INSTITUTE OF HYDROLOGY, ROORKEE

Abstract

The Ganges River, along with its primary tributaries, originates from the Himalayas and transports a significant amount of sediment in the Ganga River basin. These sediments play a crucial role in shaping the chemical composition of the river as well as groundwater in the basin. During the mid-Holocene period, it is believed that the Ganges River transported minerals associated with trace elements from the Himalayas to the plains through erosion and sedimentation. Interestingly, rivers originating from the Siwalik hills were found to release higher concentrations of arsenic and heavy metals from their sediment compared to the major rivers originating from the Higher Himalayas. This study aims to investigate the factors contributing to the presence of arsenic in the Ganges basin and understand how it moves from sediment to water phases. This study involves the mineralogical and geochemical analysis, as well as examining the mobilization process by studying the geochemical signature of the affected aquifers. The aquifers are also identified for safe drinking water supply and other uses. A total of 291 water samples (river water-85, groundwater-206) and 70 sediment samples were collected from Gangotri to Patna during the pre-monsoon season, 2024. The in-situ parameters like pH, EC, DO, and ORP were measured on the sampling site. The pH of the water samples of the study area varied from 6.67 to 8.62 (mean 7.59) for groundwater, and 5.37 to 9.00 (mean: 7.26) for the Ganga river. It was observed that the pH values of river water are increasing as the sampling location descends from the origin. At the origin and nearby area, pH was acidic in nature due to sulphide oxidation, and then pH increased due to carbonate dissolution. The pH of groundwater is around neutral where arsenic is present. The EC values were showing a declining trend in Bhagirathi river from Gangotri to Devprayag, thereafter the EC values follows an increasing trend up to Patna. The EC varies from 177 to 1893 µS/cm (average 693) for GW samples, 59 to 729 µS/cm (Average 227) for Ganga river. Generally, the EC of groundwater is high for the urban centers such as Prayagraj, Kanpur, Varanasi and Patna. The pH and EC of river water showed an increasing trend may be due to anthropogenic activities. The DO values in the river water was found to be good and significantly higher (mean 8.6 mg/L) than that of groundwater (mean: 2.8 mg/L) as is obvious. Geochemical analysis revealed substantial spatial and temporal variability in water quality, particularly for major cations and anions. The arsenic concentration in shallow and deep groundwater samples varies between ND to 361 ppb with mean 21 ppb and 0.13 to 14.91 with mean 1.3 ppb respectively. Arsenic in Ganga water samples varies between 0.37 to 13 ppb. About 13 % of samples showing arsenic above acceptable limit (10 ppb) of drinking water as prescribed by BIS (2012) in groundwater.

The arsenic concentration in river Ganga is below acceptable limit except very few locations. The vertical distribution of arsenic was also studied and found that generally groundwater is contaminated upto depth of 60 m bgl. Generally, major ions, trace metals except arsenic, iron, manganese and aluminium are under permissible limit of drinking water in the study area. Hydrogeochemical ratios such as $(Ca^{2+} + Mg^{2+})/TZ^{+}$ (average: 0.70) and $(Na^{+} + K^{+})/TZ^{+}$ (average: 0.30), along with elevated Na^{+}/Cl^{-} ratios, show dominant carbonate weathering processes and secondary contributions from silicate weathering and ion exchange. Gibbs diagrams and bivariate plots further confirmed rock-water interactions as the major geochemical control on groundwater composition. Saturation Index (SI) calculations showed super saturation for iron oxides (hematite, goethite, ferrihydrite), supporting arsenic immobilization via precipitation, while $FeAsO_4 \cdot 2H_2O$ and Rhodochrosite were under saturated, indicating potential dissolution. Mineralogical analysis using XRD and FE-SEM confirmed the dominance of quartz, feldspar, mica, and clay minerals, with the presence of arsenic-bearing phases like iron arsenates in select upstream sediments. In the river bed sediments, concentrations of arsenic were found up to 113 µg/g, iron up to 26,540 µg/g, and elevated concentration of other trace metals, particularly in the Himalayan regions. However, these trace metal concentrations decreased in downstream due to dilution, sediment deposition, and hydrodynamic sorting. Isotopic analysis ($\delta^{18}O$ and $\delta^{2}H$) was also carried out to understand the exchange between river and groundwater. The $\delta^{18}O$ value of the Alaknanda river varies between -14.4‰ to -8.9‰ with an average of -11.8‰, the Mandkini river's $\delta^{18}O$ ranges between -12.3‰ to -9.3‰ with an average of -10.7‰ while the Bhagirathi has $\delta^{18}O$ value of -11.9‰. The Ganga river $\delta^{18}O$ value ranges between –11.6‰ to -3.2‰ with an average of -5.6‰. Most of the river water samples laying above the LMWL as well as GMWL but few samples fall below the LMWL which indicates about the storng evaportion, this can also be supported by their d-excess values which fall below zero. The groundwater (which is devided into two categories i.e. GW close to river and away from river) in the same region revealing distinct regression lines: $\delta^{2}H = 5.78\ \delta^{18}O - 8.9$ ($R^2 = 0.94$) for samples close to the river, and $\delta^{2}H = 6.28\ \delta^{18}O - 6.0$ ($R^2 = 0.92$) for those farther away, while river water followed $\delta^{2}H = 5.68\ \delta^{18}O - 11.6$ ($R^2 = 0.98$). The results revealed the hydraulic connectivity between river water and adjacent groundwater in the lower part of the basin, especially on the right bank, indicating active river-aquifer interaction and variable recharge patterns influenced by evaporation.

The majority of public water supply is sourced from deeper aquifers in arsenic-affected areas, which remain free from arsenic and trace metal contamination, and are currently suitable for drinking use.

Project Team

Team of Scientists:

Dr. Sumant Kumar, Sc.-E, GWHD & PI
Dr. Surjeet Singh, Sc.-G, C4S
Dr. Rajesh Singh, Sc.-D, EHD
Dr. M.K. Sharma, Sc.-F, EHD
Dr. Nitesh Patidar, Sc.-C, GWHD
Dr. Vinay Kumar Tyagi, Sc.-D, EHD
Dr. Gopal Krishan, Sc-E, GWHD
Dr. Amit Pandey, Sc.-B, HID
Dr. Soban Singh Rawat, Sc.-F, C4S
Dr. P.K. Mishra, Sc.-D, WRSD
Dr. M.K. Goel, Director

Supporting Project Staffs:

Er. Vinod Kumar, Project Scientist-II, GWHD
Dr. Shashi Ranjan, Research Associate, GWHD
Er. Rahul Kumar, Resource Person (Jr.), GWHD
Miss Vishakha Pandey, Resource Person (Jr.), GWHD
Mr. Siddharth, Project Assistant, GWHD

Collaborators	Central Ground Water Board, Dehradun
	National Institute of Technology, Patna

List of Figures

List of tables

1. Introduction

Arsenic (As) contamination in groundwater is a major environmental issues and public health challenge in India, due to carcinogenic nature and widespread occurrence in regions like the Ganga and Brahmaputra river basins. Arsenic is categorized as a top-priority pollutant by the World Health Organization (WHO), and also it has been classified as a group 1 carcinogen by the International Agency for Research on Cancer (IARC). The severity of arsenic contamination varies across regions, but some areas have alarmingly high concentrations of arsenic in the groundwater, exceeding the permissible limits set by national and international standards. In the Ganga river basin arsenic contamination in groundwater has been found to be widespread, affecting millions of people who rely on groundwater for drinking and other domestic uses. Arsenic contamination in the Ganges Plain was first reported in the early 1980s, and since then, various studies have been conducted to assess the extent of contamination and its impact on public health. Long-term exposure to arsenic-contaminated water in the Ganges plain has been linked to several health problems, including skin lesions, cancers (such as skin, lung, bladder, and kidney cancers), and developmental issues in children (Kumar et al., 2021, Shaji et al., 2021). Arsenic presence in soil and water is mainly due to natural geological sources, may be induced by anthropogenic activities (Garcia-Sanchez, A., et al., 2003). The arsenic sediment originates from the Himalayan foothills, and its accumulation in aquifers is primarily associated with iron oxides or hydroxides in the presence of phosphate compounds in the part of West Bengal which is severely contaminated by arsenic (Ranjan et al., 2021). Amongst the various theories proposed for the mechanism of arsenic mobilization in groundwater, reductive dissolution is considered as the most appropriate mechanism for arsenic mobilization in this area. Arsenic availability and its concentration level in groundwater are significantly controlled by pH and redox conditions of the soil–water system. Depending on the soil–water pH-redox conditions, arsenic commonly exists in the subsurface in forms of inorganic compounds of As (V) and As (III). The predominant As (V) occurs in oxic water as oxy-anions of arsenic acid, whereas As(III) exists as the arseneous acid (H_3AsO_3, $H_2AsO_3^-$, $HAsO_3^{2-}$) in reducing conditions.

Arsenic is naturally present in bedrock and soil; it's found in low concentrations averaging 1–2 mg/kg in the Earth's crust (Taylor, S. R., & McLennan, S. M. 1985; Parviainen, A et al., 2015). However, it can be enriched in specific rock formations, particularly those associated with gold and sulphide-rich ore deposits. Common sulphide minerals that host arsenic include pyrite (FeS_2 or arsenian pyrite, $Fe(AsS)_2$) and arsenopyrite (FeAsS). The weathering of rocks

and minerals is considered a primary source of arsenic in soils. Arsenic tends to accumulate in the colloidal fractions during weathering and translocation, often resulting in higher concentrations in soil compared to the original parent rock. Under normal soil formation conditions, the behavior and distribution of arsenic in soil are controlled by factors such as the composition of the parent rock, volcanic inputs, biological activity, weathering processes, transportation mechanisms, sorption, and precipitation (Kathleen et al., 2011). The Ganga River and its major tributaries originate in the Himalayas, transporting large volumes of sediment that influence the river's water chemistry. During the mid-Holocene period, the Ganga likely carried metals from the Himalayan region to the plains through processes of erosion and sediment deposition. Rivers emerging from the Siwalik Hills have been found to release greater amounts of arsenic and heavy metals from their sediments compared to the main rivers sourced from the Higher Himalayas.

Groundwater chemistry is primarily shaped by chemical weathering, which itself is influenced by several factors, including the type of parent rock, topography, climate conditions, and biological processes. Weathering significantly contributes to the geochemical evolution of groundwater, as it facilitates the release and redistribution of major and trace elements via mechanisms such as mineral dissolution, co-precipitation, and ion exchange. The leaching of metals during monsoon rainfall poses a considerable environmental risk (Oke et al., 2012). Additionally, the geological nature of the formations and the duration groundwater remains in contact with rocks (residence time) play a crucial role in determining groundwater quality through rock-water interactions.

The river Ganga and its major tributaries, the Bhagirathi, the Alaknanda, and the Mandakini, originate from the Himalaya and carry high sediment, and these sediments determine the chemistry of the water (Chakraborti et al., 2004). The geology of the Himalaya region through which these rivers pass may be classified into three regions: (i) Higher Himalayan unit comprising granites, gneisses, schist, marbles with carbonates and calc-silicates (Kansakar, 2004); (ii) The Lesser Himalaya consists of shales, slates, limestones, and dolomites. The exposed crystalline rocks in the Lesser Himalaya are granites, schists, gneisses, calc-silicates, and amphibolites (Kansakar, 2004); (iii) The Siwaliks mainly consist of the eroded materials transported by the Himalayan rivers from the Higher Himalaya and Lesser Himalaya (Quade et al., 1997).

The Alaknanda and Bhagirathi rivers, the headwaters of the Ganga River, originate in the Higher Himalayas of Uttarakhand and converge at Devprayag, where the Ganga assumes its formal name. The Alaknanda originates from the Satopanth and Bhagirath Kharak glaciers near the Chaukhamba Mountain, while the Bhagirathi originates from Gomukh (3920 m), the snout of the Gangotri glacier. Both rivers drain through geologically diverse terrains that influence their geochemistry. The Alaknanda flows through carbonates, massive quartzites, slates, phyllites, and greywackes, traversing the Central Crystalline Zone with sedimentary and highly metamorphosed gneissic rocks. It encounters limestones, marbles, and quartzites of the Tejam and Berinag Formations, and before merging with the Bhagirathi, it passes through the limestone and dolomite-rich Uttarkashi Formation and the phyllitic and micaceous greywackes of the Chandpur Formation. The Bhagirathi, characterized by a rugged terrain with waterfalls and cascades, also flows through the Central Crystalline Zone, encountering schists, micaceous quartzites, calc-silicates, amphibolites, gneisses, granites, slates, and phyllites. Its middle and lower reaches are rich in limestone and dolomite, and it similarly traverses through phyllites and micaceous greywackes before the confluence. The geochemical cycling in these rivers is primarily driven by weathering and erosion, which mobilize elements from the surrounding soils and rocks into the river system.

The Mandakini River emerges from the Chorabari glacier in Uttarakhand, a tributary of the Alaknanda River. Geologically, the Mandakini River catchment lies within the Main Central Thrust (MCT) zone of the central Himalaya and is divided into three key morphotectonic units—Munsiari thrust (bottom), Vaikrita thrust (middle), and Pindari thrust (top) (Valdiya, 1980, 1998; Valdiya et al., 1999). The Chorabari Glacier, situated between the Pindari thrust and the Trans-Himadri fault, belongs to the Pindari Formation of the Higher Himalayan Crystallines (HHC). Initially termed the Schistose Series (Griesbach, 1891), these rocks were later reclassified as granitic gneisses with associated metasedimentary rocks (Heim and Gansser, 1939). The Pindari Formation features highly metamorphosed rocks, mainly banded calc-silicate gneisses and calc-schists, interbedded with biotite-psammitic gneiss and schist. The Chorabari Glacier area is dominated by granite-gneisses and migmatites, intruded by aplite and pegmatite dykes and veins, with occasional occurrences of carbonates and calc-silicate rocks (Valdiya, 1980).

The present study aims to study the mineralogy of the sediment which is being carried out by river Ganga. The geochemistry has been studied to understand the causes of arsenic occurrence in Ganga basin and its mobilization from solid to water phase. The isotopic investigation has

also been carried out to understand the surface water and groundwater interaction. It has been attempted to evaluate the performance of existing treatment units functioning in the arsenic contaminated areas. The significance of the study is to help in demarcating safe aquifer, improved monitoring and mitigation measures at regional level.

With above background, the objectives framed under the study are:

- Mineralogical characteristic of sediments and water focusing in the Indian Himalayan region to detect genesis of arsenic.
- Demarcating safe aquifer for drinking water supply in arsenic affected areas.
- Performance evaluation of existing treatment units and their comparison in terms of cost, efficiency and ease of operation etc.
- Developing a new treatment technique with high removal efficiency in optimized cost.

2. Literature review

Arsenic is a naturally occurring toxic element commonly found in groundwater across many parts of the world. The most severely affected regions, in terms of population exposure, are located in Asia—particularly along the Himalayan foothills in countries such as Pakistan, India, Bangladesh, Myanmar, and Taiwan. This region is often referred to as the Southeast Asian Arsenic Belt (SSAAB) (Ravenscroft et al., 2009). The Ganges River Basin (GRB) is a highly populated and productive region, crucial for the livelihoods of its residents who depend on it for water, food, and agriculture. India encompasses a significant portion of the GRB, with an impact on several states including Uttarakhand, Uttar Pradesh, National Capital Territory (NCT) of Delhi, Madhya Pradesh, Bihar, Jharkhand, Rajasthan, Chhattisgarh, Punjab, Haryana, and West Bengal. The contamination of groundwater with arsenic was initially documented in 1976 in Chandigarh, as well as various villages in Punjab and Haryana (Chakraborti et al., 2018).

Studies revealed that most arsenic affected aquifers are alluvial sediments that are geologically young and formed by the deposits derived from the tectonically active areas (Edmunds et al., 2015; Mukherjee et al., 2019, References). The major alluvium aquifer known for the arsenic contamination is Ganga-Brahmaputra-Meghna basin(Fendorf et al., 2010). The origin of arsenic contamination in groundwater and sediments of the Ganga-Brahmaputra-Meghna basin is from the minerals found in the Himalayan foothills (Mukherjee et al. 2019). The evolution of the Bengal sedimentary basin started during the Permo-Carboniferous period, but the major geological transformations are primarily associated with the Himalayan uplift that started in the Miocene. Intense erosion from the orogenic belt led to the deposition of clastic sediments ranging from 1 to 15 km in thickness within the Bengal foredeep during the Tertiary and Quaternary periods. As a result of weathering processes, arsenite [As(III)]—predominantly existing as the $H_3AsO_3^0$ species in the pH range of 4 to 9—along with Fe(II) and sulfate, were mobilized (Mukherjee et al., 2019). The availability of oxygen and neutral conditions led to the oxidation of iron and further arsenic. $H2AsO_4$-/ $HAsO4^{2-}$, which were formed, sorbed to Fe(III) oxyhydroxides and stored in sediments. The weathering and erosion of Himalayan derived minerals and their down gradient transport deposited the arsenic-rich sediments in this basin. In the sediments, arsenic, together with phosphate ($PO43-$) appears to be primarily adsorbed on amorphous Fe oxyhydroxides (Duxbury & Panaullah, 2007). The global average of arsenic in the Earth's crust is typically varies from 2 to 6 mg/kg (Smedley & Kinniburgh, 2000). The occurrence of high arsenic concentrations in groundwater is more strongly

influenced by hydrological and biogeochemical conditions than by the arsenic source itself (Neumann, R. B. et al., 2010). Nevertheless, regional-scale geodynamic and geochemical processes also play a role in controlling arsenic mobilization in groundwater systems (Chakraborty et al., 2015). Several mechanisms of As mobilization have been discussed but reductive dissolution of iron-hydroxides is the most suitable in the Ganga River Basin. The reductive dissolution mobilization of arsenic was proposed by (Nickson et al., 2000). This hypothesis has recently accepted by scientists and researchers as a key explanation for the mobilization of arsenic in groundwater (Nickson et al., 2000; Khan, I. et al., 2023). According to this hypothesis under reducing (anaerobic) conditions, arsenic is released through desorption from ferric hydroxide minerals, which is present in subsurface sediments. In the absence of oxygen, these iron-bearing minerals break down and release the arsenic they had previously adsorbed. Iron oxides and hydroxides are widespread in sediments and act as strong adsorbents of arsenic; however, they release it when they are reduced to their ferrous form and begin to dissolve. Therefore, the movement of arsenic in groundwater is closely linked to the stability of these iron minerals.

The common inorganic forms of arsenic in soil–water environments are arsenate [As(V)] and arsenite [As(III)], with their occurrence largely governed by local environmental conditions (Wang & Mulligan, 2006). Under oxidizing conditions (Eh > 200 mV, pH 6–8), arsenate [As(V)] is the dominant species and tends to be adsorbed onto metal hydroxides. Conversely, arsenite [As(III)] typically prevails in reducing conditions, low-pH settings and is more mobile in the environment due to its limited sorption to soils and sediments (Grafe et al., 2001).

The occurrence of secondary arsenate minerals in mine environments is strongly governed by geochemical conditions. Minerals such as arsenolite, kaatialaite, pharmacolite, brassite, and rösslerite are reported as key secondary phases controlling arsenic mobility. X-ray spectroscopy analysis indicate that arsenolite and kaatialaite typically precipitate under strongly acidic and oxidizing conditions during the weathering of arsenic-rich sulfides, whereas interaction of these acidic solutions with carbonate-bearing rocks promotes the formation of Ca–Mg arsenates (Majzlan et al., 2021). More recently, XRD datasets have demonstrated the ability to simulate peak shifts, broadening, and background noise, with validation on experimental datasets confirming strong predictive performance, thereby providing a powerful framework for arsenic-related crystallographic investigations (Lee et al., 2023). The peat enriched in organic carbon plays a significant role in arsenic dynamics within anoxic aquifers. High-resolution spectroscopic analyses reveal that pyrite and greigite act as major hosts for As,

immobilizing up to 60 wt.% in contaminated peat sediments. Pyrite forms mainly via polysulfide pathways, while Fe-rich conditions stabilize greigite, limiting its transformation. Despite temporary sequestration, redox shifts may destabilize ferrihydriten As associations, leading to potential groundwater As release (Wang et al., 2020).

Stable isotopes of hydrogen and oxygen are increasingly applied to study water fluxes and storage that influence arsenic behavior in aquifers. These isotopes trace recharge sources, flow pathways, and residence times, which are critical for understanding As mobilization under changing climate and water demand. Case studies show their value in linking hydrologic processes with arsenic distribution in natural and managed systems. Future integration of isotope methods into water management can improve strategies for mitigating arsenic contamination (Scandellari et al, 2024). Isotopic signatures have proven highly effective in characterizing surface water–groundwater (SW–GW) interactions and identifying recharge sources within aquifers. particularly in regions where recharge occurs through river–aquifer exchange (Jafari et al, 2021)

Various physicochemical techniques like chemical precipitation/coagulation and flocculation, oxidation, ion-exchange, membranes, and adsorption based techniques are developed to remove arsenic from aqueous solutions. Chemical precipitation/coagulation and flocculation methods are the most common techniques available for arsenic removal. In these methods, metal-based coagulants are added to arsenic containing aqueous solution for changing the surface charge of the solids to form clogs made of larger particles, which get settled down by gravity or filtered mechanically. The common coagulants used for arsenic removal are Ferric chloride ($FeCl_3$), Ferric sulfate ($Fe_2(SO_4)_3$ $7H_2O$) and aluminum sulfate ($Al_2(SO_4)_3 18H_2O$) (Pallier et al., 2010; Zouboulis & Katsoyiannis, 2002). Through oxidation process As(III) is converted to less mobile As(V) by addition of chemical oxidants such as gaseous chlorine, ozone, hydrogen peroxide, potassium permanganate, and Fenton's reagent (Shrivastava et al., 2015). This process involves the oxidation of available soluble forms of iron and manganese to their insoluble forms along with arsenic. The oxidized forms are then precipitated and filtered out to remove the arsenic from the aqueous solution (Singh et al., 2015). The ion-exchange process is a physiochemical process of exchanging ions on the solid resin in the feed water. For arsenic, strong base anion exchange resins are used to exchange the oxy-anionic forms of As(V) (Dominguez-Ramos et al., 2014). Membrane techniques are also found effective for arsenic removal, but its effectiveness under reducing conditions is doubted by some researchers for the As(III) removal (Walker et al., 2008; Yoon et al., 2009). Adsorption

remains a widely studied and promising method for arsenic removal due to its simplicity, cost-effectiveness, and high removal efficiency. Various adsorbent materials such as zero-valent iron, iron oxides, activated alumina, granular activated carbon, biological substrates, and polymer-based resins are employed—either individually or in combination—in different forms to enhance performance (Kanel & Choi, 2017; Liu et al., 2014; Ramos et al., 2009; Ranjan et al., 2020, 2021).

Biochar is considered a cost-effective environmentally-friendly, and sustainable, sorbent with the potential to efficiently remove toxic elements, including arsenic (As), from water. Biochar is a carbon-rich material produced from the pyrolysis or heating of organic biomass, such as wood chips, agricultural waste, or plant residues, in the absence of oxygen. The porous structure of biochar, along with its high surface area, makes it an excellent sorbent for various contaminants, including heavy metals like arsenic. The carbonaceous composition of biochar provides binding sites for these contaminants, allowing them to absorb onto its surface Biochar is commonly produced from agricultural and food industry waste materials, which are readily available, low-cost, and abundant (Luo et al., 2016). A variety of biochar—such as those derived from plant leaves, oak wood, sewage sludge, cotton stalks, rice husks, and municipal solid waste—have been explored for their potential to remove arsenic from water (Agrafioti et al., 2014; Sari et al., 2014). Notably, efforts have been made to enhance the arsenic adsorption efficiency of biochar through surface modifications and impregnation techniques, including the incorporation of organic functional groups, zero-valent iron (ZVI), metal nanoparticles, and coatings with iron or aluminum-based minerals (Cope et al., 2014; Samsuri et al., 2013; C. Wu et al., 2017).

WHO has listed Arsenic as the priority pollutant, and it has also been identified as a type 1 carcinogen by the IARC (Z. Wu et al., 2019). There are two possible pathways of arsenic consumption; one through the direct ingestion of arsenic-contaminated water, and the other is by the consumption of food contaminated with arsenic. In many arsenic affected areas, groundwater is used extensively for irrigation of crops, through which arsenic gets bio-accumulated in grains and vegetables providing an alternate route for arsenic poisoning (Mondal et al., 2021; Sidhu et al., 2012; Suman et al., 2020). Toxicity of As(III) is also quite higher than As(V) due to its high binding affinity towards thiol or sulfhydryl groups in tissue proteins of the important organs (Hughes, 2002; Ratnaike, 2003).

3. Study Area

The Ganga River and its key tributaries have their sources in the Himalayas and transport of sediment, which significantly influence the water's chemical composition. During the mid-Holocene period, the Ganga likely played a major role in carrying metals from the Himalayan region to the plains through erosion and sediment deposition. Studies indicate that rivers arising from the Siwalik Hills tend to release higher concentrations of arsenic and heavy metals from their sediments compared to the larger rivers originating in the Higher Himalayas.

The Ganga River Basin envelops an immense topographical region, extending across various states in northern India, including Uttarakhand, Uttar Pradesh, Bihar, Jharkhand, and West Bengal. Nepal and Bangladesh, two of the basin's neighbours, are also included. One of the world's largest deltas, the greater Ganga basin's Sundarbans are named after the 60,000 square kilometres of Sundari trees found there. It houses over 500 million people and occupies nearly 26% of India's land area. One of the world's largest river basins, the Ganga River Basin spans approximately 1,080,000 square kilometers. Prevalent soil types found in the basin are sand, topsoil, earth and their mixes, for example, sandy topsoil, topsoil, silty dirt topsoil and loamy sand soils. More than 600 million Indians live there, which is close to half the country's population; and this region accounts for more than 40% of the nation's GDP. From its western Himalayan beginnings to its junction with the Bay of Bengal, the Ganga River's main stem travels approximately 2,525 kilometers. At Devprayag in Uttarakhand, the Bhagirathi River and the Alaknanda River, two major tributaries, meet to form the Ganga River. Along its course, it is joined by a number of other tributaries, such as the Yamuna, Son, Gandak, and Kosi. The Bhagirathi River, which originates near Gomukh at an elevation of approximately 7,010 meters above sea level in the Uttarkashi district of Uttarakhand, is regarded as the River Ganga's source. The Ganga River has a total length of 2,525 kilometers. The Upper Ganga Reach, which stretches from the Ganga's source to Narora Barrage in Uttar Pradesh's Bulandshahar district, can be divided into three sections from a hydrological perspective: The Central Ganga reach from Narora Blast to Ballia district in Uttar Pradesh, and the lower Ganga reach from Ballia to its delta. Though, this study focuses on the upper Ganga including the Bhagirathi and Alaknanda stretch and the middle Ganga region up to Patna, Bihar (Fig3.1).

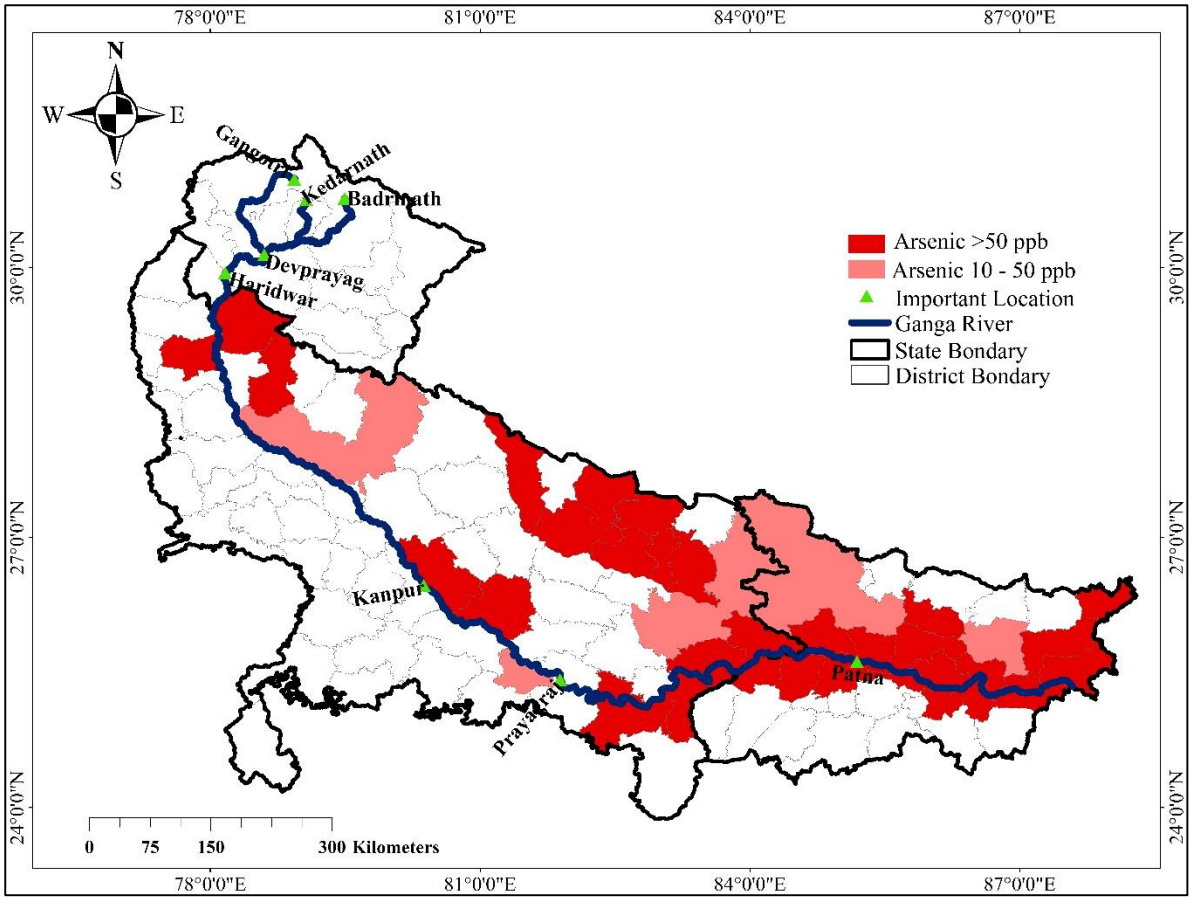

Figure 3.1: Study area map showing the river Ganga and arsenic-affected districts in the study area.

4. Methodology

4.1. Water and sediment sampling of the Ganga River and groundwater

The study covers the detailed hydrogeology and geochemistry of the As-contaminated aquifer of the Ganga basin. A pre-monsoon sampling was carried out in upper and middle Ganga basin to study the spatial variation of water quality parameters of river and groundwater (Fig. 4.1). The sediment samples at different location was collected from upper and middle Ganga basin focusing on Himalayan sediments for sediment characterization using XRD techniques (Fig. 4.2). Phase wise sampling of sediment and water was done in the study area as discussed below. The sampling locations was decided based on the geomorphology of the area, major bends in the river and point of confluence of major tributaries. Water and sediment samples were taken after every 10 Km in upper Ganga region and after Haridwar it was taken at the interval of 20-25 Km depending upon the approachability and practical limitation in the field for the Ganga river. Corresponding to each point of river Ganga, three/four groundwater samples were taken across the river (both sides at the interval of 10 Km).

Pre-Monsoon (2024) Sampling ((Figure: -4.1)

- Phase 1: Haridwar to Varanasi (RW-25, GW-123, Sediment-23; May 2024)
- Phase 2: Varanasi to Patna (RW-12, GW-86, Sediment-14; June 2024)
- Phase 3: Gangotri (Bhagirathi), Badrinath (Alaknanda), and Kedarnath (Mandakini) to Haridwar (Alaknanda River) (RW-48, Sediment-33; Nov. 2024)

The mineralogical study would help in identifying the minerals of arsenic present in the Ganga basin. The sediment samples were collected from bed of river Ganga and analysed for XRD, XRF and SEM. The locations of the sampling point are marked using a hand-held global positioning system (GPS). Field measurements including temperature, pH, electrical conductivity (EC), and dissolved Oxygen (DO) are measured on site. The measured stable value of these water quality parameters will be representative of in-situ conditions. Three sets of water samples are being collected at every location for cation/anion (500 ml), trace elements (125 ml) and isotopes (15 ml) analysis.

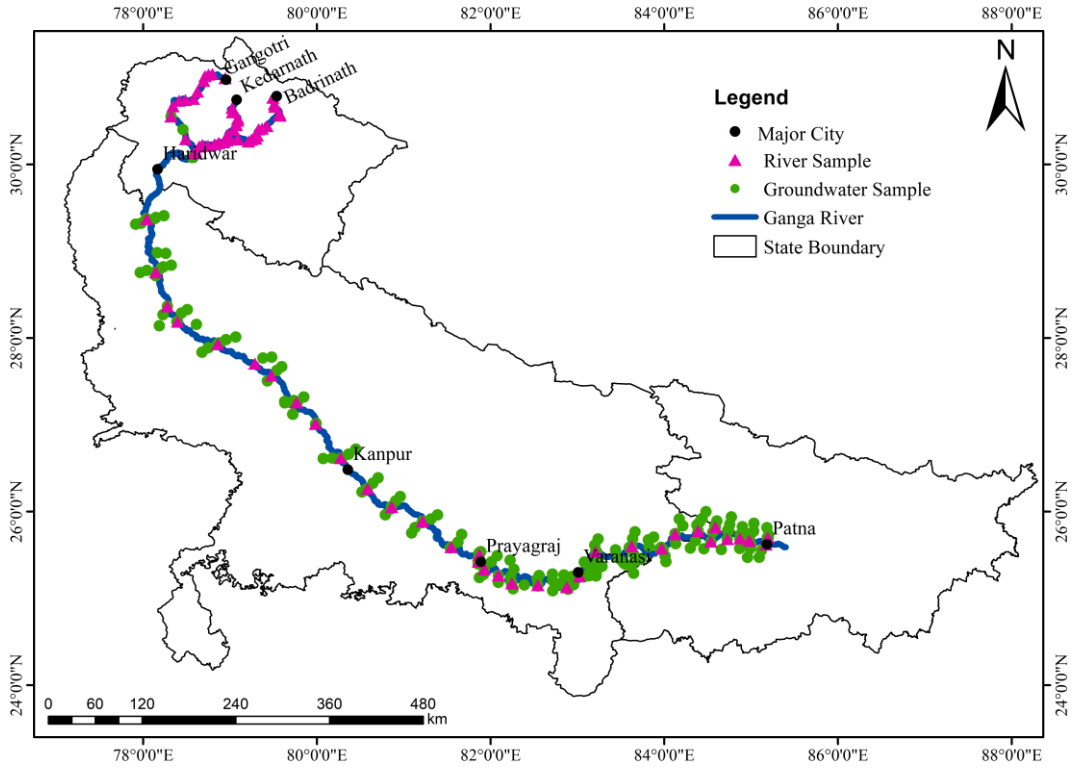

Figure 4.1: River water and groundwater sampling location map.

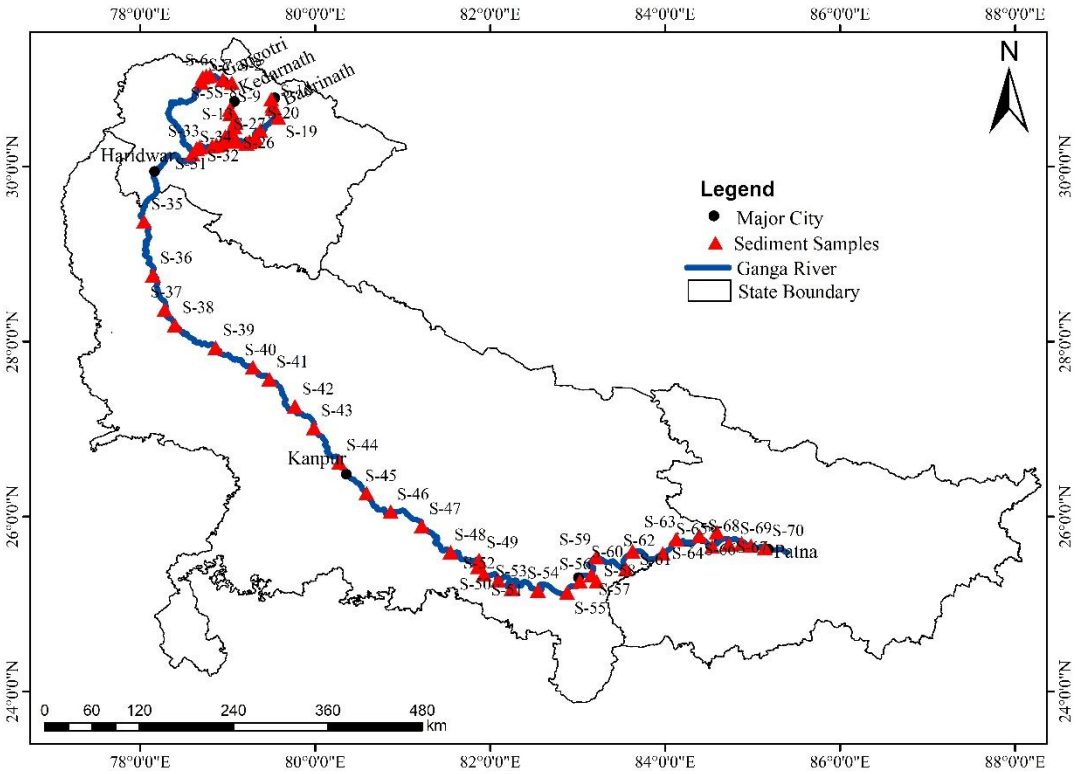

Figure 4.2: Sediment sampling locations in the study area

4.2. Water sample analysis

Major cations (Ca^{2+}, Mg^{2+}, Na^{+}, and K^{+}) and anions (Cl^{-}, SO_4^{2-}, NO_3^{-}, and F^{-}) in the water samples were analyzed using Ion Chromatography (IC, Dionex ICS-5000 series). Trace metals concentrations, including As, Fe, Mn, Zn, Cu, Cr, Cd, Ni, and Pb, were determined using an Inductively Coupled Plasma–Mass Spectrometry (ICP-MS, Agilent 7850) at the National Institute of Hydrology (NIH), Roorkee (Table 4.1).

Table 4.1: Analytical methods and equipment used for water samples analysis

Sr. No.	Parameter	Method	Equipment Used
Water Chemistry Analysis			
A.	**Physico-chemical (Major Ions)**		
1	pH	Electrometric	pH meter – Hach
2	Electrical Conductivity	Electrometric	Conductivity meter – Hach
3	Bicarbonate	Titration	Volumetric glassware
4	Calcium	Conductivity Method	Ion Chromatography
5	Magnesium		
6	Sodium		
7	Potassium		
8	Chloride		
9	Fluoride		
10	Nitrate		
11	Sulfate		
12	Ammonia		
B.	**Trace/Heavy Metals**		
13	Arsenic	Spectrometry Method	ICP-MS
14	Cobalt		
15	Cadmium		
16	Total Chromium		

17	Copper		
18	Zinc		
19	Iron		
20	Aluminum		
21	Manganese		
22	Nickel		
23	Lead		

4.3. Sediment Sample Analysis

The soil particle size distribution was analysed using sieve shaker and Mastersizer particle size analyser (Malvern Mastersizer 2000 E). The soil particle having size of more than 75 μm was processed by sieve analysis whereas the soil particles passing through 75 μm sieve was measure through Mastersizer. Sodium hexa-meta phosphate was used as dispersing agent to disperse any aggregate. The Mastersizer (Malvern Instruments, 2004) operates by continuously circulating a portion of the soil suspension through a narrow gap between two glass lenses. As particles pass through this gap, their sizes are determined based on the laser light scattering patterns they produce. The analysis relies on the principles of the Fraunhofer diffraction model and Mie theory to interpret the scattering data. The calculated percentage of sand, silt and clay in a soil sample was used in determining textural classification using textural triangle of United State Department of Agriculture (USDA). The ICP-MS was used for determining trace metals in the digested sediment samples. The Multiwave PRO microwave reaction system was used to digest soil samples for carrying out chemical analysis of these sediment samples. Analytical methods and equipment used for sediment samples analysis Table 4.2.

4.4 Methodology for XRD analysis

X-ray diffraction (XRD) were used to determine the mineralogical composition of the sediment samples. Collected sediment samples were oven-dried at 40–60 °C, fine crushed using an agate mortar, and pass through a 200 μm mesh to obtain a fine homogeneous powder. X-ray diffractometer (Bruker D8 Advance) radiation source (λ = 1.5406 Å), operating at 40 kV and 30 mA, the diffraction patterns were recorded in the 2θ range of (5°–90°) with a step size of (0.02°) and a scanning speed of (1°/min) at IIT Kanpur was used for mineralogical study. Phase identification was carried out by comparing the obtained diffraction patterns with standard

reference data from the International Centre for Diffraction Data (ICDD) Powder Diffraction File (PDF) database using software Xpert HighScore.

Table 4.2: Analytical methods and equipment used for sediment samples analysis

Sr. No.	Parameter	Method	Equipment Used
1	Grain Size Analysis	Sieve & Laser diffraction method	Sieve Shaker and Malvern Instruments
2	All trace metals including As	Spectrometry Method	ICP-MS
3	Minerals (major and minor mineral)	XRD Technology	D8 Advance (Bruker) X-ray diffractometer
5	Elemental composition	Scanning Electron Microscopy	FE-SEM

4.5 Isotopic analysis

The isotopic analysis of water samples is being carried out for stable isotope analysis of oxygen-18 ($\delta^{18}O$) and deuterium (δD), Water samples were collected in 30 mL airtight high-density polyethylene (HDPE) bottles and transported to the Nuclear Hydrology Laboratory at the National Institute of Hydrology, Roorkee. Isotopic analysis was carried out using both continuous-flow and dual-inlet isotope ratio mass spectrometers. Standard equilibration techniques were followed during preparation and analysis of oxygen and hydrogen (δ18O and δ2H), to identify the source and pathways of groundwater recharge and getting insight about the recharged water based on residence time. The analytical uncertainty for $\delta^{18}O$ was ±0.1‰, while for δD it was ±1.0‰. All isotope ratios are reported in per mil (‰) notation relative to the Vienna Standard Mean Ocean Water (V-SMOW) reference standard, using the delta (δ) notation as defined below:

$$\delta(‰) = \left\{\left(\frac{R_{Sample}}{R_{Standard}}\right) - 1\right\} \times 1000 \ldots\ldots\ldots \text{(Eq.1)}$$

where *R* represents the ratio of the less abundant to the more abundant isotope in the sample and standard.

To evaluate evaporative processes affecting surface and groundwater, the deuterium excess (d-excess) parameter was calculated using the formula:

$$\text{d-excess} = \delta D - 8 \times \delta^{18}O \ldots\ldots \text{(Eq.2)}$$

This derived parameter helps in distinguishing different water sources and understanding the role of non-equilibrium (kinetic) evaporation processes in shaping isotopic signatures. To understand the processes river, SWM rain along with groundwater samples were collected along and across the river. In upper reaches only river water (Alaknanda, Mandakini, and one sapmple drom Bhagirathi) samples were collected.

5.0 Result and analysis

5.1 Geochemical Characteristics of Groundwater and Surface Water

For understanding the geochemical characteristics of groundwater and surface water, and sediment samples were collected during different seasons and were analyzed for pH, Electrical Conductivity (EC), Dissolve Oxygen (DO), which were measured in-situ and presented in Table 5.1. The samples were brought to the NIH lab for analysis of major cations, viz. Sodium (Na^+), Potassium (K^+), Calcium (Ca^{2+}), Magnesium (Mg^{2+}), major anions viz., Bicarbonate (HCO_3^-), Sulphate (SO_4^{2-}), Nitrate (NO_3^-), Chloride (Cl^-), and trace metals (Arsenic, Chromium, Copper, Cobalt, Cadmium, Nickel, Manganese, Iron, and Zinc).

Table 5.1: Statistical summary of in-situ parameters for river water and groundwater

	BIS		Ganga River				Groundwater			
	Acceptable	**Permissible**	**Min**	**Max**	**Mean**	**Stdev**	**Min**	**Max**	**Mean**	**Stdev**
pH	**6.5-8.5**	**-**	**5.37**	**9**	**7.26**	**0.84**	**6.67**	**8.62**	**7.59**	**0.41**
EC (µs/cm)	**-**	**-**	**59**	**729**	**227**	**139**	**177**	**1893**	**693**	**294**
DO (mg/L)	**-**	**-**	**5**	**13**	**8.6**	**1.4**	**0.78**	**5.25**	**2.27**	**0.87**

5.1.1 In-situ Parameters (pH, EC, and DO)

pH is an important water quality parameter that indicates the concentration of hydrogen ions ($[H^+]$). It serves as a measure of acidity or alkalinity, ranging from 0 to 14 on a scale. For drinking water purposes, the Bureau of Indian Standards (BIS, 2012) recommends a pH value within the range of 6.5 to 8.5. The pH of the water samples of study area varies from 6.67 to 8.62 (average 7.59) for GW samples, 5.37 to 9.0 (average 7.26) for Ganga river. It can be observed that the pH values are increasing in the upper stretch (Gangotri to Devprayag) and decreasing in the lower stretch (Mirzapur to Patna) of the river samples, however pH is showing decreasing trend in the groundwater samples.

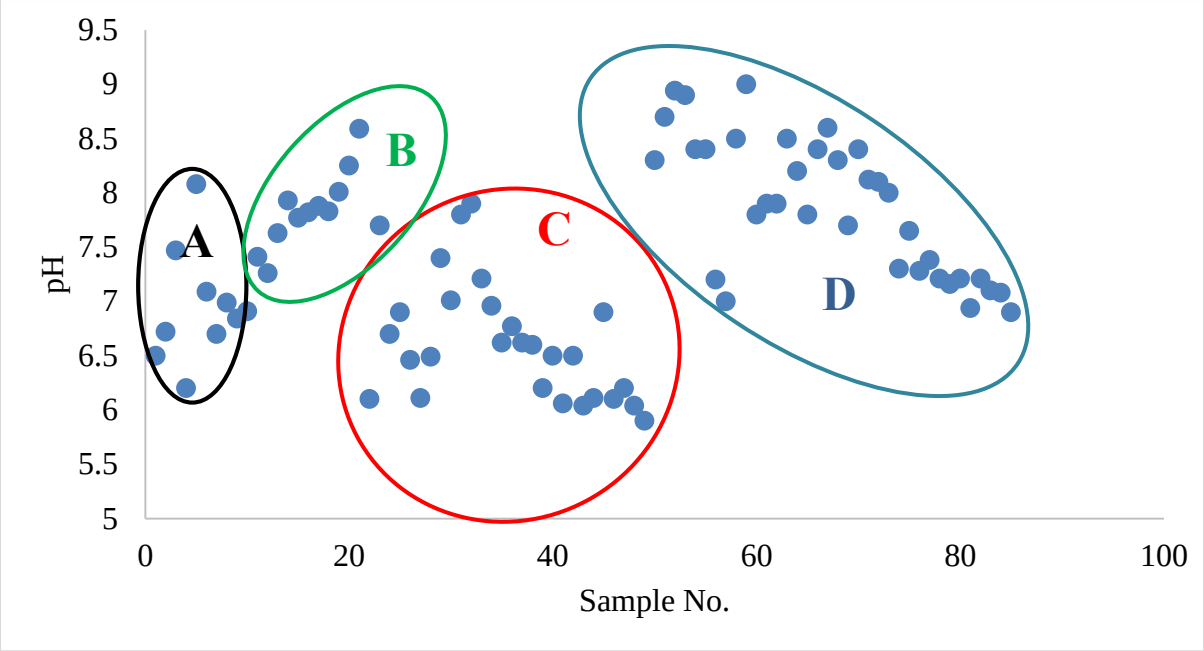

Figure 5.1: pH variation in river water (A-Mandakini River, B- Bhagirathi River, C-Alaknanda River, D-Ganga River.

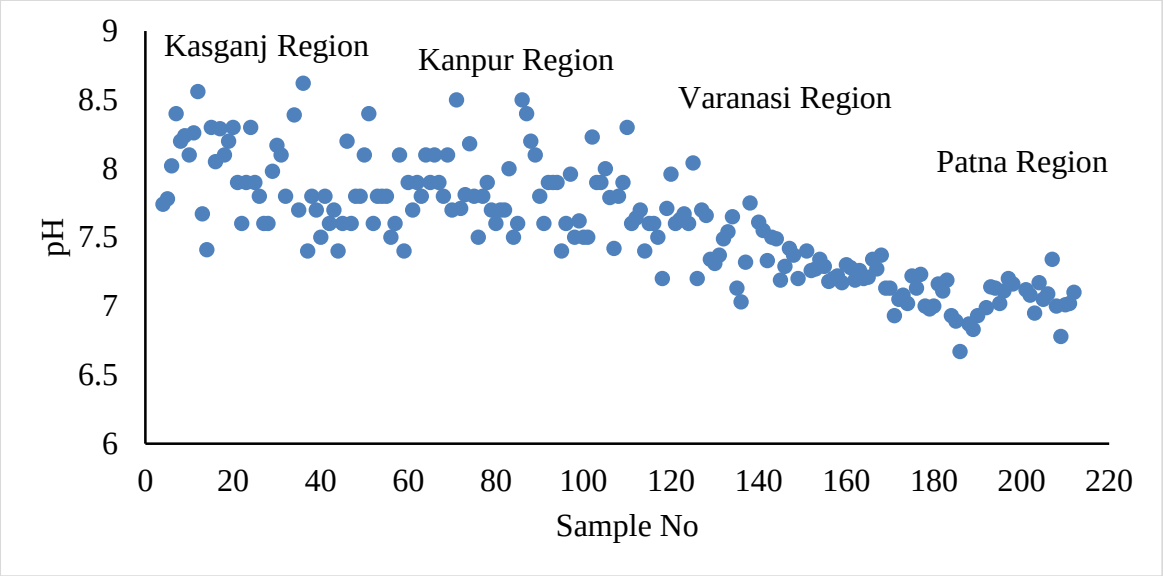

Figure 5.2: pH variation in groundwater of the study area.

Electrical conductivity (EC) of water refers to its ability to conduct an electric current. It is a measure of the dissolved salts, minerals, and other charged particles present in the water. Higher concentrations of dissolved ions and minerals in water result in higher electrical conductivity. TDS of water includes all dissolved material in solution, whether ionized or not. TDS is numerical sum of all mineral constituents dissolved in water and is expressed in mg/l. BIS (2012) have prescribed 500 mg/l as the acceptable limit and 2000 mg/l as permissible limit

in absence of alternate source for drinking and other domestic usage. The EC varies from 177 to 1893 (average 693) for GW samples, 59 to 729 (Average 227) for Ganga river (Fig 5.3). It has been observed that the EC values were showing a declining trend in Bhagirathi river from Gangotri to Devprayag, thereafter the EC values follows an increasing trend up to Mirzapur. The increase in EC might be due to many anthropogenic activities happening along the river. Dumping of domestic as well as industrial sewage and agricultural runoff carrying residual fertilizers are the most possible reasons for elevated EC. The EC values in groundwater samples are higher in and around the urban centers of the study area may be due to anthropogenic activities (Fig. 5.4).

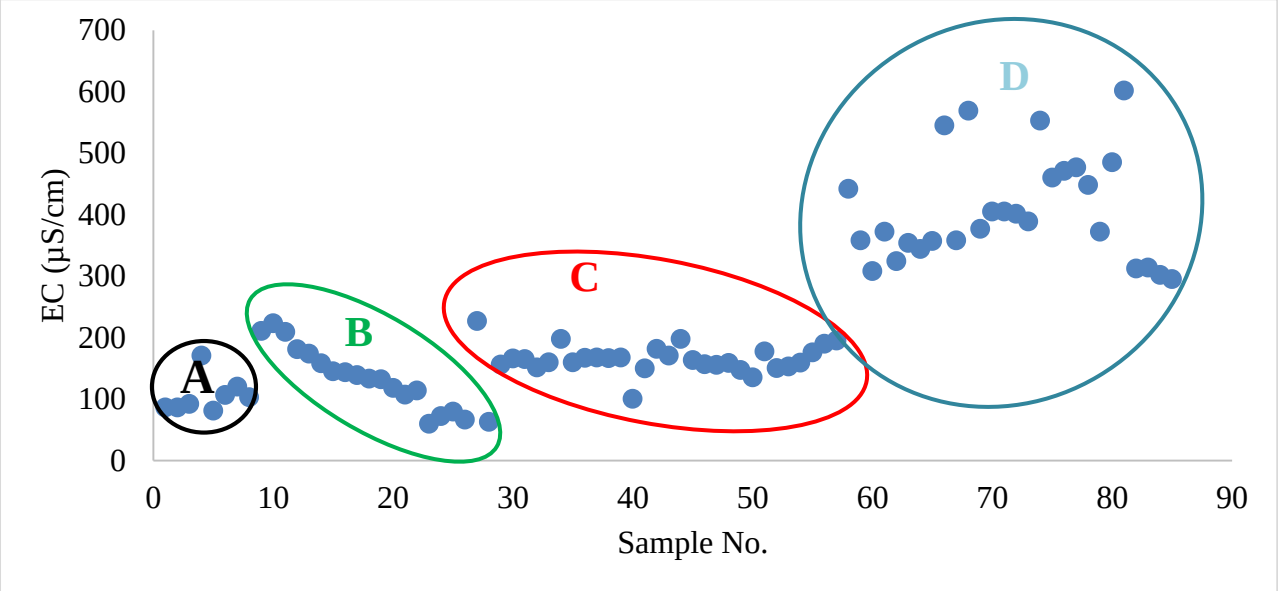

Figure 5.3: EC variations in river water (A-Mandakini River, B- Bhagirathi River, C-Alaknanda River, D-Ganga River).

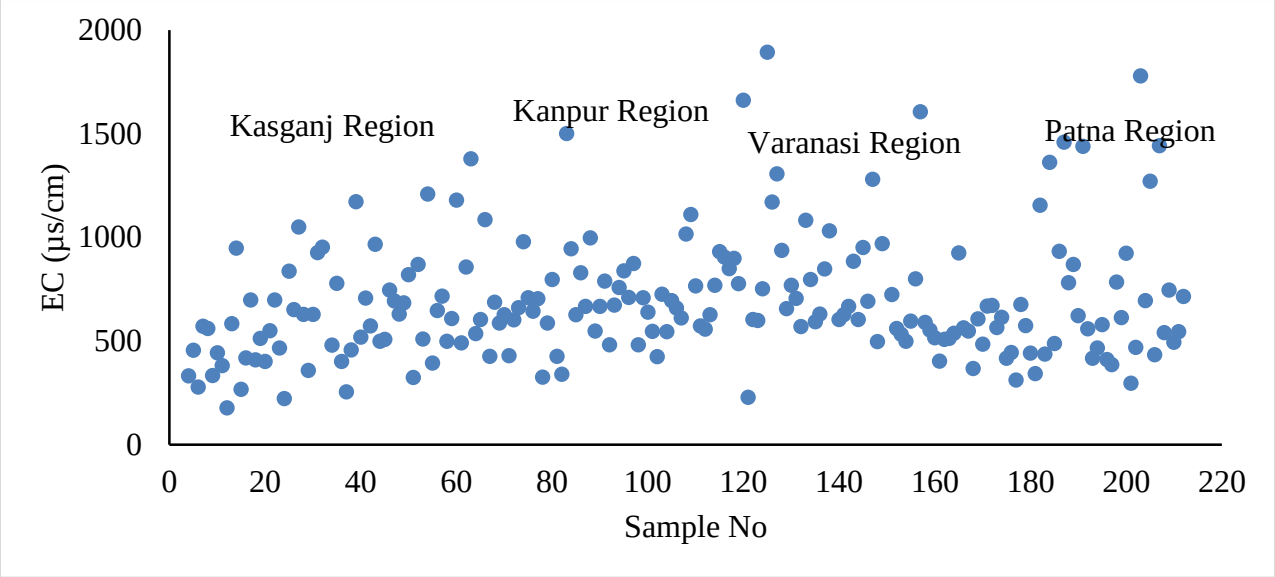

Figure 5.4: EC variation in Groundwater Samples of the study area.

Dissolved Oxygen (DO) in water refers to the amount of oxygen gas (O_2) that is dissolved and available for aquatic organisms to use. It is an essential parameter for assessing water quality and the health of aquatic ecosystems. Dissolved oxygen levels in water are influenced by various factors such as temperature, pressure, and the presence of photosynthetic organisms and oxygen-consuming processes. High dissolved oxygen levels are usually indicative of well-oxygenated, healthy water bodies, while low levels can be an indication of pollution, organic matter decomposition, or other factors leading to oxygen depletion. The DO varies from 0.78 to 5.25 mg/L (average 2.27 mg/L) for GW samples, 5.0 to 13 mg/L (Average 8.6 mg/L) for Ganga river (Fig. 5.4). Overall, DO was found to be good for river water and generally arsenic was present in those samples where DO was less.

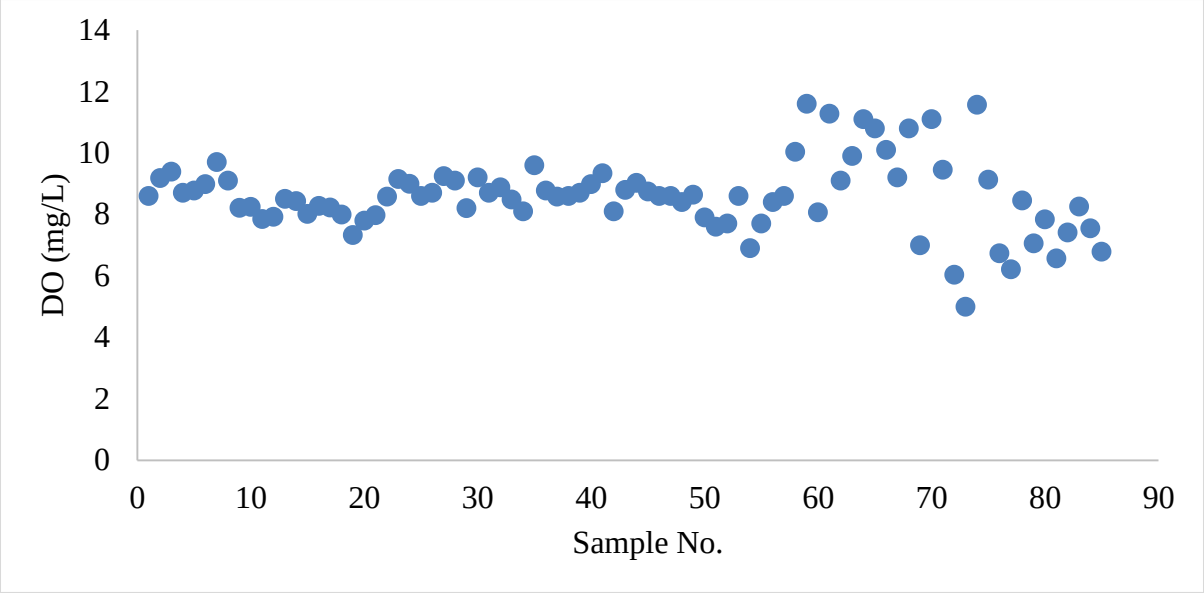

Figure 5.5: DO variation in river water Samples.

5.1.2 Major Ions

Major ions play a crucial role in determining its chemical composition and characteristics of water. Summary of the major ions, which include calcium (Ca^{2+}), magnesium (Mg^{2+}), sodium (Na^{+}), potassium (K^{+}), chloride (Cl^{-}), Fluoride, Nitrate, and bicarbonate (HCO_3^{-}) (Table 5.2). (Calcium and magnesium ions contribute to water hardness, which can affect the taste, efficiency of soaps and detergents, and the formation of scale in pipes and appliances. Sodium and potassium ions are electrolytes that help maintain proper fluid balance in the body. Chloride ions are anions often present in water and are associated with salinity levels. Bicarbonate ions play a significant role in water alkalinity and buffering capacity. They can affect the pH of water and are involved in chemical reactions and equilibrium. The presence and concentrations of these major ions in water can vary depending on the geological characteristics of the region, human activities, and water treatment processes. Monitoring and managing these ions are important for assessing water quality, determining suitability for various purposes such as drinking, irrigation, and industrial use, and implementing appropriate treatment methods.

The water chemistry of the area is dominated by alkaline metals. In general, water sampling results showing elemental abundance follow the order $Ca^{2+} > Na^{+} > Mg^{2+} > K^{+}$ for river water and groundwater samples. Generally, all the ions, including cations and anions are within the permissible limit prescribed by BIS.

Table 5.2: Statistical summary of major ions for river and groundwater

	BIS		Ganga River			Groundwater		
	Acceptable	Permissible	Min	Max	Mean	Min	Max	Mean
Na (mg/L)	-	-	1.1	68	14	2.61	135	45
K (mg/L)	-	-	0.56	10.4	3.4	0.25	83	5.37
Ca (mg/L)	75	200	9.2	65	25	0.193	138	44
Mg (mg/L)	30	100	0.79	35	10	6.71	94	31
Cl (mg/L)	250	1000	0.26	88	12	1.51	176	34
SO4 (mg/L)	200	400	5.4	98	25	1.33	267	36
NO3 (mg/L)	45	NR	0.009	6.7	0.65	0.005	104	10
F (mg/L)	1	1.5	0.03	1.24	0.22	0.009	1.85	0.4
Alk (mg/L)	200	600	13	398	122	86	615	248

Calcium (Ca^{2+}): Calcium in water primarily originates from the dissolution of calcium-bearing minerals present in the aquifer formations, and it is often the most abundant cation in groundwater. The weathering and dissolution of calcium carbonate minerals (such as limestone and dolomite) and calcium-rich silicate minerals (including amphiboles, pyroxenes, olivine, biotite, etc.) are the main sources of calcium in aquatic systems. Calcium concentrations range from 0.193 to 138 mg/L (mean: 44 mg/L) in groundwater, and from 9.2 to 65 mg/L (mean: 25 mg/L) in the Ganga River. According to the Bureau of Indian Standards (BIS, 2012), the acceptable limit for calcium in drinking water is 75 mg/L, while the permissible limit, in the absence of an alternative source, is 200 mg/L. All samples fall within the permissible limit prescribed by the Bureau of Indian Standards (BIS, 2012).

Magnesium (Mg^{2+}): Magnesium (Mg^{2+}) is abundant in the Earth's crust and is a common constituent of natural waters. It originates primarily from the weathering and dissolution of clay minerals, dolomite, and pyroxenes. The main sources of magnesium in natural waters include ferromagnesian minerals in igneous rocks and magnesium carbonate in sedimentary rocks. Magnesium sulphate and chloride are highly soluble, contributing to its mobility in

aquatic systems. In the present study, magnesium concentrations range from 6.71 to 94 mg/L (mean: 31 mg/L) in groundwater, and from 0.79 to 35 mg/L (mean: 10 mg/L) in the Ganga River. The presence of calcium and magnesium ions contributes to water hardness. According to the Bureau of Indian Standards (BIS, 2012), the acceptable limit for magnesium in drinking water is 30 mg/L, and the permissible limit, in the absence of an alternative source, is 100 mg/L. All samples within permissible limit for magnesium as prescribed by the Bureau of Indian Standards (BIS, 2012)

Sodium (Na^+): Sodium in the aquatic system is primarily derived from atmospheric deposition, evaporite dissolution, and silicate weathering. The formation of evaporite encrustations containing sodium and potassium salts can also occur due to cyclic wetting and drying, which leads to the development of alkaline or saline soils—an additional source of sodium in water. The weathering of sodium and potassium-bearing silicate minerals, such as albite, anorthite, orthoclase, and microcline, is a major contributor to the presence of Na^+ in natural waters. In the present study, sodium concentrations range from 2.61 to 135 mg/L (mean: 45 mg/L) in groundwater, and from 1.1 to 68 mg/L (mean: 14 mg/L) in the Ganga River. According to WHO (2011), no health-based guideline value has been established for sodium, as its contribution from drinking water to total daily intake is generally low. However, based on taste threshold, sodium concentrations in drinking water should ideally be less than 200 mg/L (Sharma, N. et al., 2023).

Potassium (K^+): Potassium is nearly as abundant as sodium in igneous and metamorphic rocks; however, its concentration in groundwater is typically one-tenth to one-hundredth that of sod (Sharma et al. 2023). Similar concentrations of sodium and potassium are found only in very low mineral water. Two main factors contribute to the scarcity of potassium in groundwater: The resistance of potassium-bearing minerals to weathering and decomposition, and the fixation of potassium by clay minerals, which are formed as weathering products. Potassium concentrations range from 0.253 to 83 mg/L (mean: 5.37 mg/L) in groundwater, and from 0.56 to 10.4 mg/L (mean: 3.4 mg/L) in the Ganga River.

Bicarbonate (HCO_3^-): Bicarbonates and carbonates in natural waters are primarily derived from soil-zone CO_2 and the weathering of parent minerals. The subsurface soil zone typically contains elevated carbon dioxide (CO_2) pressure, which is produced through the decay of organic matter and root respiration. This CO_2 combines with rainwater to form carbonic acid, which then reacts with minerals to produce bicarbonate ions. Bicarbonates may also form

through the dissolution of carbonate and/or silicate minerals by carbonic acid. These ions contribute significantly to the alkalinity (acid-neutralizing capacity) of water. According to the Bureau of Indian Standards (BIS, 2012), the acceptable limit for bicarbonate in drinking water is 200 mg/L, and the permissible limit, in the absence of an alternative source, is 600 mg/L. In the present study, bicarbonate (HCO_3^-) concentrations range from 104 to 750 mg/L (mean: 302 mg/L) in groundwater, and from 15.8 to 485 mg/L (mean: 148 mg/L) in the Ganga River. Few samples exceeded the permissible bicarbonate concentration limit set by the Bureau of Indian Standards (BIS, 2012) respectively. The high bicarbonate concentrations observed in the samples indicate active weathering of carbonate minerals in the study area. Higher bicarbonate is observed in lower stretches for both river and groundwater (Fig. 5.6).

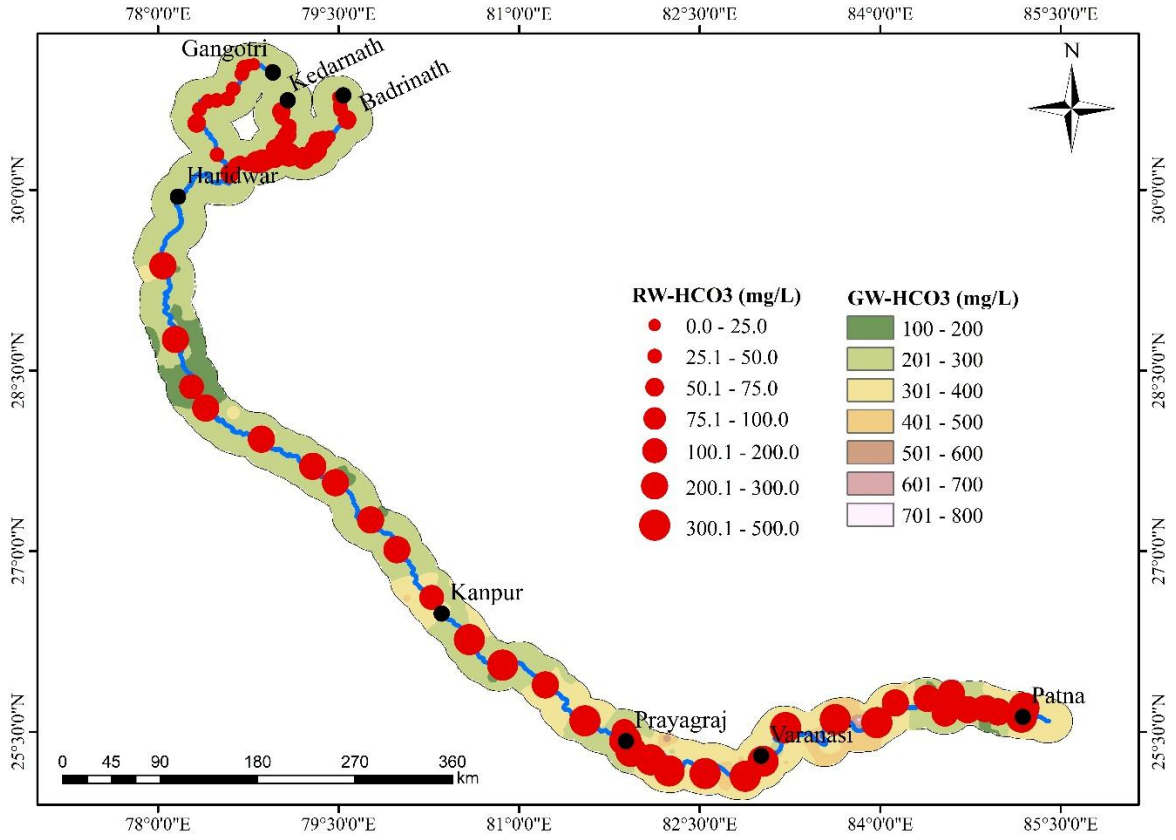

Figure 5.6: Spatial variation of HCO_3 (red dots present the river water concentration and spatial colour coding shows the GW concentration).

Chloride (Cl^-): Chloride is generally found in lower concentrations in most common rock types compared to other major ions in natural water. The primary sources of chloride in groundwater are atmospheric deposition, seawater intrusion, and anthropogenic activities. Abnormally high chloride levels may also result from pollution by sewage or other waste

discharges. According to the Bureau of Indian Standards (BIS, 2012), the acceptable limit for chloride in drinking water is 250 mg/L, while the permissible limit, in the absence of an alternative source, is 1000 mg/L. In this study, chloride concentrations in all analyzed samples during both seasons remained within the permissible limit prescribed by BIS. Chloride concentrations range from 1.51 to 176 mg/L (mean 34 mg/L) in groundwater, and from 0.126 to 88 mg/L (mean: 12 mg/L) in the Ganga River. Higher Cl (larger red circles) in the river is noticed in the stretch from Kannauj to Mirzapur showing anthropogenic activities in the river. For GW, high chloride was observed in Kasganj, Kannauj, Kanpur, Varanasi and Patna region (Fig. 5.7).

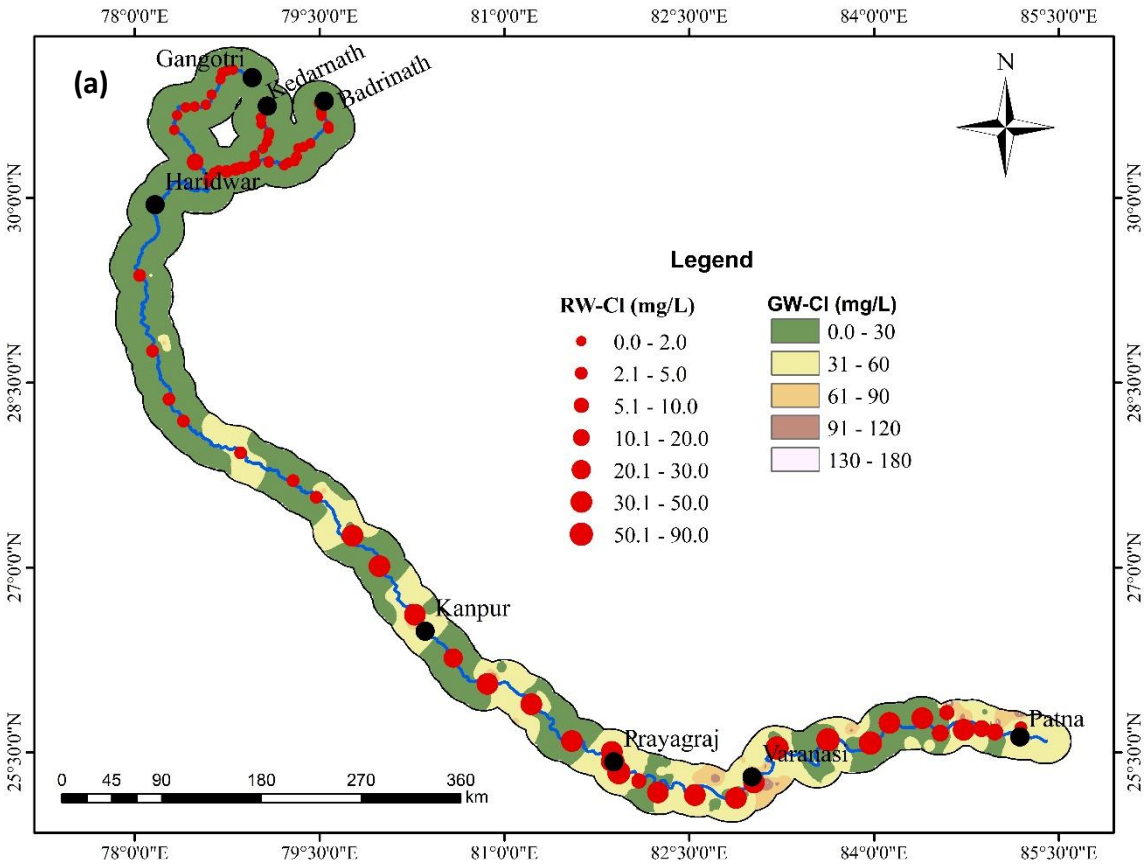

Figure 5.7: Spatial variation of Cl. (red dots present the river water concentration and spatial colour coding shows the GW concentration).

Sulphate (SO_4^{2-}): High sulphate concentrations in drinking water can impart a noticeable taste, and very high levels may have a laxative effect, especially in individuals who are not accustomed to it. Elevated sulphate levels in drinking water may also lead to gastrointestinal disorders. In the present study, sulphate concentrations range from 1.3 to 267 mg/L (mean 36 mg/L) in groundwater samples, and from 5.4 to 98 mg/L (mean: 25 mg/L) in the Ganga River.

According to the Bureau of Indian Standards (BIS, 2012), the acceptable limit for sulphate in drinking water is 200 mg/L, while the permissible limit, in the absence of an alternative source, is 400 mg/L. All analysed samples show sulphate concentrations within the permissible limit, indicating that the water is safe with respect to sulphate content. SO_4 is high in the middle stretch and also at near origin of rivers and high sulphate was observed in GW where Cl was also more that shows anthropogenic activities (Fig. 5.8).

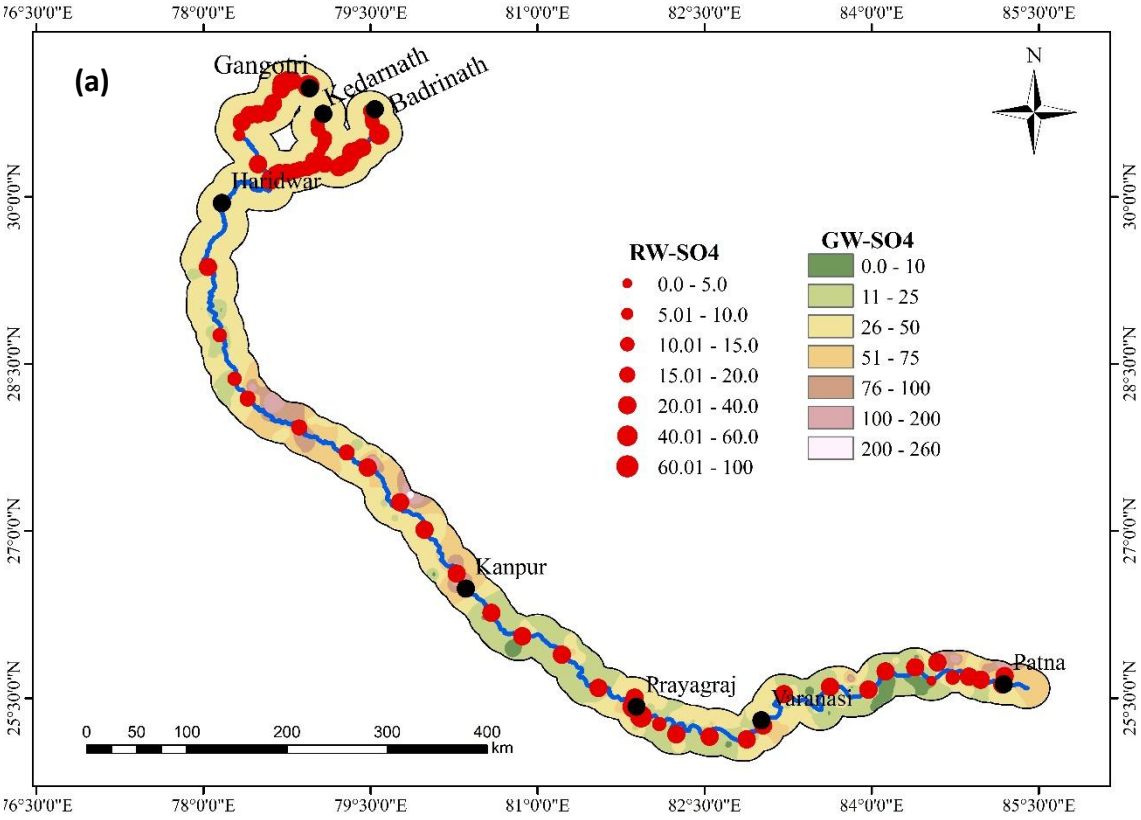

Figure 5.8: Spatial variation of SO_4. (red dots present the river water concentration and spatial colour coding shows the GW concentration).

Nitrate (NO_3^-): Nitrate occurs naturally in the environment and is highly soluble in water. It is found in varying concentrations in all plants and plays an essential role in the nitrogen cycle. Nitrate can enter surface water and groundwater primarily through agricultural activities including the excessive application of inorganic nitrogenous fertilizers and organic manures as well as through wastewater discharge and the oxidation of nitrogenous waste from human and animal excreta, including septic tanks. Nitrate concentrations range from 0.005 to 104 mg/L (mean: 10 mg/L) in groundwater, and from 0.009 to 6.76 mg/L (mean: 0.65 mg/L) in the Ganga River. According to the Bureau of Indian Standards (BIS, 2012), the acceptable limit for nitrate in drinking water is 45 mg/L. Exceeding this limit can pose serious health risks, particularly

for infants, as high nitrate levels are associated with methemoglobinemia, commonly known as “Blue Baby Syndrome.” In the present study, most of the samples were found to have nitrate concentrations below the BIS permissible limit but few samples exceed the limit of BIS. Higher NO_3 (larger red circles) in the river is present in the stretch from Kannauj to Mirzapur showing anthropogenic activities (Fig. 5.9). However, it is comparatively higher near the urban centers in GW samples.

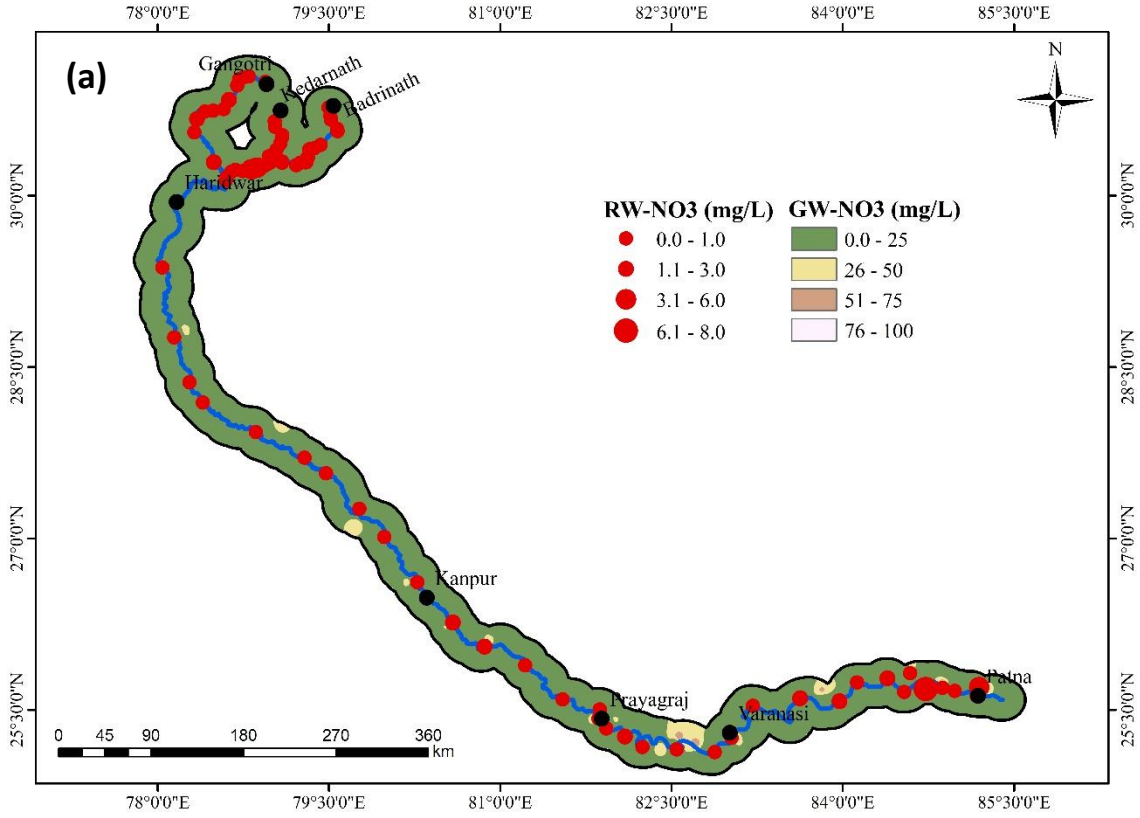

Figure 5.9: Spatial variation of NO_3^- during pre-monsoon. (red dots present the river water concentration and spatial colour coding shows the GW concentration).

Fluoride (F^-): Fluoride is present in all natural water to varying degrees. While seawater typically contains about 1.0 mg/L, rivers and lakes generally exhibit fluoride concentrations below 0.5 mg/L. In groundwater, fluoride concentrations may vary widely, depending on the geological characteristics and the presence of fluoride-bearing minerals in the aquifer. A certain level of fluoride intake is beneficial for human health, particularly for dental health, but only within safe limits. According to the Bureau of Indian Standards (BIS, 2012), the maximum permissible limit of fluoride in drinking water is 1.5 mg/L. However, long-term intake of fluoride above this level may lead to fluorosis, especially dental and skeletal fluorosis. Fluoride concentrations range from 0.009 to 1.85 mg/L (mean: 0.4 mg/L) in groundwater, and from 0.03

to 1.24 mg/L (mean: 0.22 mg/L) in the Ganga river. In the present study, all analysed samples Fluoride concentrations within the permissible limit (exceed few samples).

5.1.3 Hydro-geochemical processes

The chemical constituents of groundwater are influenced by many factors such as rainwater chemical properties, mineral composition of rock, groundwater residence time and anthropogenic activities involved in the area (Andre et al., 2005, Gautam, A.et al., 2022). The atmospheric sources may contribute to the dissolved salts present in the groundwater and it may be evaluated by calculating the ratios of elements to Cl- (Zhang et al., 1995). The average Na^+/Cl^- and K^+/Cl^- ratios for the groundwater shows the relative concentrations of sodium and potassium ions compared to chloride ions in groundwater samples. A Na^+/Cl^- ratio of 4.0 indicates that sodium is significantly more abundant than chloride, suggesting that sources other than halite (NaCl) dissolution such as silicate weathering, cation exchange, or anthropogenic activity may be contributing to the sodium levels in the groundwater. On the other hand, the K^+/Cl^- ratio of 0.34 implies that potassium is present in lower amounts relative to chloride. This lower ratio is commonly observed, as potassium tends to be immobilized in soils through adsorption onto clay minerals or uptake by vegetation. Together, these ratios serve as useful indicators of the geochemical processes influencing groundwater composition.

The ratio $HCO_3^- / (SO_4^{2-} + Cl^-)$ with a value of 6.9 indicates the relative dominance of bicarbonate ions (HCO_3^-) compared to the combined concentration of sulfate (SO_4^{2-}) and chloride (Cl^-) ions in groundwater. A high value like 6.9 means that bicarbonate is the dominant anion in the groundwater. Carbonate weathering (from minerals like calcite or dolomite) is a major geochemical process controlling the water composition, rather than the input of salts such as gypsum ($CaSO_4 \cdot 2H_2O$), halite (NaCl), or anthropogenic sources like sewage or industrial waste. Such a high ratio also reflects a freshwater environment with minimum salinity and strong influence from natural geochemical processes rather than contamination (Rose, 2002).

The average ratio of $(Ca^{2+} + Mg^{2+})/TZ^+$ being 0.70 indicates that calcium and magnesium ions 70% of the total cations (TZ^+) present in the groundwater. TZ^+ refers to the sum of all major cations, typically including calcium (Ca^{2+}), magnesium (Mg^{2+}), sodium (Na^+), and potassium (K^+). A high value like 0.70 suggests that alkaline earth metals (Ca^{2+} and Mg^{2+}) are dominant in the groundwater chemistry, pointing toward carbonate weathering as a primary source of

dissolved ions. This is characteristic of regions where limestone, dolomite, or other carbonate-rich rocks are prevalent. The dominance of these divalent cations also implies that the water has undergone significant rock-water interaction**,** particularly with carbonate minerals, contributing to its hardness and overall geochemical makeup.

The average ratio of $(Na^+ + K^+)/TZ^+$ is 0.29 means that sodium and potassium ions together 29% of the total cations (TZ^+) present in the groundwater. TZ^+ represents the total concentration of major cations, including calcium (Ca^{2+}), magnesium (Mg^{2+}), sodium (Na^+), and potassium (K^+). A $(Na^+ + K^+)/TZ^+$ ratio of 0.29 suggests a moderate contribution from alkali metals**,** which are typically released through silicate weathering, cation exchange processes, or in some cases, human activities such as agriculture or wastewater discharge. This ratio reflects the relative significance of silicate weathering in the geochemical evolution of groundwater, especially when compared to carbonate weathering, which is usually responsible for the dominance of Ca^{2+} and Mg^{2+}. Therefore, a 0.29 ratio indicates that while carbonate minerals may still be the primary contributors to groundwater composition, silicate mineral weathering also plays an important secondary role in influencing the water's chemical characteristics. $(Ca^{2+} + Mg^{2+})/(Na^+ + K^+)$ ratio of 3.3 in groundwater indicates that the combined concentration of calcium and magnesium ions is more than three times greater than that of sodium and potassium ions. This ratio provides insight into the dominant geochemical processes influencing groundwater composition. A high value like 3.3 suggests that carbonate weathering involving minerals such as calcite and dolomite is the primary source of dissolved cations, as calcium and magnesium are major products of carbonate dissolution.

In contrast, sodium and potassium are typically derived from silicate weathering or anthropogenic sources, and their relatively lower contribution (reflected in the ratio) indicates that these processes are less dominant in the groundwater system. Therefore, a $(Ca^{2+} + Mg^{2+})/(Na^+ + K^+)$ ratio of 3.3 strongly points toward carbonate-rich lithology and natural rock-water interactions as the main drivers of groundwater chemistry in the study area, with limited influence from silicate weathering or human activities.

Gibbs's diagram is a widely used geochemical tool for identifying the mechanisms controlling the chemical composition of natural waters. It relates the weight ratio of major cations Na/(Na+Ca) and major anions $Cl/Cl+HCO_3$ to the total dissolved solids (TDS) concentration. By plotting water samples on these diagrams, the dominant geochemical processes influencing water chemistry can be inferred. Gibbs (1970) proposed three main controlling mechanisms:

(i) Precipitation dominance**,** where rainfall and atmospheric inputs govern water chemistry; (ii) Rock dominance, where water and rock interaction and mineral weathering are the main sources of solutes; and (iii) Evaporation dominance, where evaporation enhances salinity and leads to mineral precipitation. The spatial distribution of sample points within the diagram helps to evaluate the relative contribution of these processes in a given hydrogeological. In the present study, Gibbs's diagram (Fig. 5.10) indicates that rock–water interaction is the dominant process controlling groundwater geochemistry.

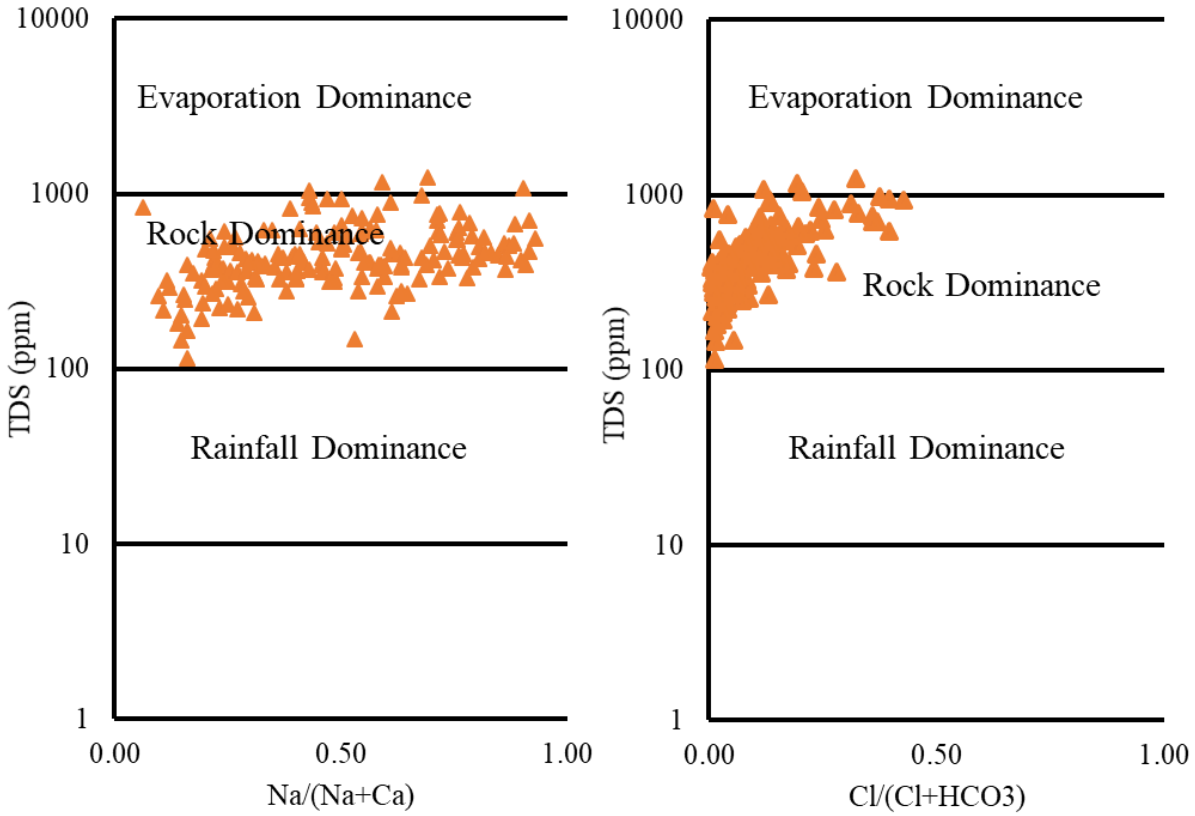

Figure 5.10: Gibbs Plot showing rock water interaction in the study area

Several hydrogeochemical bivariate diagrams have been constructed and are shown in (Fig. 5.11). The plot of (Ca^{2+} + Mg^{2+}) versus (HCO_3^- + SO_4^{2-}) illustrates the dissolution of carbonate and sulfate minerals such as calcite, dolomite, and gypsum within the groundwater system. In this study, the majority of samples plot below the equiline, although a few points lie directly on it. Data points below the equiline indicate that the combined concentration of bicarbonate and sulfate exceeds that of calcium and magnesium, suggesting additional input from non-carbonate sources. In carbonate weathering, the stoichiometric relationship dictates that the amount of Ca^{2+} and Mg^{2+} released should be equivalent to the bicarbonate produced (Singh et

al., 2013). The (Ca^{2+} + Mg^{2+}) versus HCO_3^- plot helps to identify the dominant weathering process either carbonate or silicate. A few samples plot along the equiline, indicating contributions from both carbonate and silicate weathering. However, most samples cluster near the Ca^{2+} + Mg^{2+} axis, highlighting the dominance of carbonate weathering in the region. Ca^{2+} and Mg^{2+} relative to HCO_3^-, which suggests that the excess bicarbonate may be compensated by alkali metals such as Na^+ and K^+, likely derived from silicate weathering. The origin of Ca^{2+} and Mg^{2+} ions are further assessed using the Ca^{2+} vs. HCO_3^- and Ca^{2+} vs. SO_4^{2-} plots. The Ca^{2+} vs. HCO_3^- plot indicates calcite and dolomite dissolution, as many data points are positioned near the HCO_3^- axis. Meanwhile, the Ca^{2+} vs. SO_4^{2-} plot shows that Ca^{2+} concentrations exceed those of SO_4^{2-}, suggesting that gypsum is not a significant source of calcium in the study area

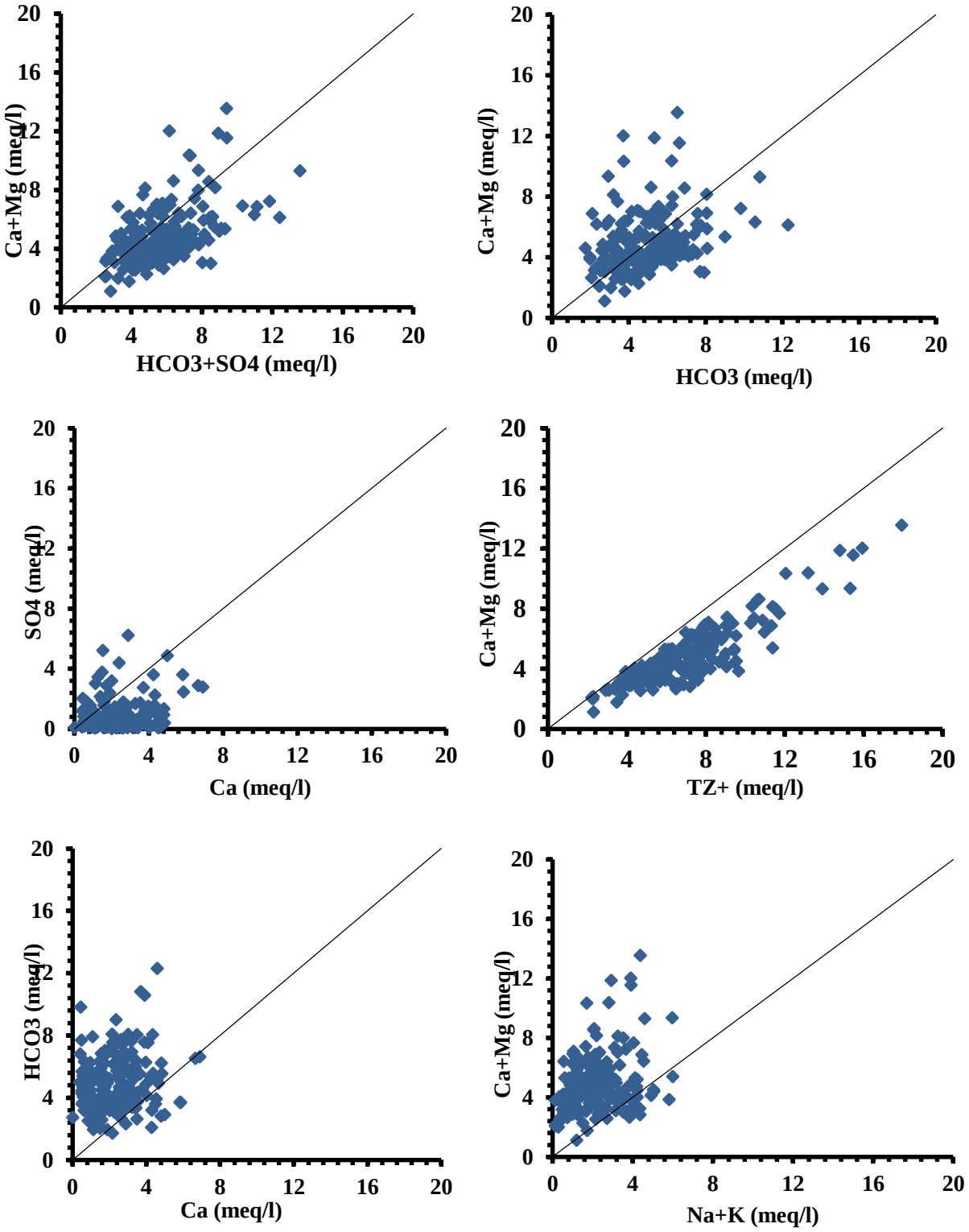

Figure 5.11: Scatter plots (a) Ca+Mg Vs HCO_3 + SO_4 (b) Ca+Mg Vs HCO_3 (c) Ca Vs SO_4 (d) Ca + Mg Vs TZ^+ (e) HCO_3 Vs Ca (f) Ca + Mg Vs Na +K.

5.1.4 Classification of water

Piper trilinear diagram or Piper trilinear plot, is a graphical representation used to analyze and display the chemical composition of water samples. It provides a visual summary of the relative concentrations of major ions in the water. The diagram is constructed on a triangular grid, with each apex representing a major ion or ion group: cations (calcium, magnesium, sodium, and potassium) on the left apex, anions (sulfate, chloride, and carbonate/bicarbonate) on the right apex, and silica in the lower apex. The concentrations of these ions are represented by points within the triangular grid. The position of a point on the diagram reflects the relative concentrations of the different ions. The location of the point within each apex triangle indicates the dominance of a particular ion, while the distance from the apex indicates the concentration level. The diagram allows for a visual comparison of different water samples and can reveal patterns, trends, and relationships among the ions. The diagram helps in understanding the hydro chemical characteristics of water samples and aids in decision-making for water resource management and environmental monitoring. In majority of the water samples, anions are dominated by HCO_3, with abundance order: $HCO_3 > SO_4 > Cl$, Cations are dominated by Ca, with abundance order: Ca > Mg > Na. Groundwater samples are found concentrated with mixed Ca+Mg+Cl type, Ca+HCO_3 type, Na+Cl type and mixed Ca+Na+ HCO_3 type whereas river water samples are concentrated with mixed Ca+Mg+Cl type and Ca+HCO_3 type (Fig. 5.12).

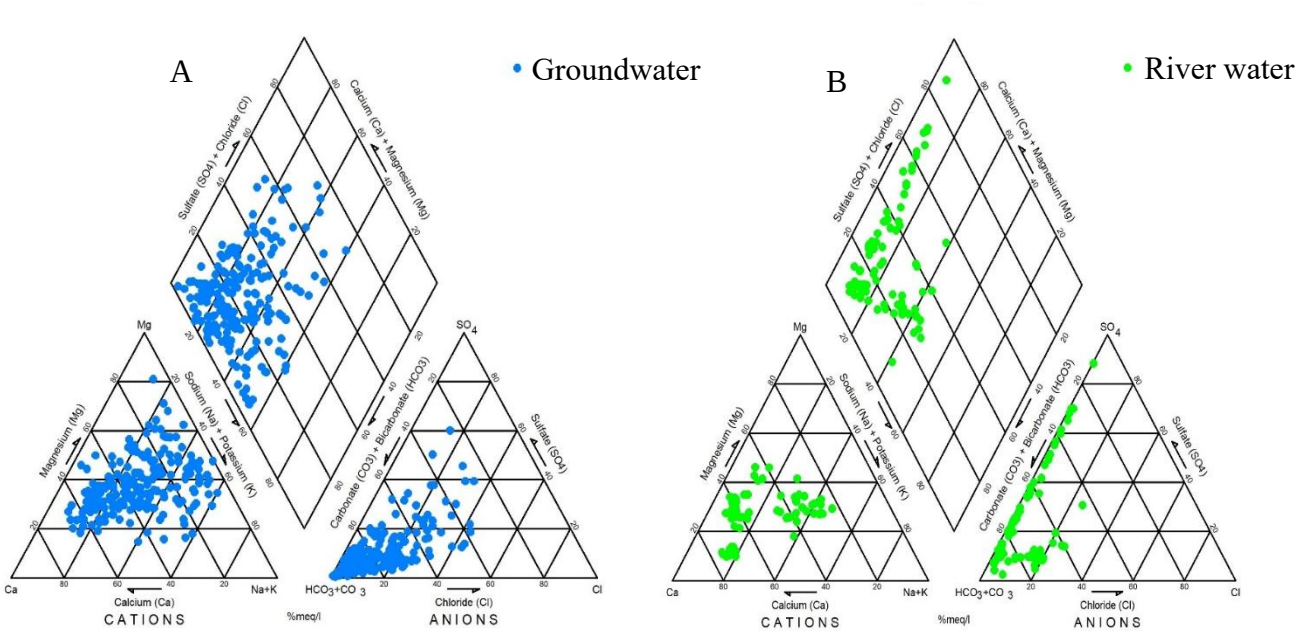

Figure 5.12: Piper diagram illustrates hydro-geochemical regime: (A) groundwater samples and (B) river water samples.

5.1.5 Trace Elements

Trace metals in water samples refer to metallic elements that are found in low concentrations in water. These metals can originate from natural sources or be introduced through human activities such as industrial processes, mining, and agricultural practices. The presence of trace metals in water samples is of concern due to their potential toxicity and the adverse effects they can have on ecosystems and human health. Monitoring and analyzing trace metals in water samples is crucial for assessing water quality, identifying potential contamination sources, and implementing appropriate mitigation measures when necessary. The detection and quantification of trace metals help ensure the safety and suitability of water for various purposes such as drinking, irrigation, and industrial use. Additionally, understanding the levels of trace metals in water samples aids in evaluating the effectiveness of water treatment processes and implementing regulatory measures to protect both human and environmental health. Statistical summary of trace elements for Ganga river, shallow and deep groundwater are presented in Table 5.3.

Table 5.3: Statistical summary of trace elements for Ganga River, Shallow and Deep Groundwater

	BIS		Ganga River				Shallow Groundwater				Deep Groundwater			
	Acceptable	Permissible	Min	Max	Mean	Stdev	Min	Max	Mean	Stdev	Min	Max	Mean	Stdev
Al (ppb)	30	200	0.47	1597	588	337	3.4	615	50	78	9.30	668	74	122
Cr (ppb)	50	NR	0.077	40	2.43	4.9	0.097	14	1.25	1.821	0.08	20	2.0	3.43
Mn (ppb)	100	300	0.11	1411	79	161	1.71	1410	223	268	0.94	685	81	135
Fe (ppb)	300	NR	0.76	2431	879	517	40	12764	2007	2647	29	5000	1184	1217
Ni (ppb)	20	NR	ND	19	3.4	3.2	0.12	53	1.99	5.37	0.11	15	1.5	2.34
Cu (ppb)	50	1500	0.28	74	6.98	13	0.24	94	4.69	10.73	0.34	38	4.1	5.86
Zn (ppb)	5000	15000	7.49	242	60	33	3.5	5798	280	656	25	4032	245	501
As (ppb)	10	NR	0.37	13	6.3	3.13	0.084	361	21	58	0.13	14.91	1.3	2.05
Cd (ppb)	3	NR	ND	1.3	0.13	0.17	ND	0.87	0.065	0.11	ND	0.49	0.1	0.076
Pb (ppb)	10	NR	0.04	12.6	2.1	2.17	0.35	46	2.63	5	0.41	37	3.1	5.54

Arsenic (As): Arsenic is usually present in natural waters at concentrations of less than 1-2 ppb. However, the arsenic concentration can be significantly elevated in groundwater, where there are sulfide mineral deposits and sedimentary deposits deriving from volcanic rocks. In the study area concentration of arsenic in shallow and deep groundwater samples varies between ND to 361 ppb with mean 21 ppb and 0.13 to 14.91 with mean 1.3 ppb respectively. Arsenic in Ganga water samples varies between 0.37 to 13 ppb. It may be observed that As concentration is more in middle stretch around Kanpur and in lower stretch (Varanasi to Patna) in the shallow groundwater, whereas As is relatively higher in middle stretch of river water (Fig. 5.13,5.14 and 5.15).

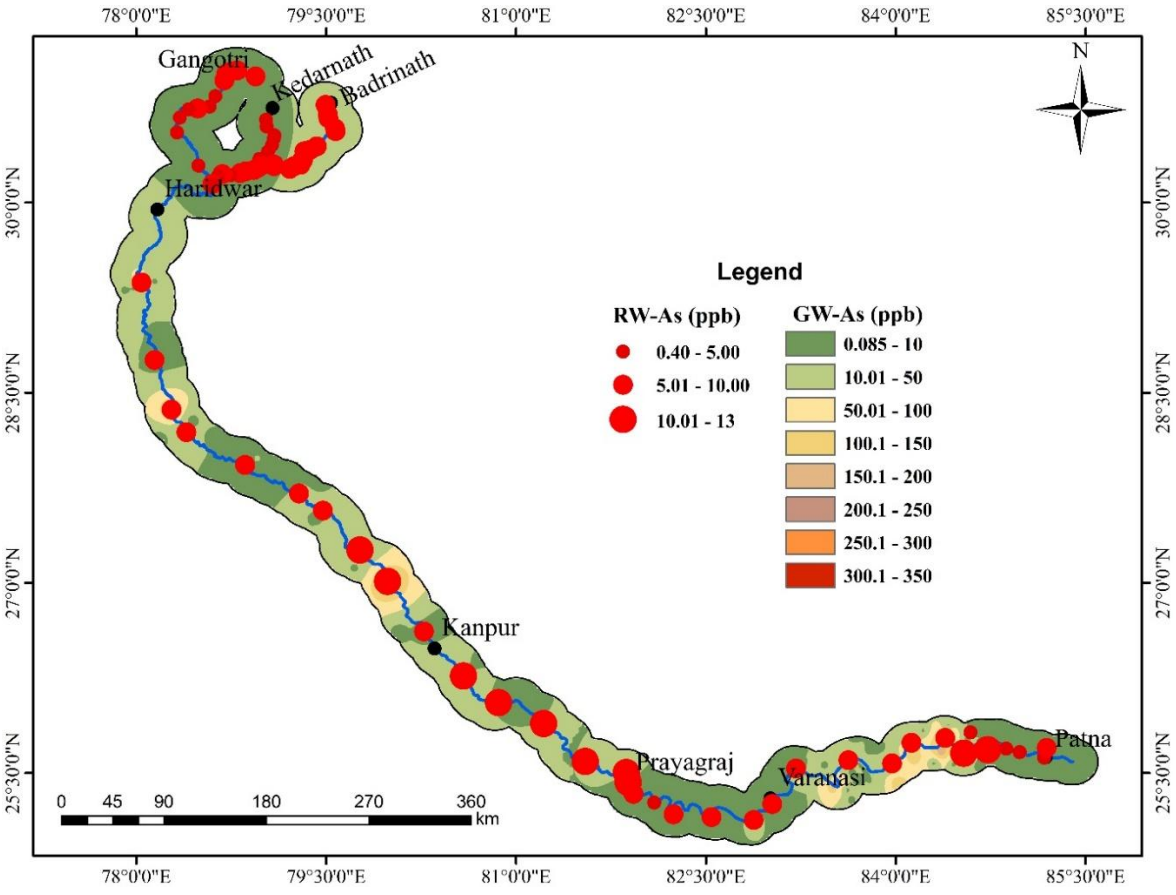

Figure 5.13: Spatial distribution of Arsenic concentration in shallow groundwater.

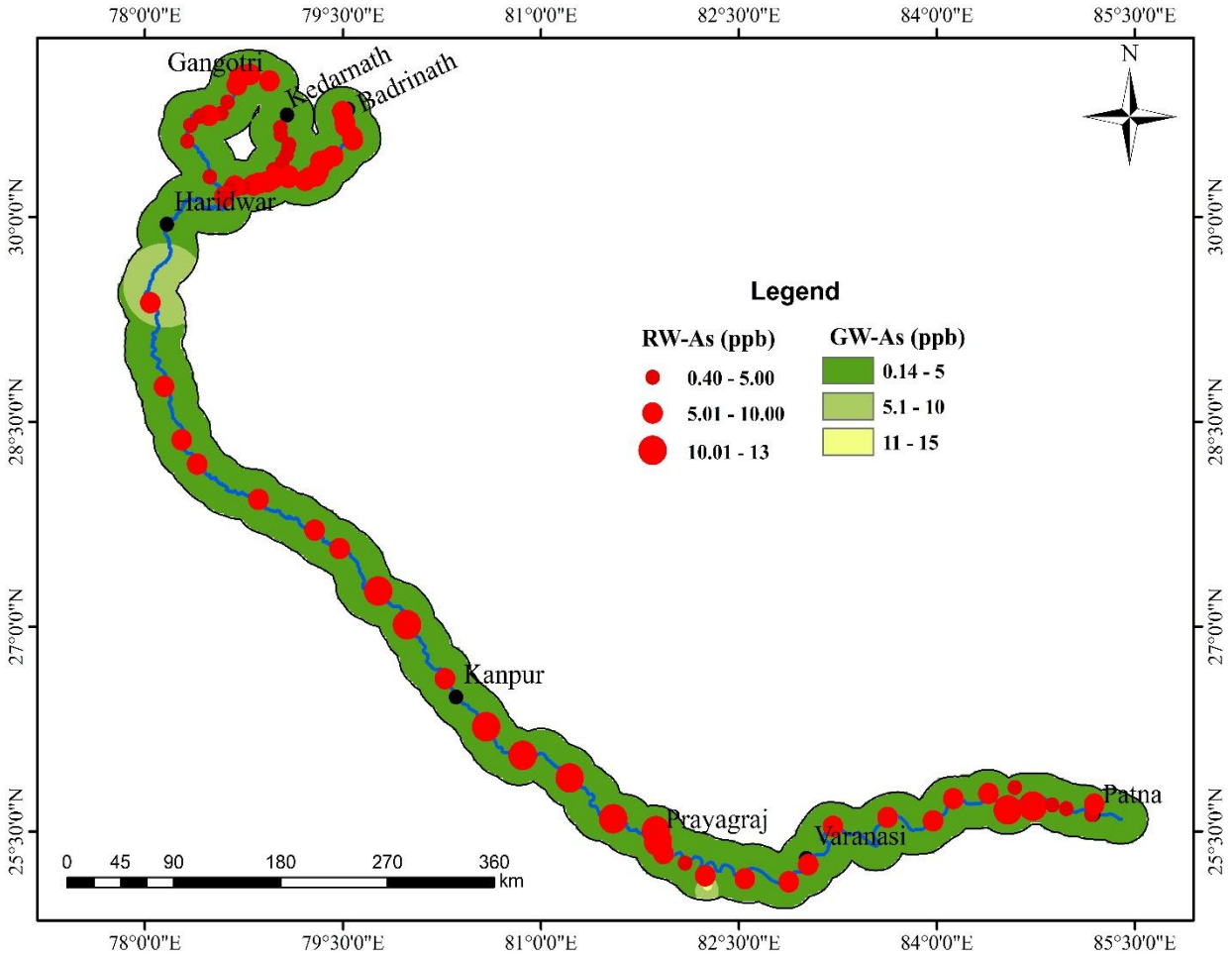

Figure 5.14: Spatial distribution of Arsenic concentration in deep Groundwater.

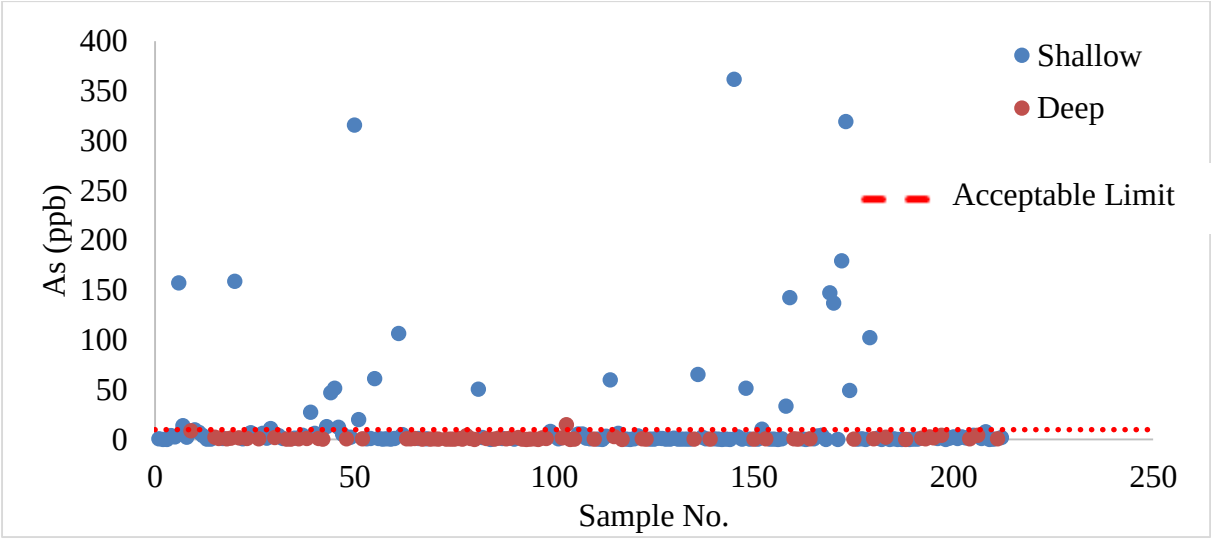

Figure 5.15: Scatter plot of As concentration in shallow and deep groundwater samples.

The groundwater samples collected during sampling were generally from hand pumps with depth ranging from 15 to 150 m because of potential sand zones at shallow depth. Depth vs. As conc. cross-plot of samples from study area reveals a rapid decrease in As conc. beyond 60 m bgl (Fig 5.16). It implies that only unconfined shallow aquifer is contaminated by As.

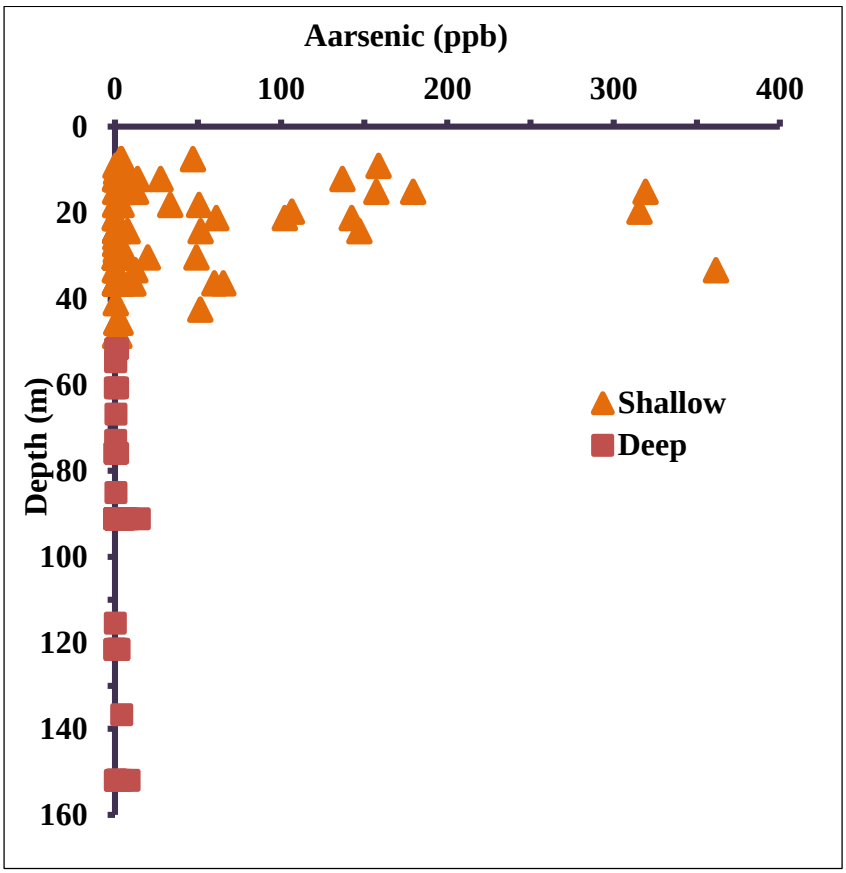

Figure 5.16: Depth wise variation of Arsenic in the groundwater

Iron (Fe): Iron in trace amounts is essential for nutrition. High concentrations of iron generally cause inky flavor, bitter and astringent taste to water. Groundwater containing soluble iron remain clear while pumped out, but exposure to air causes precipitation of iron due to oxidation, with a consequence of rusty color and turbidity. The objection to iron is not due to health reason though there is a taste and odour problem. The concentration of Fe in shallow, deep groundwater and Ganga river water samples of the study area varies between 40 to 12764 ppb (mean 2007 ppb), 29 to 5000 ppb (mean 1184 ppb) and 0.76 to 2431 ppb (mean 879 ppb)

respectively (Fig. 5.17, 5.18). The Bureau of Indian Standards has recommended 300 ppb as the acceptable limit for iron in drinking water.

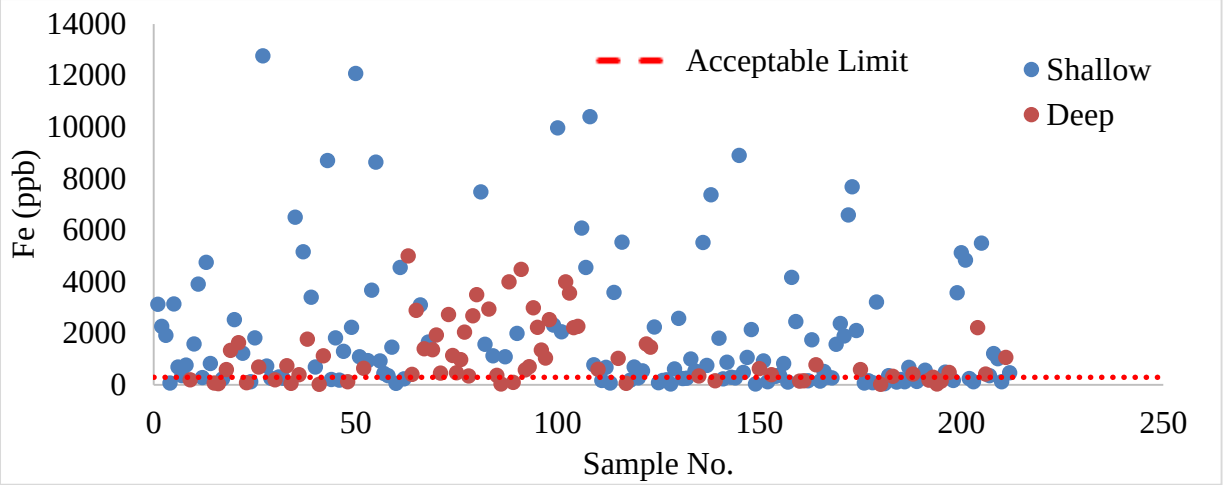

Figure 5.17: Scatter plot of Fe concentration in shallow and deep groundwater samples.

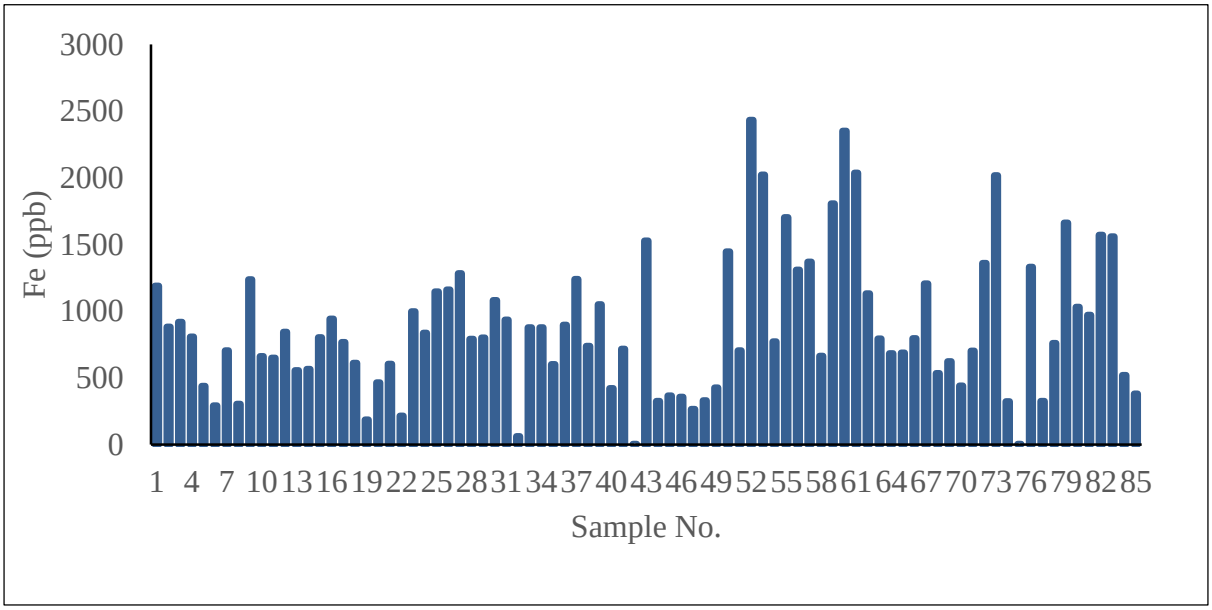

Figure 5.18: Scatter plot of Fe concentration in ganga river during pre-monsoon.

Manganese (Mn): Manganese is a naturally occurring element found in many surface water and groundwater sources, especially under anaerobic or low-oxidation conditions. When manganese concentrations exceed 100 ppb, it can cause an undesirable taste in beverages and

lead to staining of sanitary ware and laundry. Additionally, the presence of manganese in drinking water can result in the accumulation of deposits within the distribution system. The manganese concentrations range from 1.71 to 1410 ppb in shallow groundwater samples (mean: 223 ppb), 0.94 to 685 ppb (mean 81ppb) in deep groundwater samples and from 0.11 to 1411 ppb in the Ganga River (mean: 79 ppb) (Fig. 5.19 and 5.20).

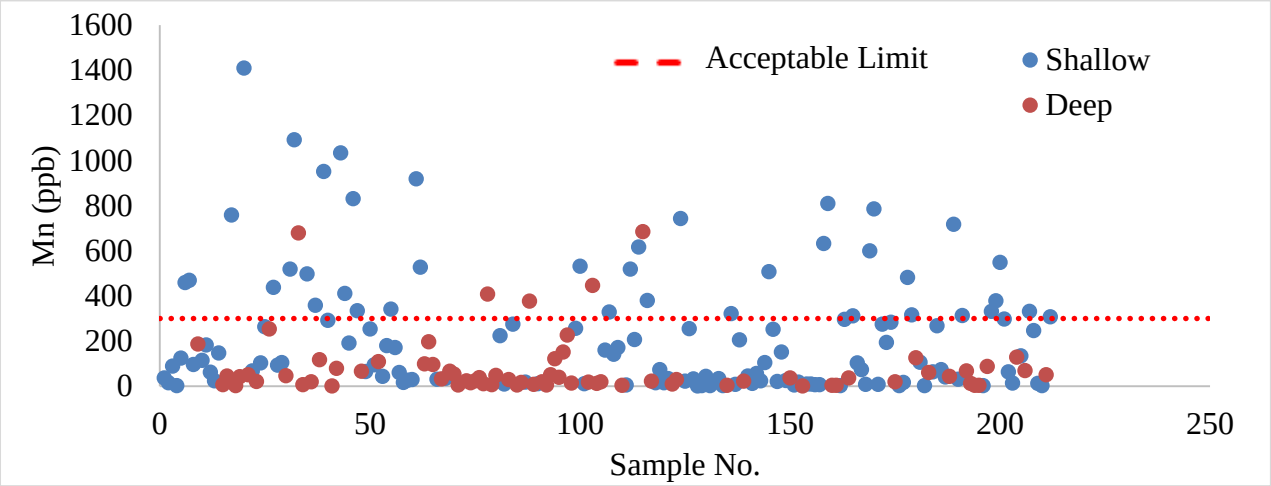

Figure 5.19: Scatter plot of Mn concentration in shallow and deep groundwater.

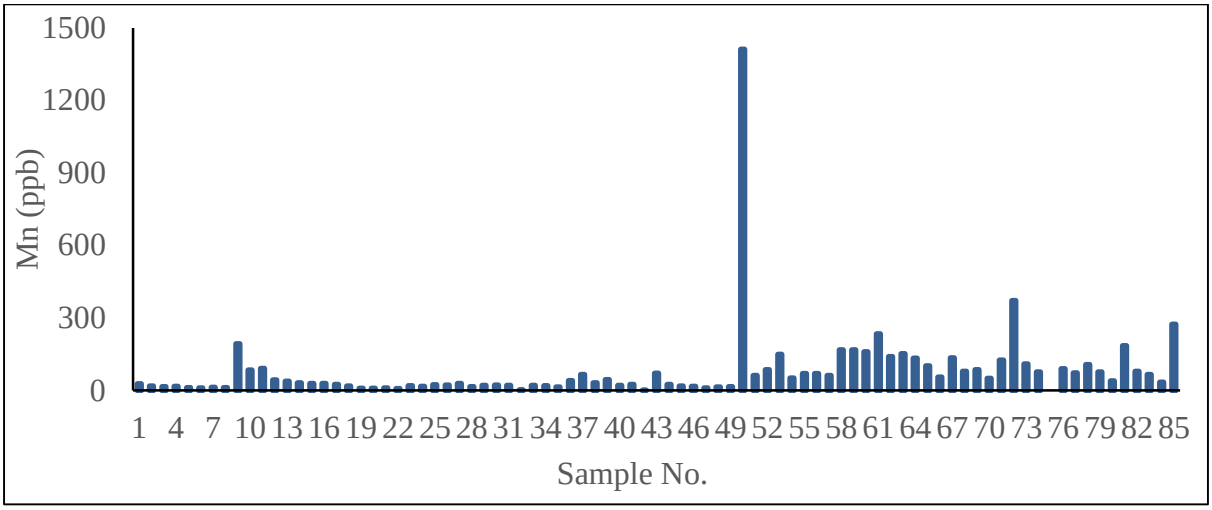

Figure 5.20: Scatter plot of Mn concentration in Ganga river during pre-monsoon.

Cadmium (Cd): Cadmium is a non-essential and non-beneficial element, known for its high toxicity even at low concentrations. It can enter the environment through various industrial

activities, including mining and smelting, electroplating, and the production of pigments and plasticizers. In the pre-monsoon season, cadmium concentrations in shallow and deep groundwater samples range from ND to 0.87 ppb (mean: 0.065 ppb) and ND to 0.49 ppb (mean 0.1 ppb). In the Ganga river Cd range from ND to 1.36 ppb (mean: 0.13 ppb) (Fig. 5.21). All observed concentrations are below the permissible limit of 3 ppb for drinking water as prescribed by the Bureau of Indian Standards (BIS, 2012).

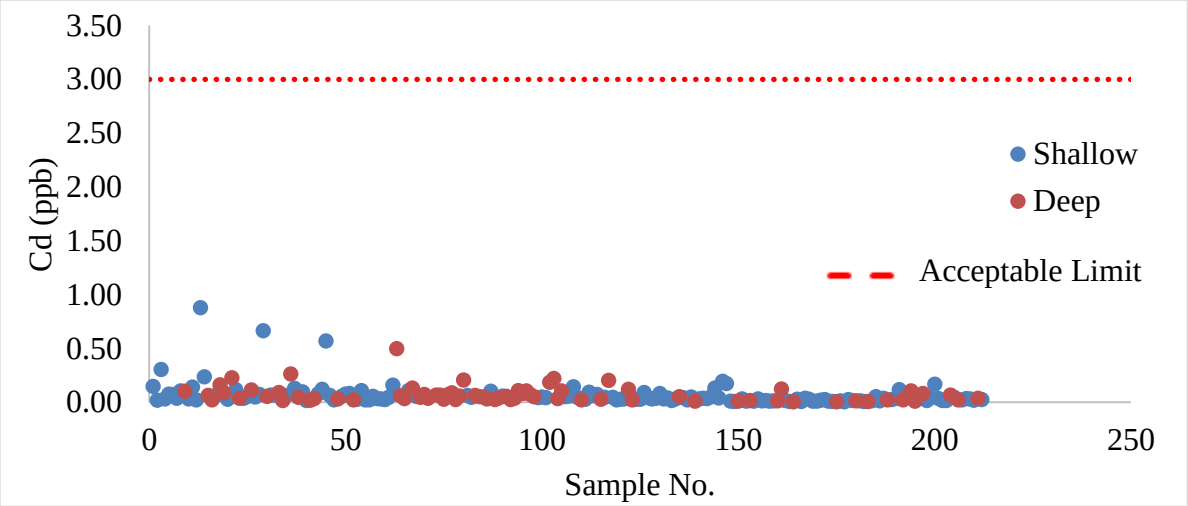

Figure 5.21: Scatter plot of Cd concentration in groundwater during pre-monsoon.

Copper (Cu): Copper is an essential nutrient and if it is in higher concentration it becomes drinking-water contaminant. It is used to make pipes, valves and fittings and is present in alloys and coatings. Beyond 0.05 mg/l the water imparts astringent taste and cause discoloration and corrosion of pipes, fittings and utensils. Recent studies have delineated the threshold for the effects of copper in drinking-water on the gastrointestinal tract, but there is still some uncertainty regarding the long-term effects of copper on human health. The concentration of copper in shallow, deep groundwater samples and Ganga river water samples of the study area varies between 0.24 to 94 ppb with mean 4.69, and 0.34 to 38 ppb with a mean value 4.1 ppb and 0.28 to 74 ppb with mean 6.98 respectively (Fig. 5.22). The Bureau of Indian Standards has recommended 50 ppb as the acceptable limit and 1500 ppb as the permissible limit in the absence of alternate source (BIS, 2012). In the study area, all the samples fall in the permissible limit of 1500 ppb.

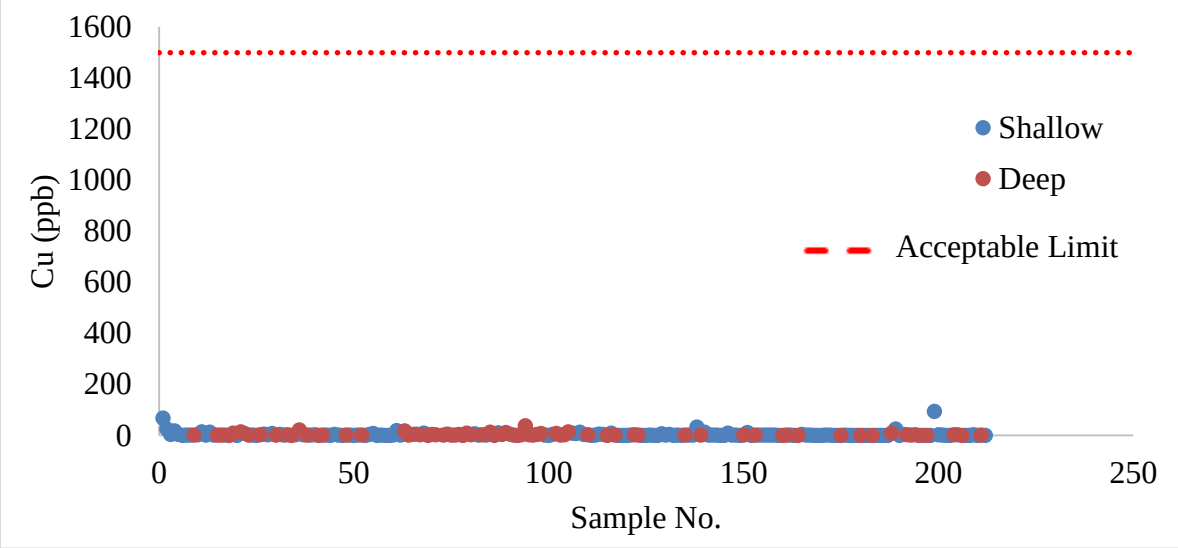

Figure 5.22: Scatter plot of Cu concentration in shallow and deep groundwater samples.

Nickel (Ni): Nickel is released into the environment primarily through the combustion of fossil fuels and the waste discharge from electroplating industries. The nickel concentrations in shallow and deep groundwater samples range from 0.12 to 53 ppb (mean 1.99 ppb), and 0.11 to 15 ppb (mean 1.5 ppb) (Fig. 5.23). In the Ganga River nickel range from not detected (ND) to 19 ppb. According to the Bureau of Indian Standards (BIS, 2012), the acceptable limit for nickel in drinking water is 20 ppb. In the present study, most of the samples fall within this permissible limit. Expected few samples of shallow groundwater samples.

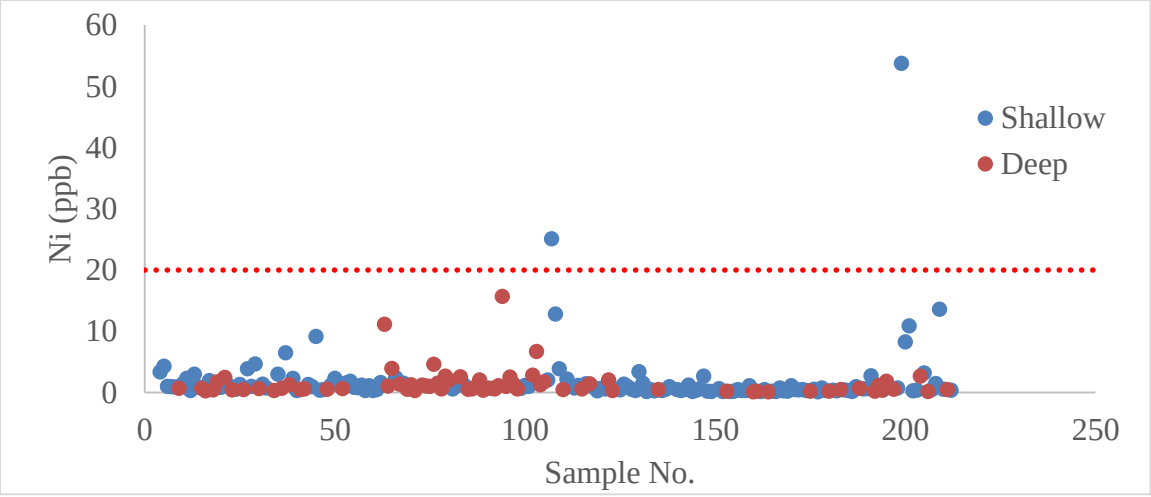

Figure 5.23: Scatter plot of Ni concentration in shallow and deep groundwater samples.

Lead (Pb) Lead is one of the most common trace metals and is extensively mined across the world. It is primarily used in the production of lead-acid batteries, solder, and alloys. Organic lead compounds, such as tetraethyl lead and tetramethyl lead, have been widely used as antiknock agents and lubricating additives in petrol. Lead is rarely present in drinking water due to natural sources. Instead, its occurrence is typically the result of corrosive water reacting with household plumbing systems that contain lead in pipes, solder, fittings, or service connections. Exposure to lead is linked to a wide range of adverse health effects, including neurodevelopmental disorders, increased mortality (mainly due to cardiovascular diseases), hypertension, impaired fertility, and adverse pregnancy outcomes. In the present study lead (Pb) concentrations range from 0.35 to 46 ppb (mean 2.63) in shallow groundwater, 0.41 to 37 ppb (mean 3.1 ppb) in deep groundwater and from 0.04 to 12.6 ppb in the Ganga River.

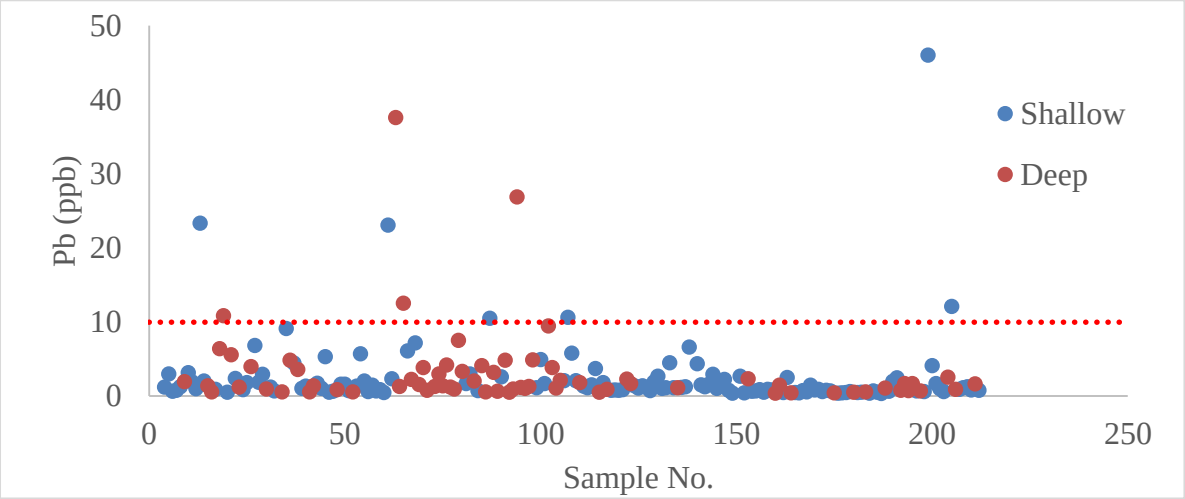

Figure 5.24: Scatter plot of Pb concentration in shallow and deep groundwater samples.

Aluminium (Al): Aluminium is the most abundant metallic element and constitutes about 8% of Earth's crust. High residual concentrations may ensure undesirable color and turbidity. There is little indication that orally ingested aluminium is acutely toxic to humans despite the widespread occurrence of the element in foods, drinking-water and many antacid preparations. It has been hypothesized that aluminium exposure is a risk factor for the development or

acceleration of onset of Alzheimer disease in humans. The concentration of Al in shallow, deep groundwater and Ganga river water samples varies between 3.4 to 615 ppb (mean 50 ppb), 9.30 to 668 ppb (mean 74 ppb) and 0.47 to 1597 ppb respectively (Fig. 5.25). The Bureau of Indian Standards has recommended 30 ppb as the acceptable limit and 200 ppb as the permissible limit for drinking water.

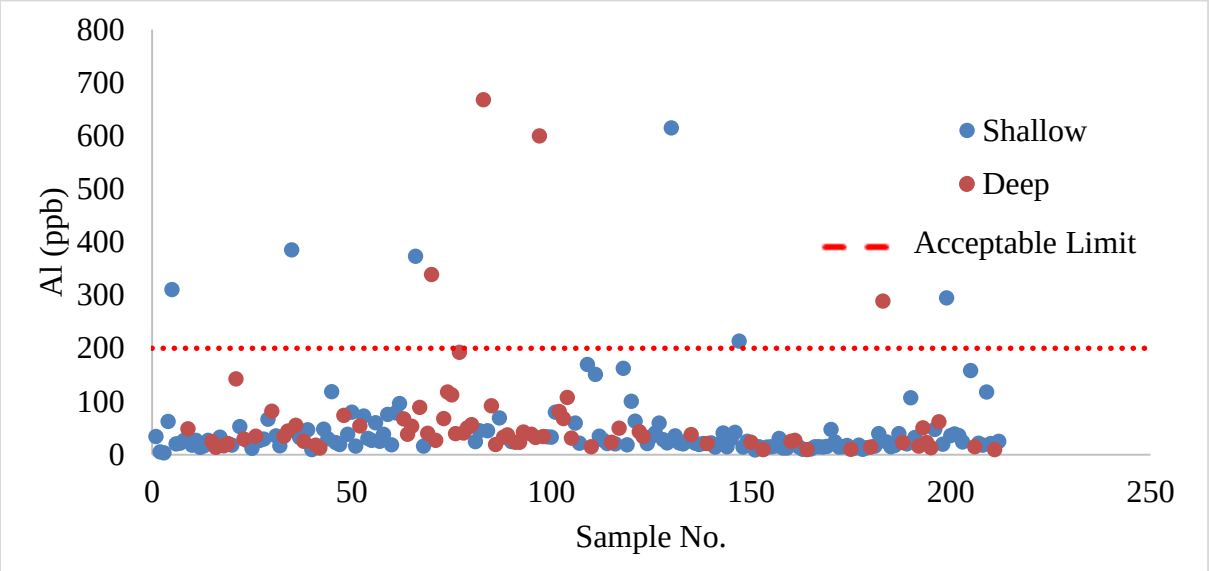

Figure 5.25: Scatter plot of Al concentration in shallow and deep groundwater samples.

5.1.6 Saturation Index

The Saturation Index (SI) in water chemistry is a numerical value used to determine whether water is in equilibrium with respect to a particular mineral, orthe mineral is likely to dissolve or precipitate. It is calculated using the logarithm of the ratio of the ion activity product (IAP) to the mineral's solubility product constant (Ksp). If the SI is greater than zero, the water is considered supersaturated, meaning the mineral is likely to precipitate out of the solution. An SI of zero indicates the water is in equilibrium with the mineral, with no net dissolution or precipitation occurring. A negative SI means the water is undersaturated**,** and the mineral is likely to dissolve. This concept is particularly important in understanding the geochemical behavior of minerals such as calcite, gypsum, silica, and iron oxides, etc. in natural waters. In groundwater and drinking water systems, SI is commonly used to assess scaling potential, corrosion risk, and the likelihood of mineral formation or depletion. The Saturation Index was

calculated for the minerals containing iron or manganese oxides/hydroxides using the Visual MINTEQ software for river water (upper stretch) and the values are shown in Figure. 5.26 and 5.27. The results indicated that Hematite, Goethite, Lepidocrocite, and Ferrihydrite fall within the supersaturated zone, suggesting a potential for precipitation, whereas $FeAsO_4 \cdot 2H_2O(s)$ and Rhodochrosite fall within the undersaturated zone, indicating a tendency toward dissolution (Fig. 5.27). Arsenic interact strongly with iron oxides like haematite, goethite and Frrihydrite and these minerals are supersaturated. These minerals precipitate and can adsorb arsenic from solution and thereby potentially removing arsenic from dissolved phase particularly in upper stretches of river Ganga. Conversely, if the condition changes such as pH changes, arsenic may be released back into the water as it is happening in the middle stretch of river. In the groundwater also, these minerals are supersaturated (Fig. 5.27).

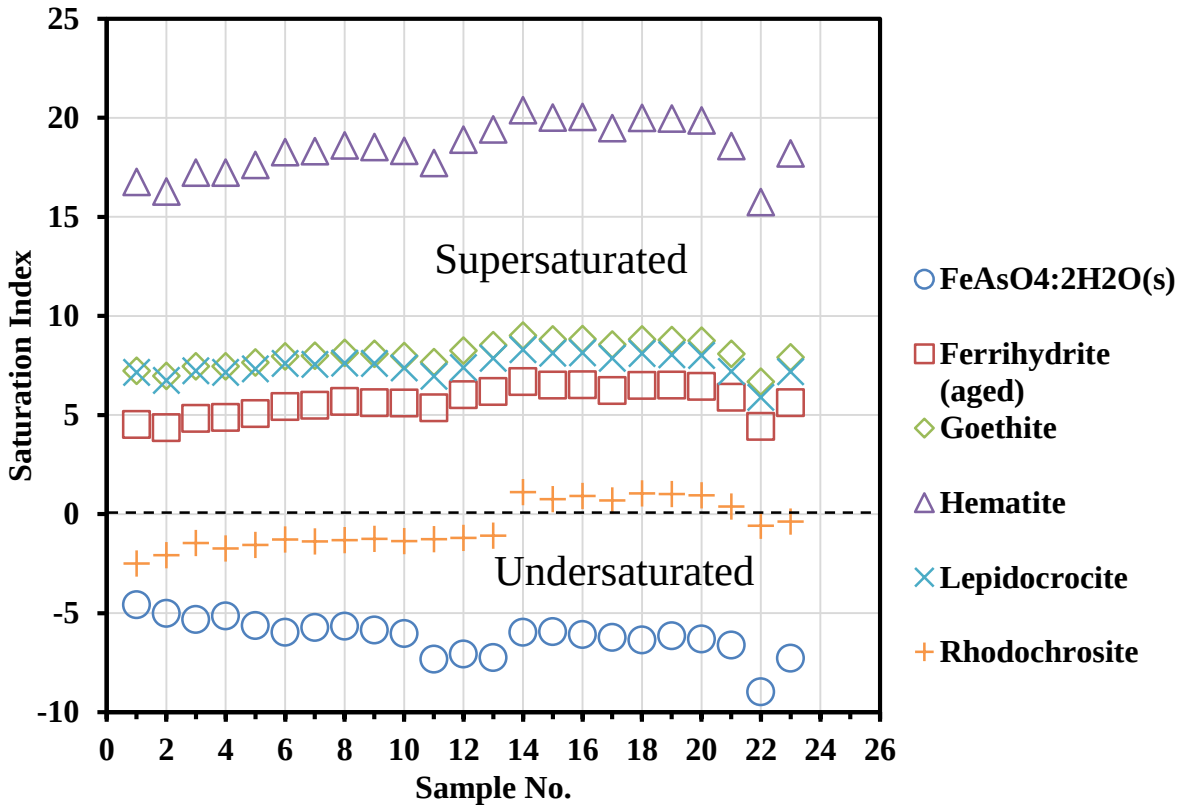

Figure.5.26: - Saturation Index of selected minerals in river water

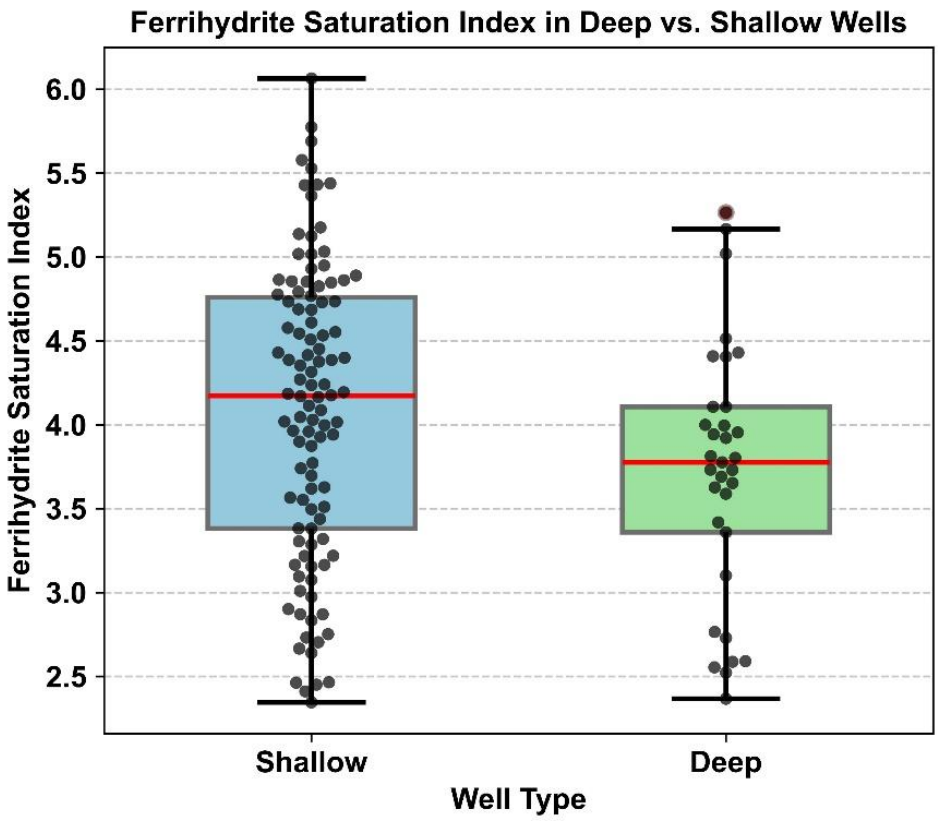
Ferrihydrite Saturation Index in Deep vs. Shallow Wells
Ferrihydrite Saturation Index
6.0
5.5
5.0
4.5
4.0
3.5
3.0
2.5
Shallow
Deep
Well Type

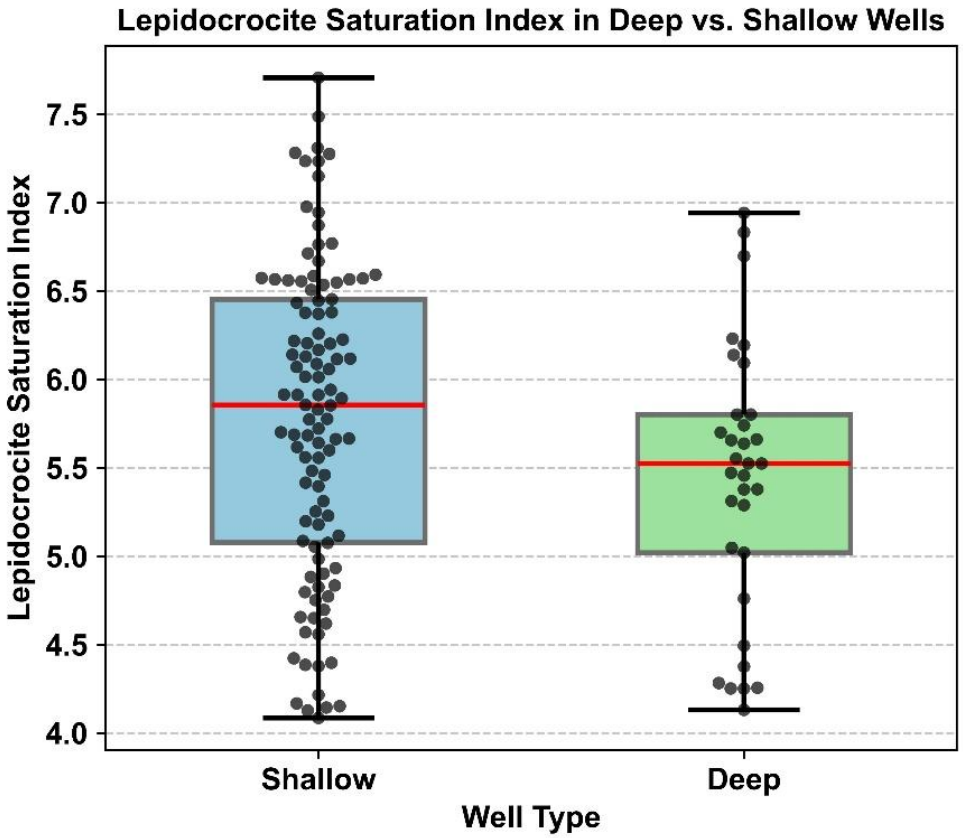
Lepidocrocite Saturation Index in Deep vs. Shallow Wells
Lepidocrocite Saturation Index
7.5
7.0
6.5
6.0
5.5
5.0
4.5
4.0
Shallow
Deep
Well Type

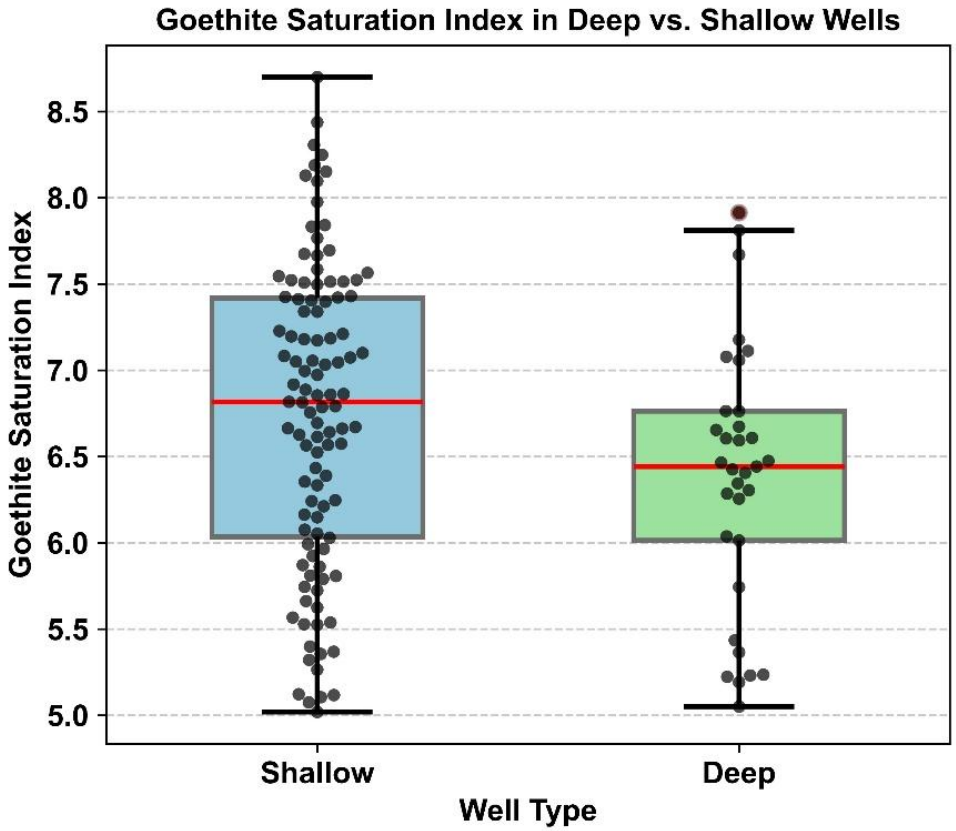

Figure 5.27: - Box plot of Saturation index with respect to different minerals (Ferrihydrite, Lepidocrocite and Goethite)

5.1.7 Sediment Characterization

Grain size analysis determines the relative amounts of sand, silt and clay in a soil. These size fractions are the mineral component of a soil and determine soil texture. Soil texture is an inherent soil property that has a major influence on several other properties that influence agricultural potential and groundwater quality. The disturbed sediment samples were collected from the river bed either by hand and by sampler. The samples were then dried in lab for further analysis. Grain size analysis reveals that the majority of the sediment samples are mainly composed of sand with an average of more than 84 % (Fig. 5.28). Texture analysis reveals the percentage of grain size of sediments in the following order:

Sand (%) > Silt (%) > Gravel (%) > Clay (%)

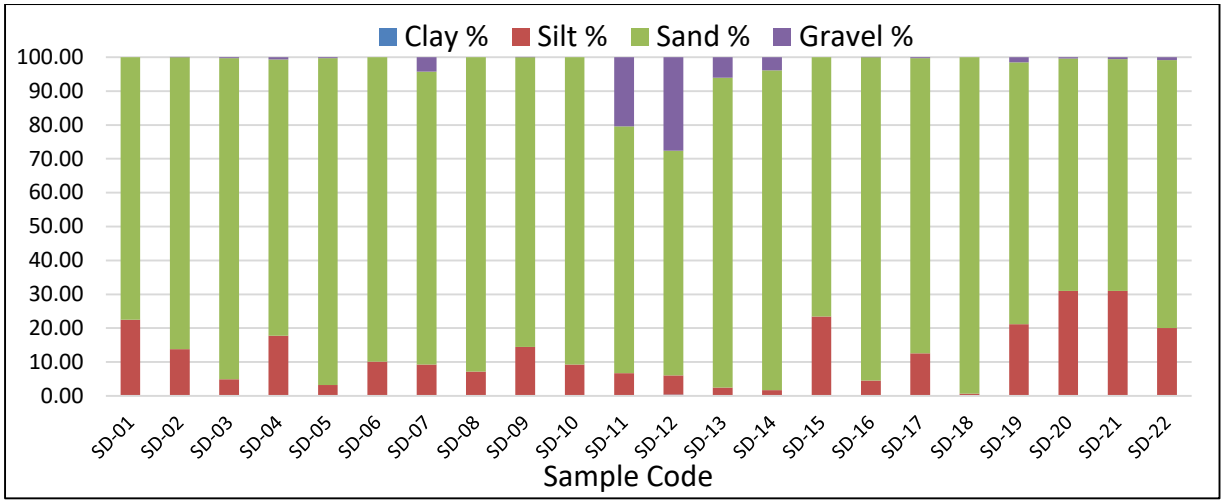

Figure 5.28: Bar graph showing the distribution of silt, sand, and gravel in sediment samples.

5.1.8 XRD and SEM-EDS analysis

In this study, we performed an XRD analysis of the sediment samples and procured XRD spectra for all the samples. Before performing the XRD analysis, the samples were sieved using a 75-micron sieve. The sediment samples were then classified according to the locations where they were collected, namely sediments from the Bhagirathi, Ganga, Alakananda, and Mandakini rivers. After procuring each sediment sample's X-ray spectra, the spectra were analysed using X'Pert High Score software. X'Pert has a high score in some mineral databases (PDF2). Upon comparison with the database of different minerals, the minerals present in the sediment were identified. The XRD spectra show the presence of minerals such as quartz (silicon dioxide), Albite (Sodium Feldspar), and arsenic-associated minerals (Calcium, Magnesium, and Potassium oxides associated with arsenic).

Further, EDS analysis was also performed on the sediment sample which shows presence of sodium, potassium, calcium, magnesium, arsenic and oxygen in different composition. Energy dispersive X-ray analysis (EDX) is performed in conjunction with Scanning electron microscopy (SEM). It provides the elemental details of near surface elements of a sample and the overall positional mapping in it. Here a high energy electron beam ~ 10–20 keV is bombarded on a sample and X-rays emitted from the sample are collected by an energy dispersive spectrometer. The energy of the X-rays generated are characteristics of the atomic structure of the element from which it is emitted, and hence provides the elemental details of

the sample. X-rays are generated in approximately 2 μm depth of the sample and, therefore, EDX is generally a bulk characterization technique.

The XRD spectra of the sediment samples collected from Bhagirathi river show major minerals as quartz albite and anorthite, while arsenic-related compounds such as calcium, aluminium and iron arsenate are present in minimal amounts (Fig. 5.29). The relatively low concentration of calcium, aluminium and iron arsenates in bulk samples hinders detection of these minerals in X-ray diffraction analyses. Figures 5.30, and 5.31 show SEM images and their corresponding EDS analyses. The SEM-EDS analyses revealed the presence of arsenic, oxygen, aluminium, silica, potassium and iron likely due to the presence of calcium, aluminium and iron arsenates.

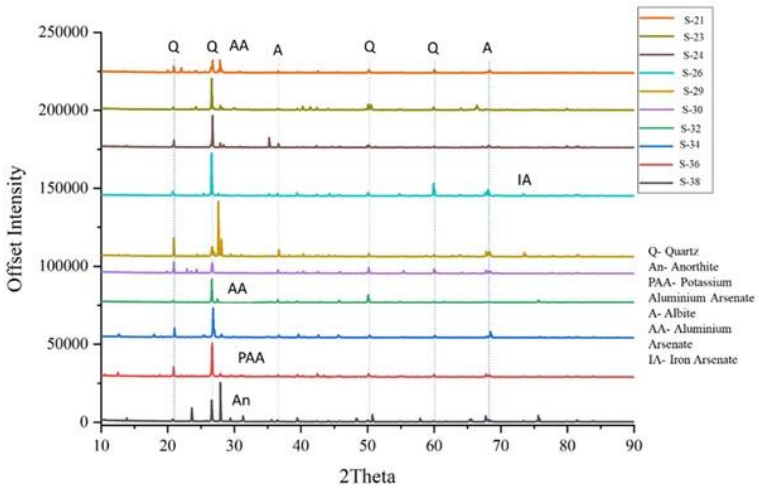

Figure 5.29: X-ray diffraction pattern of sediment samples (S22) collected from the Ganga river (upper stretch).

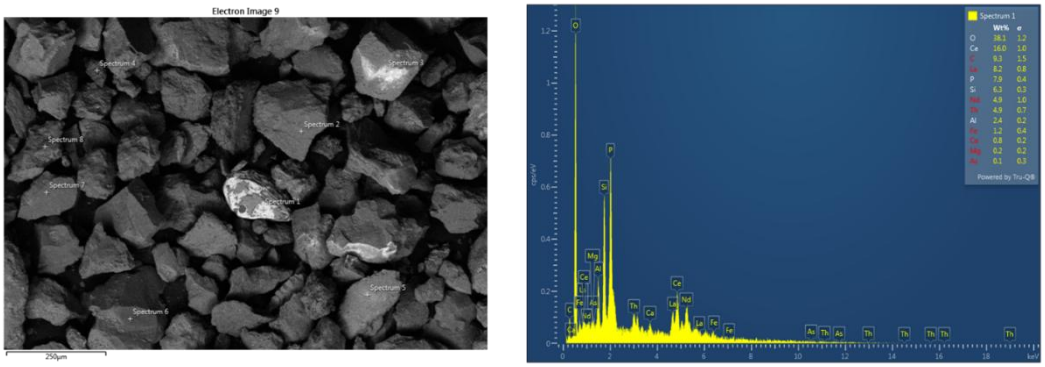

Figure 5.30: SEM image and EDS spectra of sample S22

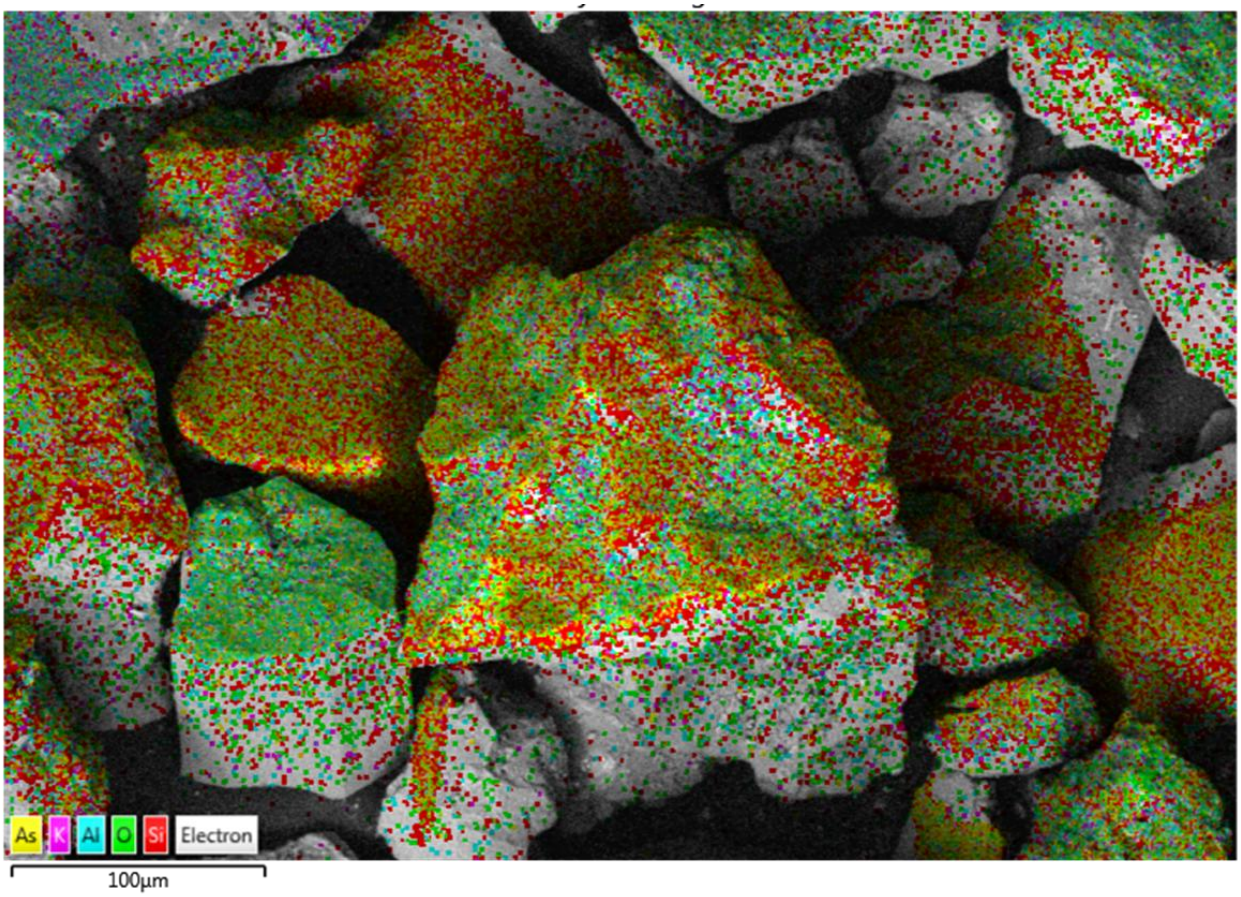

Figure 5.31: SEM image of sample S22 showing presence of different elements spatially

5.1.9 Trace metals variations of river bed sediment

The concentration of trace metals in sediment samples collected from the Mandakini, Alaknanda, Bhagirathi, and Ganga Rivers bed were analyzed using Inductively Coupled Plasma Mass Spectrometry (ICP-MS). Arsenic (As) concentrations ranges from 0.036 to 113 µg/g, Aluminum (Al) varied from 2.3 to 15,417 µg/g, Iron (Fe) ranged from 3.7 to 26,540 µg/g. Manganese (Mn) varied from 0.15 and 1,165 µg/g, cobalt (Co) ranged from 0.002 to 8.5 µg/g, and nickel (Ni) varied from 0.006 to 53.9 µg/g. Lead (Pb) concentrations ranged from 0.042 to 27.7 µg/g, while zinc (Zn) was detected in the range of ND to 49.7 µg/g.

Arsenic was detected in riverbed sediments from the source region of the Bhagirathi/Alaknanda/Mandakini river up to Rudraprayag, after which its concentration along

with other trace metals, showed a declining trend in the downstream (Fig. 5.32). Aluminum, iron, and manganese were consistently present in all sediment samples throughout the study area.

The high concentrations of trace metals in the upstream region may be natural weathering of mineral-rich Himalayan rocks, which are a significant geogenic source. As the rivers flow downstream, the concentration of these metals tends to decrease, likely due to dilution, sediment deposition, and hydrodynamic sorting processes. These processes lead to the settling of heavier or metal-rich particles in the upper reaches and the transport of finer, less metal-laden sediments downstream. Additionally, the reduction in concentration may also reflect reduced geological input or sediment dispersion in the broader river valleys downstream.

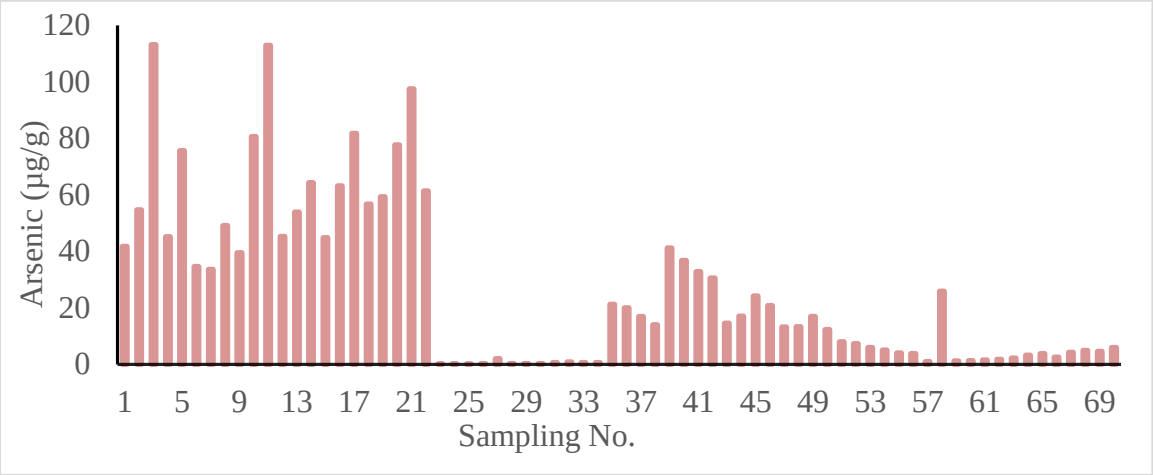

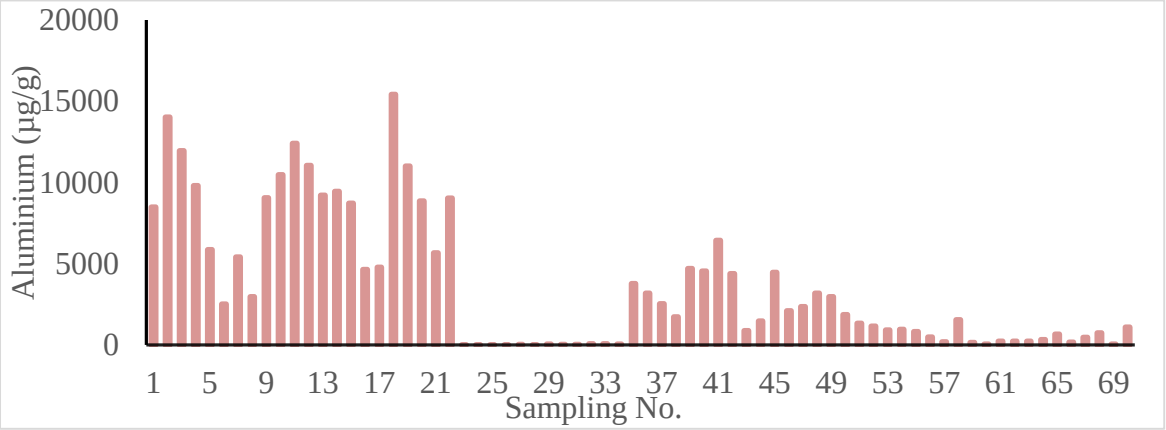

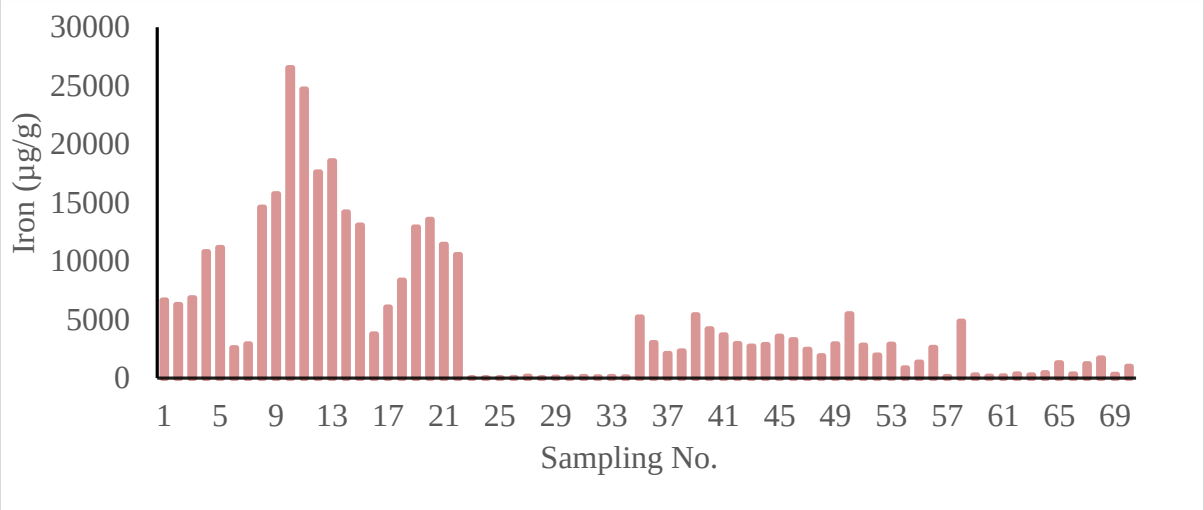
Iron (µg/g)
30000
25000
20000
15000
10000
5000
0
1 5 9 13 17 21 25 29 33 37 41 45 49 53 57 61 65 69
Sampling No.

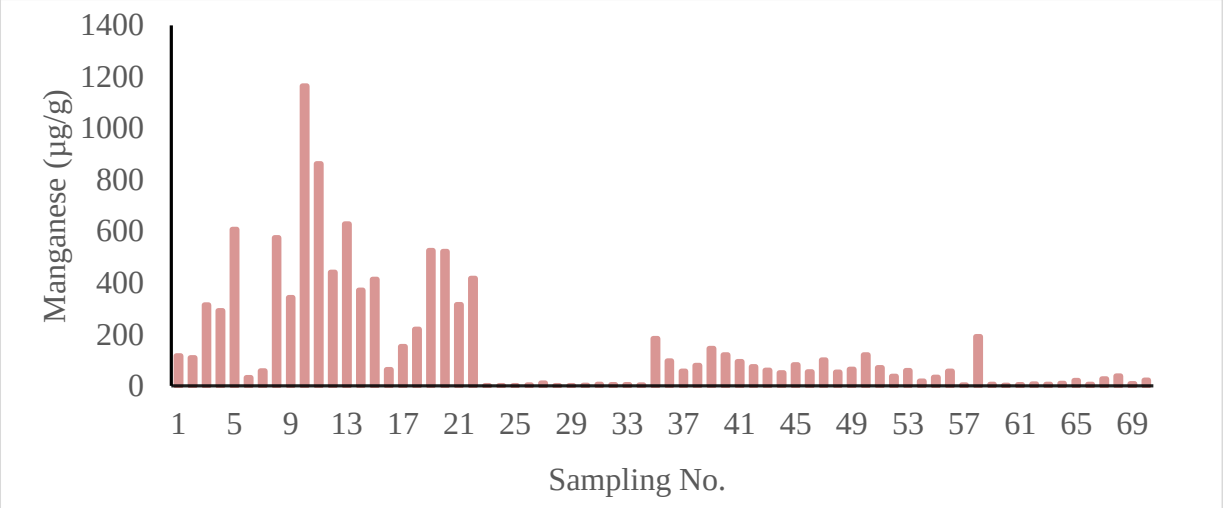
Manganese (µg/g)
1400
1200
1000
800
600
400
200
0
1 5 9 13 17 21 25 29 33 37 41 45 49 53 57 61 65 69
Sampling No.

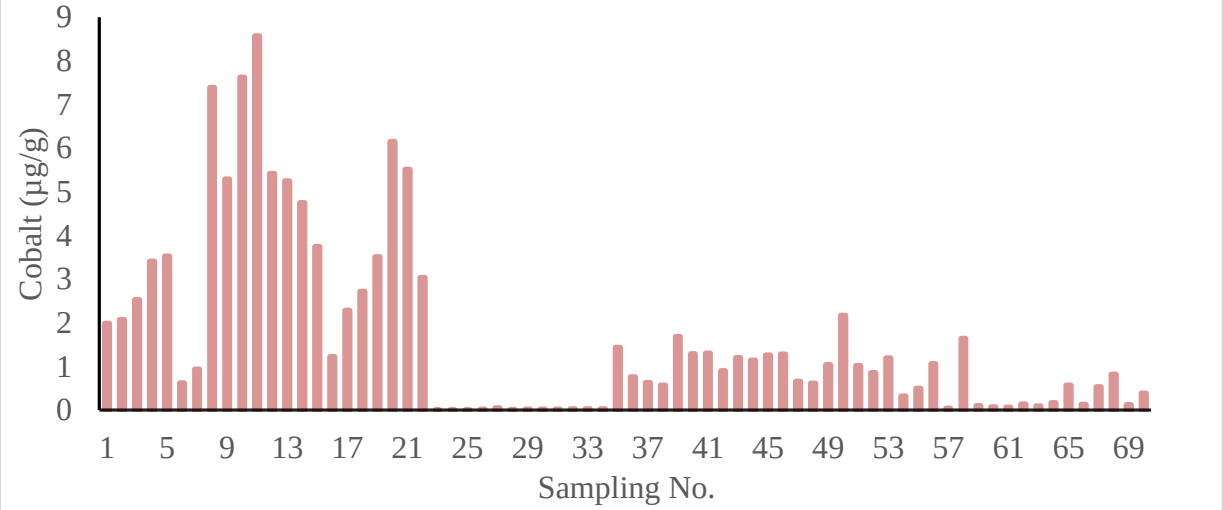
Cobalt (µg/g)
9
8
7
6
5
4
3
2
1
0
1 5 9 13 17 21 25 29 33 37 41 45 49 53 57 61 65 69
Sampling No.

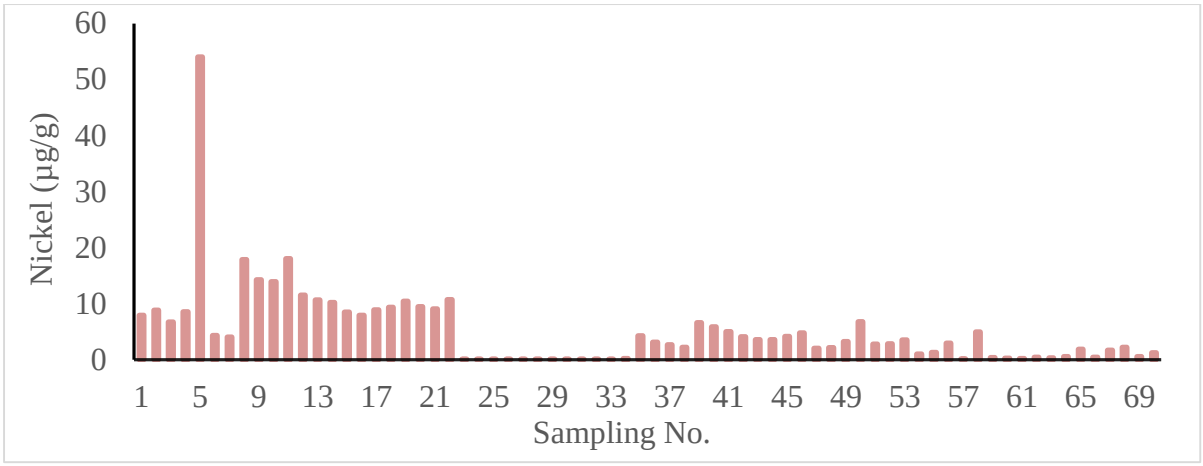

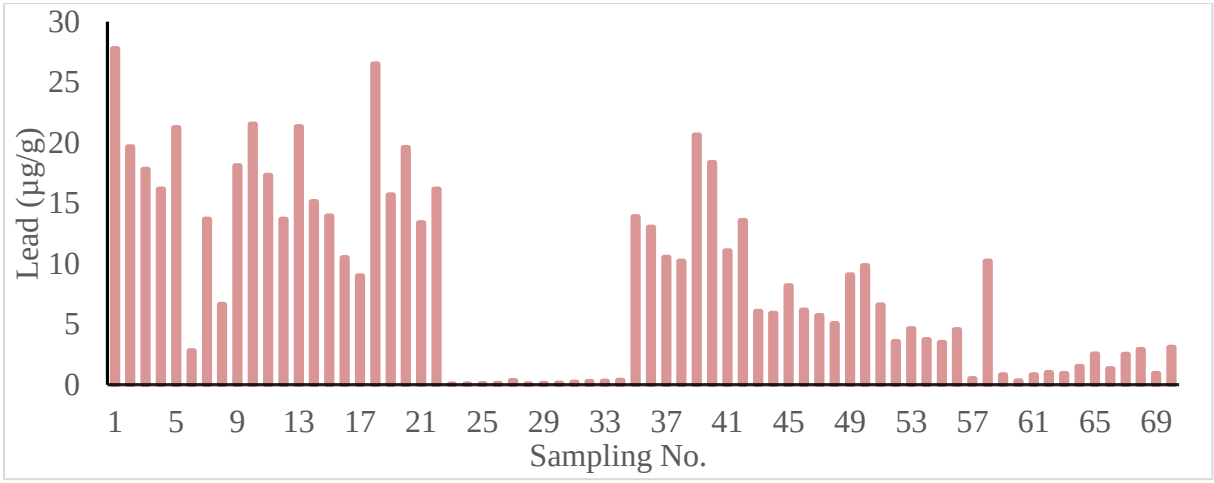

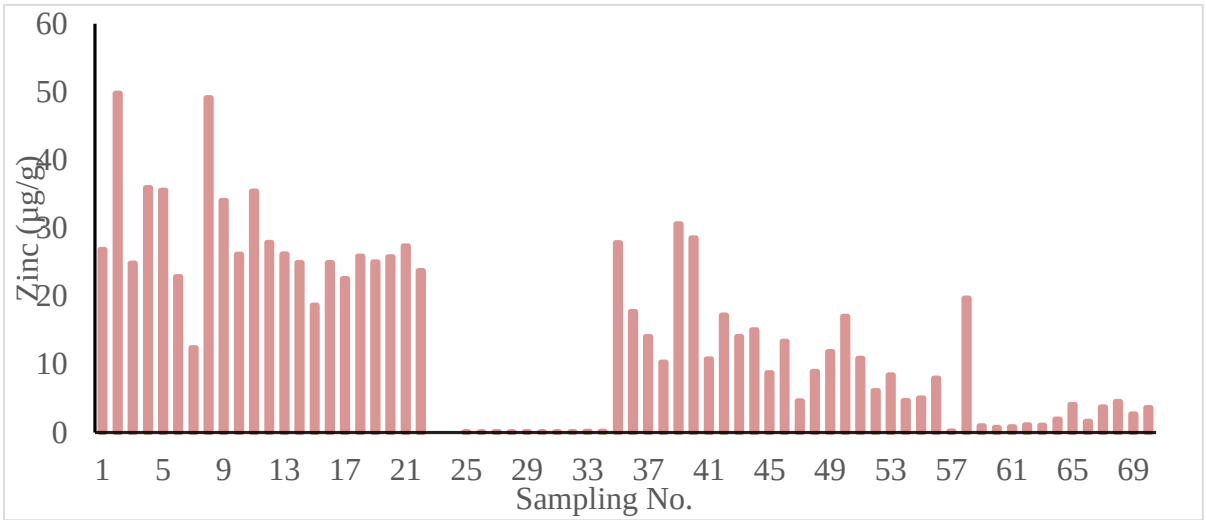

Figure 5.32: Trace metals variation of river bad sediment (As, Al,Fe,Mn,Co, Ni, Pb, and Zn).

5.1.10 Isotopic results

The $\delta^{18}O$ value of the Alaknanda river varies between -14.4‰ to -8.9‰ with an average of -11.8‰, the Mandkini river's $\delta^{18}O$ ranges between -12.3‰ to -9.3‰ with an average of -10.7‰ while the Bhagirathi has $\delta^{18}O$ value of -11.9‰. The Ganga river $\delta^{18}O$ value ranges between –11.6‰ to -3.2‰ with an average of -5.6‰. Figure 5.32 represents the relationship between δD vs $\delta^{18}O$ and d-excess vs $\delta^{18}O$ for rain, the Ganga river and its tributries. Most of the river water samples laying above the LMWL as well as GMWL but few samples fall below the LMWL which indicates about the strong evaporation, this can also be supported by their d-excess values which fall below zero. The groundwater (which is devided into two categories i.e. GW close to river and away from river, Fig 5.38) in the same region revealing distinct regression lines: $\delta^2H = 5.78\ \delta^{18}O - 8.9$ ($R^2 = 0.94$) for samples close to the river, and $\delta^2H = 6.28\ \delta^{18}O - 6.0$ ($R^2 = 0.92$) for those farther away, while river water followed $\delta^2H = 5.68\ \delta^{18}O - 11.6$ ($R^2 = 0.98$). Similarity in slope and intercept between river water and groundwater near the river suggests a strong hydraulic connection, likely through bank infiltration. The d-excess vs $\delta^{18}O$ The plot further supports this interpretation, with near-river groundwater and river samples showing moderate to low d-excess values, indicating limited evaporation, some groundwater samples near river have high d-excess (marked by rectangle in Fig 5.33) which indicate lower evaporation and faster recharge rate. Groundwater farther from the river displays a narrow range and slightly higher d-excess values, reflecting lower evaporation and lower interactions with surface water compared to the groundwater close to river. A few high d-excess values (>10‰) in both groundwater groups likely result from recent recharge by rainfall with distinct isotopic signatures. Conversely, river water and some enriched groundwater samples show low or negative d-excess, indicating evaporation from open surfaces or shallow stagnant sources. Overall, the data highlight regional hydrogeological variability and demonstrate that stable isotope signatures effectively capture the influence of river proximity and evaporation on groundwater recharge across the Ganga basin.

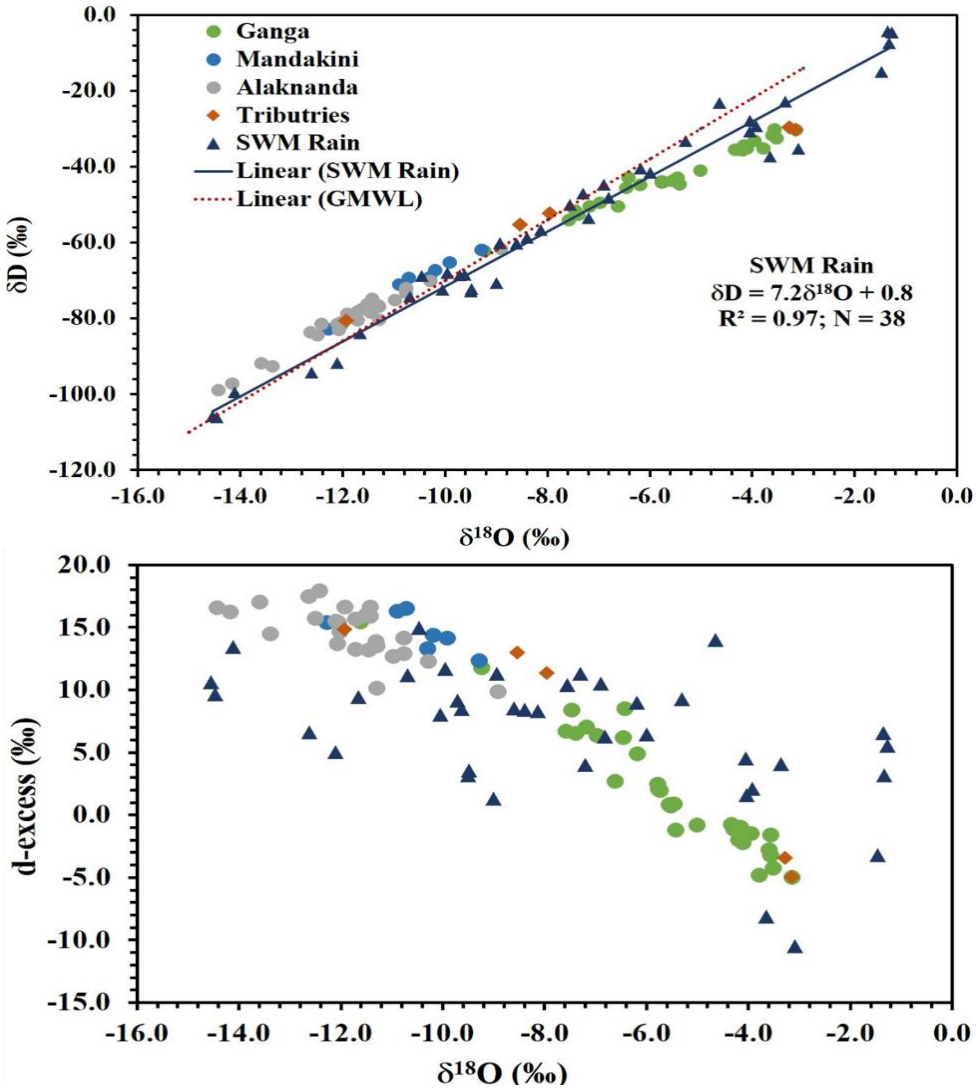

Figure 5.33 Plot showing relationship between δD vs $\delta^{18}O$ and d-excess vs $\delta^{18}O$ for rain

The Figure 5.33 illustrates both the isotopic relationships (δD vs $\delta^{18}O$) and the spatial distribution of $\delta^{18}O$ values in shallow and deep groundwater across the left and right banks of the Ganga River. The Figure 5.35 (a) presents linear regression plots for three distinct water groups: left bank groundwater, right bank groundwater, and river water. Each group exhibits a well-defined linear trend between δD and $\delta^{18}O$ values, indicative of meteoric origins with varying degrees of evaporative enrichment. The slope (4.7) of the river water line is lower than

the Global Meteoric Water Line (GMWL), confirming the influence of evaporation, which is expected in large river systems exposed to open atmosphere over long flow distances.

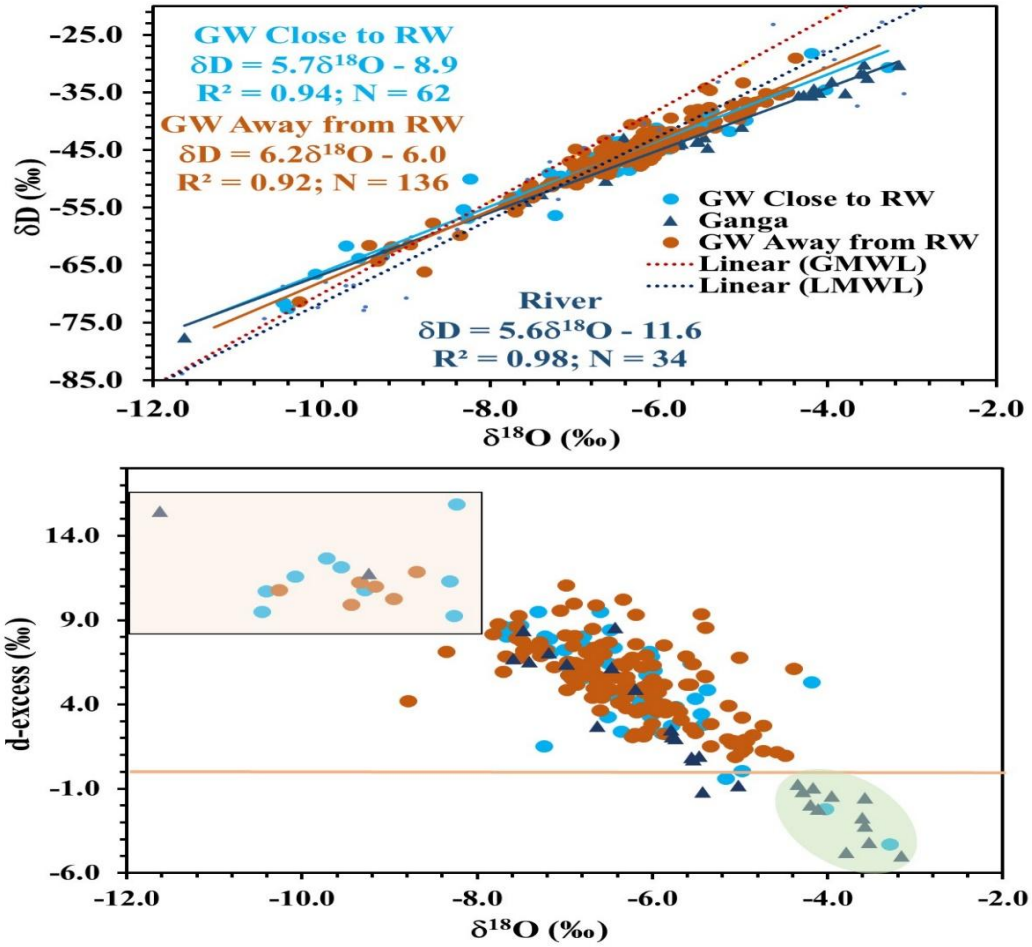

Figure 5.34 GW close to river and away from river

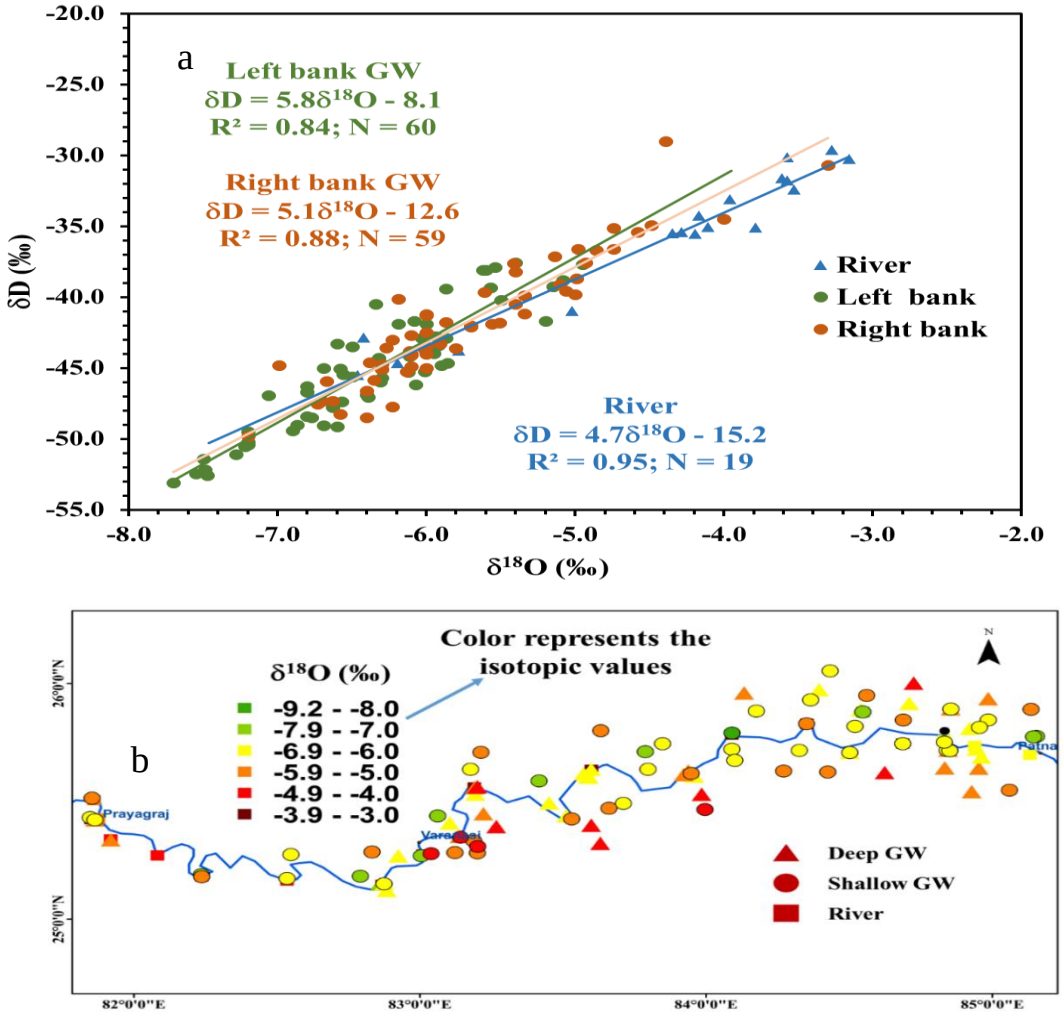

Figure 5.35: (a) Plot showing isotopic relationships δD and $\delta^{18}O$. (b) the spatial distribution of $\delta^{18}O$ values in shallow and deep groundwater

Considering the fact that in this aerial extent (left bank and right bank of groundwater from Prayagraj to Patna) rainwater isotopic composition will not very much, the difference in isotopic composition of left bank and right bank groundwater samples and deep and shallow aquifer samples indicates about difference in recharge rate and process of recharges. The left bank groundwater shows a regression line with a higher slope ($\delta D = 5.85 \times \delta^{18}O - 8.1$). This slope is closer to the GMWL, indicating recharge from recent local precipitation with minimal evaporative loss prior to infiltration compare to right bank groundwater. In contrast, right bank groundwater displays a distinct isotopic signature, with a regression equation of $\delta D = 5.18 \times \delta^{18}O - 12.6$ ($R^2 = 0.88$, N = 59), implying a slightly lower slope and higher $\delta^{18}O$ values. The lower slope and higher $\delta^{18}O$ values in groundwater of right bank side compared to left suggest

that slower recharge rate or connectivity with surface water or irrigation return flow. The spatial variation in $\delta^{18}O$ values shown in the bottom panel further supports these interpretations. The map clearly demonstrates that groundwater on the left bank is more isotopically depleted than that on the right bank. The difference in isotopic slope and intercept between river water and adjacent bank groundwater reveals that the exchange between river and aquifer systems is not uniform along the banks. The stronger similarity in isotopic values between river water and right bank groundwater suggests a greater degree of river water infiltration or hydraulic connectivity on that side of the river. These spatial and isotopic differences between the two banks are likely influenced by the contrasting geological and geomorphological settings of the region. The left bank is predominantly composed of younger alluvial deposits with shallow water tables and high infiltration potential, while the right bank often consists of older alluvium or interbedded sandy-clayey layers, which may facilitate deeper infiltration or preserve older groundwater. The isotopic signals captured in the groundwater therefore integrate both the immediate recharge dynamics and the long-term hydrogeological framework of the basin.

Isotopic Variation in the Ganga River System from Source to Mid-Plains: Insights from $\delta^{18}O$ Trends

The isotopic study presents the spatial variation in $\delta^{18}O$ values along the course of the Ganga River, extending from its glacial origin in the Himalayas to the city of Patna, covering a stretch of nearly 1400 km. The figure displays $\delta^{18}O$ values measured in the main river, its major tributaries, and shallow groundwater located near the river. These isotopic trends help in understanding the hydrological processes at play, including contributions from tributaries, groundwater interaction, and evaporation effects across different geomorphic zones.

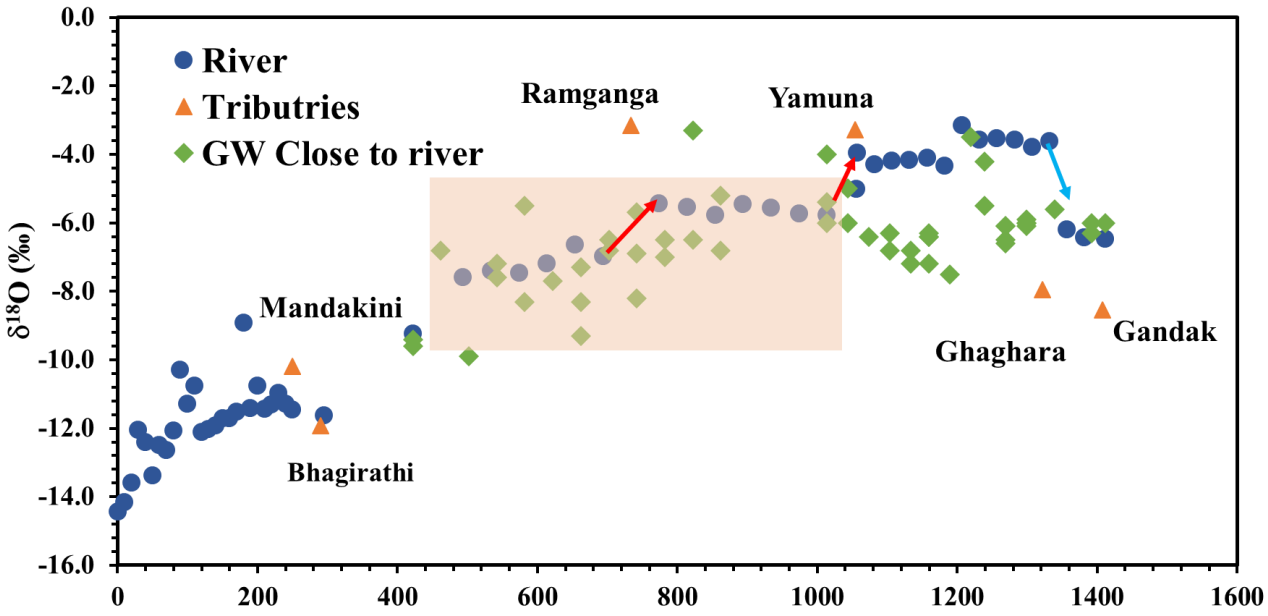

Figure 5.36: spatial variation in $\delta^{18}O$ values along the course of the Ganga River

In the headwater region (0–400 km), which forms part of the Upper Ganga Basin, significant isotopic differences are observed between the two main tributaries—Bhagirathi and Mandakini. The Bhagirathi River, which originates from glacial meltwaters in the Gangotri region, shows highly depleted $\delta^{18}O$ values (around –14‰). In contrast, the Mandakini River exhibits slightly enriched values (approximately –12‰). These variations can be attributed to differences in altitude, snowpack contribution, and the extent of glacial melt influencing each stream. Such isotopic depletion is a characteristic feature of Himalayan glacier-fed rivers and has been highlighted in earlier studies (e.g., Lambs, 2000; Rai et al., 2009; Khan et al., 2022), which report that high-altitude and snow/glacier-fed waters typically have more negative $\delta^{18}O$ signatures due to cooler condensation temperatures and higher elevation precipitation.

As the Ganga descends from the mountains and enters the alluvial plains, there is a marked shift in its isotopic composition. Within the boxed region shown in the figure—representing the Ganga's entry into the Indo-Gangetic Plain—the river water becomes progressively enriched in $\delta^{18}O$, transitioning from approximately –10‰ to about –6‰. This enrichment trend closely aligns with the isotopic signatures of shallow groundwater in this stretch, suggesting

significant groundwater-river interaction. This relationship points to either groundwater contribution with higher $\delta^{18}O$ values (resulting from regional recharge and evaporation) or evaporative enrichment of river water as it flows through warmer, lower-elevation environments. Such interaction is crucial in determining the hydrological balance between surface and subsurface waters in the Ganga basin, particularly in its middle reaches.

A noticeable shift occurs near the confluence with the Ramganga River, around 800 km from the source. Here, the Ganga's $\delta^{18}O$ value increases abruptly from –6.9‰ to –5.4‰. The Ramganga itself is relatively enriched, with a $\delta^{18}O$ value of around –3.2‰, and its input substantially alters the isotopic composition of the Ganga. The impact of this mixing is evident in the figure and highlights how tributary inputs can modify the mainstem river's isotopic character. This enrichment is consistent with the Ramganga's catchment, which includes agricultural and urbanized areas where evaporation and localized recharge may increase the $\delta^{18}O$ values of surface waters. Following this point, and up to the city of Prayagraj, the $\delta^{18}O$ values in the Ganga show a declining trend, decreasing from –5.4‰ to around –5.8‰. This region lacks major tributary inflows with isotopically depleted water, suggesting that the reduction in $\delta^{18}O$ is likely driven by baseflow contributions from shallow groundwater systems. Groundwater in this stretch typically has lower $\delta^{18}O$ values, and its seepage into the river could explain the observed isotopic dilution. This segment of the basin has been further investigated using hydrochemical and trace metal data to better understand the source and composition of the baseflow.

A major isotopic shift is again observed near the confluence with the Yamuna River (–3.3‰), which contributes significantly to this change. Based on mixing calculations, it is estimated that the Yamuna contributes up to 60% of the discharge at this point, making it one of the most influential tributaries in terms of both volume and isotopic impact. Further downstream, the Ganga receives water from tributaries such as the Ghaghara and Gandak Rivers. However, the $\delta^{18}O$ values in this section of the main river remain relatively stable, hovering around –4.5‰ to –5.0‰. The green diamonds in the Figure 5.36 representing groundwater near the river show similar values, reinforcing the ongoing exchange between surface and subsurface water in this lower part of the basin.

Overall, the longitudinal $\delta^{18}O$ profile of the Ganga River reveals important insights into its hydrological dynamics. In the upper reaches, the isotopic signature is primarily controlled by altitude and glacial sources. As the river flows through the plains, groundwater interaction and tributary mixing become the dominant factors influencing its isotopic composition. This analysis helps in understanding the surface water and groundwater interaction. The arsenic concentration varies between left and right bank of river as isotopic values are also different for these banks, thus it shows that interaction of SW-GW also playing a major role in the occurrence and mobilization of arsenic.

5.1.11 Performance evaluation of existing treatment units and supply wells

One of the objectives of the study was to evaluate the performance of existing treatment units and suggest the alternate water supply. The field survey was carried out in the arsenic-affected areas, but very few ex-situ treatment systems were installed and functioning. The reason was drinking water supply is being done to each household through a piped water supply under under Har Ghar Jal Nal Yojna. Water samples were collected from three existing treatment units to evaluate the performance of treatment systems that are installed in the arsenic affected areas. The filtration systems are functioning effectively for the removal of the ions, with a significant reduction of electrical conductivity (EC). Trace metals show a slight reduction across the treatment process, except for iron (Fe), which has increased
possibly due to the exhaustion of iron-based adsorbent media. Arsenic removal efficiency in the filters ranges from 35% to 66%. The drinking water supply wells were also tested for evaluating drinking water suitability. All major ions and trace metals are within the acceptable limits of drinking water standards. Although there is no significant removal of major ions in the Water Treatment Plant (WTP) but all measured parameters within permissible limits. The inlet and outlet samples from Water Treatment Plant (WTP) installed at Bhojpur on river Ganga were also collected and tested for various parameters. It is observed that the treated water of WTP are safe for drinking water, all major ions and trace metals remain within the acceptable range for drinking water.

Table 5.4:-Performance evaluation of existing treatment units and supply wells basis on In-situ and Ions concentrations

		pH	EC (µs/cm)	Na (mg/L)	K (mg/L)	Ca (mg/L)	Mg (mg/L)	Cl (mg/L)	SO4 (mg/L)	NO3 (mg/L)	F (mg/L)	Alk (mg/L)
Filter 1	**Inlet**	7.08	460	15.23	3.31	68.65	16.54	4.35	4.97	2.12	0.16	300
	Outlet	7.34	140	10.06	2.64	21.21	4.92	6.01	1.53	0.96	0.05	109
Filter 2	**Inlet**	7.26	467	25.89	2.54	56.42	24.92	2.05	10.99	0.08	0.39	231
	Outlet	7.35	85	8.07	0.85	12.42	5.92	0.69	2.02	0.05	0.09	87
Filter 3	**Inlet**	6.50	517	18.17	5.54	62.55	20.73	9.76	12.10	0.16	0.19	258
	Outlet	6.64	127	15.06	3.11	61.29	17.10	4.11	5.52	0.03	0.17	65
WTP	**Inlet**	8.30	514	41.76	7.16	41.46	18.73	43.12	31.87	1.05	0.21	167
	Outlet	8.20	495	28.86	2.72	33.38	14.89	7.92	10.81	0.14	0.12	161
Water Supply TW		**7.48**	**476**	**22.50**	**1.45**	**71.11**	**19.05**	**4.63**	**2.89**	**0.28**	**0.22**	**215**
Water Supply TW		**7.44**	**568**	**19.24**	**0.41**	**45.83**	**18.78**	**8.13**	**13.48**	**ND**	**0.72**	**277**
Water Supply TW		**7.51**	**577**	**40.39**	**5.88**	**29.79**	**18.36**	**40.12**	**30.84**	**1.17**	**0.26**	**243**

Table 5.5: -Performance evaluation of existing treatment units and supply wells basis on Trace metals concentrations

		Al (ppb)	Cr (ppb)	Mn (ppb)	Fe (ppb)	Ni (ppb)	Cu (ppb)	Zn (ppb)	As (ppb)	Cd (ppb)	Pb (ppb)
Filter 1	**Inlet**	9.68	0.54	54.20	362	0.22	0.60	108.06	20.06	0.19	0.60
	Outlet	9.16	0.53	26.36	946	0.22	0.97	30.26	10.67	0.05	0.89
Filter 2	**Inlet**	7.45	0.48	106.05	1083	0.34	19.26	223.48	12.58	0.03	0.52
	Outlet	13.03	0.38	41.04	1552	0.33	2.53	111.08	4.17	0.03	0.68
Filter 3	**Inlet**	714	3.08	278.67	2410	54.20	8.61	111.79	14.07	ND	15.74
	Outlet	275	ND	118.87	940	23.93	4.37	57.48	9.47	ND	ND
WTP	**Inlet**	900	2.12	51.46	1300	7.18	2.37	93.06	12.36	ND	ND
	Outlet	784	ND	52.25	1100	9.42	2.08	25.43	6.94	ND	ND
Water Supply TW		**715.29**	**ND**	**43.62**	**1060**	**3.64**	**2.93**	**51.70**	**8.92**	**ND**	**ND**
Water Supply TW		**124.57**	**ND**	**15.80**	**210**	**ND**	**ND**	**25.21**	**ND**	**ND**	**ND**
Water Supply TW		**626.96**	**ND**	**72.81**	**770**	**13.09**	**5.40**	**70.51**	**8.31**	**ND**	**ND**

6.0 Conclusions

The hydrochemical and geochemical investigation of the Ganga river basin, with a focus on the mineralogical characteristics of sediments and water in the Indian Himalayan region, highlights the genesis, mobility, and spatial behavior of arsenic and associated trace metals. The study reveals that arsenic contamination is closely linked with iron-rich mineral phases, with high As concentrations predominantly confined to shallow aquifers (up to 60 meters) in the Mirzapur to Patna stretch. These zones are strongly influenced by anthropogenic inputs, including sewage, agricultural runoff, and industrial discharge, particularly evident from high concentration of chloride, sulphate, and nitrate in both river and groundwater. Trace metals such as Fe, Al, and Mn are widely distributed due to geogenic sources, with local anthropogenic influence near urban centers. Upstream river bed sediments are enriched with As and other trace metals, likely due to weathering of mineral-rich Himalayan rocks. Downstream dilution, hydrodynamic sorting, and sediment deposition contribute to declining metal concentrations.

The chemical behavior of arsenic in sediments is influenced by its strong affinity for supersaturated iron oxides, favoring immobilization through precipitation. In headwater tributaries like Bhagirathi, Alaknanda, and Mandakini, acidic pH conditions arise from sulphide oxidation, while downstream, pH increases due to carbonate dissolution. Additionally, increasing trends of pH and electrical conductivity in the mid-region (Kanpur to Varanasi) reflect growing anthropogenic impacts, whereas dissolved oxygen levels generally indicate good river health. River bed sediment analysis using ICP-MS shows variation of trace metal concentrations, with arsenic ranging from 0.036 to 113 μg/g, Fe up to 26,540 μg/g, and other metals like Mn, Co, Ni, Pb, and Zn also present. The mineral saturation index, calculated using Visual MINTEQ, reveals that iron oxides such as Hematite, Goethite, and Ferrihydrite are supersaturated, indicating precipitation potential, while minerals like $FeAsO_4 \cdot 2H_2O$ and Rhodochrosite remain undersaturated, suggesting potential dissolution.

Groundwater composition is shaped by factors including rainwater chemistry, rock mineralogy, residence time, and human activities. High Na^+/Cl^- and K^+/Cl^- ratios point toward significant silicate weathering and cation exchange, while the dominance of Ca^{2+} and Mg^{2+}, with $(Ca^{2+} + Mg^{2+})/(Na^+ + K^+)$ ratio of 3.3, confirms carbonate weathering as the main geogenic process. The high $HCO_3^-/(SO_4^{2-} + Cl^-)$ ratio (6.9) and Gibbs plots further reinforce the influence of rock-water interaction over evaporative or anthropogenic processes. Hydrogeochemical plots of $(Ca^{2+} + Mg^{2+})$ vs. $(HCO_3^- + SO_4^{2-})$ and Ca^{2+} vs. HCO_3^-/SO_4^{2-} indicate that carbonate dissolution is prominent. Rock-water interaction, particularly carbonate weathering, controls

the groundwater chemistry, with limited contribution from silicate weathering. The isotopic analysis reveals that groundwater near the river exhibits strong river aquifer interaction, and groundwater on the right bank is more enriched due to higher evaporation. The arsenic treatment units in arsenic affected area were found to be very few and most of them are non-functional. The majority of public water supply is sourced from deeper aquifers, which remain free from arsenic and trace metal contamination, and are currently suitable for drinking use.

References

Agrafioti, E., Kalderis, D., & Diamadopoulos, E. (2014). Arsenic and chromium removal from water using biochars derived from rice husk, organic solid wastes and sewage sludge. *Journal of Environmental Management*, *133*, 309–314. https://doi.org/10.1016/j.jenvman.2013.12.007

Chakraborti, D., Singh, S. K., Mahmudur Rahman, M., Nath Dutta, R., Chandra Mukherjee, S., Pati, S., & Bijoy Kar, P. (2018). Groundwater Arsenic Contamination in the Ganga River Basin: A Future Health Danger. *International Journal of Environmental Research and Public Health*, *15*(180). https://doi.org/10.3390/ijerph15020180

Chakraborty, M., Mukherjee, A., & Ahmed, K. (2015). A Review of Groundwater Arsenic in the Bengal Basin, Bangladesh and India: from Source to Sink. *Current Pollution Reports*, *1*, 220–247. https://doi.org/10.1007/s40726-015-0022-0

Cope, C. O., Webster, D. S., & Sabatini, D. A. (2014). Arsenate adsorption onto iron oxide amended rice husk char. *Science of The Total Environment*, *488-489*(1), 554–561. https://doi.org/10.1016/J.SCITOTENV.2013.12.120

Dominguez-Ramos, A., Chavan, K., García, V., Jimeno, G., Albo, J., Marathe, K. V., Yadav, G. D., & Irabien, A. (2014). Arsenic removal from natural waters by adsorption or ion exchange: An Environmental Sustainability Assessment. *Industrial and Engineering Chemistry Research*, *53*(49), 18920–18927. https://doi.org/10.1021/ie4044345

Duxbury, J. M., & Panaullah, G. M. (2007). *Remediation of arsenic for agriculture sustainability, food security and health in Bangladesh*.

Edmunds, W. M., Ahmed, K. M., & Whitehead, P. G. (2015). A review of arsenic and its impacts in groundwater of the Ganges-Brahmaputra-Meghna delta, Bangladesh. *Environmental Sciences: Processes and Impacts*, *17*(6), 1032–1046. https://doi.org/10.1039/c4em00673a

Fendorf, S., Michael, H. A., & Van Geen, A. (2010). Spatial and temporal variations of groundwater arsenic in South and Southeast Asia. *Science*, *328*(5982), 1123–1127. https://doi.org/10.1126/science.1172974

Grafe, M., Eick, M. J., & Grossl, P. R. (2001). Adsorption of arsenate (V) and arsenite (III) on goethite in the presence and absence of dissolved organic carbon. *Soil Science Society of America Journal*, *65*(V), 1680–1687. https://doi.org/10.2136/sssaj2001.1680

Hughes, M. F. (2002). Arsenic toxicity and potential mechanisms of action. *Toxicology Letters*, *133*(1), 1–16. http://www.ncbi.nlm.nih.gov/pubmed/12076506

Kanel, S. R., & Choi, H. (2017). Removal of arsenic from groundwater by industrial byproducts and its comparison with zero-valent iron. *Journal of Hazardous, Toxic, and Radioactive Waste*, *21*(3), 1–7. https://doi.org/10.1061/(ASCE)HZ.2153-5515.0000349

Liu, T., Wang, Z. L., Yan, X., & Zhang, B. (2014). Removal of mercury (II) and chromium (VI) from wastewater using a new and effective composite: Pumice-supported nanoscale zero-valent iron. *Chemical Engineering Journal*, *245*, 34–40. https://doi.org/10.1016/j.cej.2014.02.011

Luo, S., Shen, M. N., Wang, F., Zeng, Q. R., Shao, J. H., & Gu, J. D. (2016). Synthesis of Fe3O4-loaded porous carbons developed from rice husk for removal of arsenate from

aqueous solution. *International Journal of Environmental Science and Technology*, *13*(4), 1137–1148. https://doi.org/10.1007/s13762-016-0955-x

Mondal, D., Rahman, M. M., Suman, S., Sharma, P., Siddique, A. B., Rahman, M. A., Bari, A. S. M. F., Kumar, R., Bose, N., Singh, S. K., Ghosh, A., & Polya, D. A. (2021). Arsenic exposure from food exceeds that from drinking water in endemic area of Bihar, India. *Science of the Total Environment*, *754*, 142082. https://doi.org/10.1016/j.scitotenv.2020.142082

Mukherjee, A., Gupta, S., Coomar, P., Fryar, A. E., Guillot, S., Verma, S., Bhattacharya, P., Bundschuh, J., & Charlet, L. (2019). Plate tectonics influence on geogenic arsenic cycling: From primary sources to global groundwater enrichment. *Science of The Total Environment*, *683*, 793–807. https://doi.org/https://doi.org/10.1016/j.scitotenv.2019.04.255

Nickson, R. T., McArthur, J. M., Ravenscroft, P., Burgess, W. B., & Ahmed, K. Z. (2000). Mechanism of arsenic poisoning of groundwater in Bangladesh and West Bengal. *Applied Geochemistry*, *15*, 403–413.

Pallier, V., Feuillade-Cathalifaud, G., Serpaud, B., & Bollinger, J.-C. (2010). Effect of organic matter on arsenic removal during coagulation/flocculation treatment. *Journal of Colloid and Interface Science*, *342*(1), 26–32. https://doi.org/https://doi.org/10.1016/j.jcis.2009.09.068

Ramos, M. A. V, Yan, W., Li, X., Koel, B. E., & Zhang, W. (2009). Simultaneous Oxidation and Reduction of Arsenic by Zero-Valent Iron Nanoparticles: Understanding the Signi cance of the Core-Shell Structure. *The Journal of Physical Chemistry C*, *113*, 14591–14594. https://doi.org/10.1021/jp9051837

Ranjan, S., Yadav, B. K., & Joshi, H. (2020). Development of nZVI-Pumice / Zeolite Composites for Effective Removal of Arsenic (III) from Aqueous Solution. *Journal of Hazardous, Toxic, and Radioactive Waste*, *24*(3), 1–10. https://doi.org/10.1061/(ASCE)HZ.2153-5515.0000507

Ranjan, S., Yadav, B. kumar, & Joshi, H. (2021). Removal of arsenic (III and V) from aqueous solution using stable maghemite (γ -Fe2O3) loaded pumice composite. *International Journal of Environmental Science and Technology*, 1–12. https://doi.org/10.1007/s13762-021-03326-x

Ratnaike, R. N. (2003). Acute and chronic arsenic toxicity. *Postgraduate Medical Journal*, *79*(933), 391–396. https://doi.org/10.1136/pmj.79.933.391

Ravenscroft, P., Brammer, H., & Richards, K. (2009). Introduction. In K. Ward & J. Bullard (Eds.), *Arsenic pollution: A global synthesis* (1st ed., pp. 1–22). Willey-Blackwell.

Samsuri, A. W., Sadegh-Zadeh, F., & Seh-Bardan, B. J. (2013). Adsorption of As(III) and As(V) by Fe coated biochars and biochars produced from empty fruit bunch and rice husk. *Journal of Environmental Chemical Engineering*, *1*(4), 981–988. https://doi.org/10.1016/J.JECE.2013.08.009

Sari, N. A., Ishak, C. F., & Bakar, R. A. (2014). Characterization of oil palm empty fruit bunch and rice husk biochars and their potential to adsorb arsenic and cadmium. *American Journal of Agricultural and Biological Science*, *9*(3), 450–456. https://doi.org/10.3844/ajabssp.2014.450.456

Shrivastava, A., Ghosh, D., Dash, A., & Bose, S. (2015). Arsenic Contamination in Soil and Sediment in India: Sources, Effects, and Remediation. *Current Pollution Reports*, *1*(1), 35–46. https://doi.org/10.1007/s40726-015-0004-2

Sidhu, S. S., Brar, J. S., Biswas, A., Banger, K., & Saroa, G. S. (2012). Arsenic contamination in soil-water-plant (rice, Oryza sativa L.) continuum in central and sub-mountainous Punjab, India. *Bulletin of Environmental Contamination and Toxicology*, *89*(5), 1046–1050. https://doi.org/10.1007/s00128-012-0799-0

Singh, R., Singh, S., Parihar, P., Singh, V. P., & Prasad, S. M. (2015). Arsenic contamination, consequences and remediation techniques: A review. *Ecotoxicology and Environmental Safety*, *112*, 247–270. https://doi.org/10.1016/j.ecoenv.2014.10.009

Smedley, P. L., & Kinniburgh, D. G. (2000). Source and behaviour of arsenic in natural waters Importance of arsenic in drinking water. *British Geological Survey*, 61.

Suman, S., Sharma, P. K., Siddique, A. B., Rahman, M. A., Kumar, R., Rahman, M. M., Bose, N., Singh, S. K., Ghosh, A. K., Matthews, H., & Mondal, D. (2020). Wheat is an emerging exposure route for arsenic in Bihar, India. *Science of the Total Environment*, *703*, 134774. https://doi.org/10.1016/j.scitotenv.2019.134774

Walker, M., Seiler, R. L., & Meinert, M. (2008). Effectiveness of household reverse-osmosis systems in a Western U.S. region with high arsenic in groundwater. *Science of The Total Environment*, *389*(2), 245–252. https://doi.org/https://doi.org/10.1016/j.scitotenv.2007.08.061

Wang, S., & Mulligan, C. N. (2006). Effect of natural organic matter on arsenic release from soils and sediments into groundwater. *Environmental Geochemistry and Health*, *28*(3), 197–214. https://doi.org/10.1007/s10653-005-9032-y

Wu, C., Huang, L., Xue, S. G., Huang, Y. Y., Hartley, W., Cui, M. qian, & Wong, M. H. (2017). Arsenic sorption by red mud-modified biochar produced from rice straw. *Environmental Science and Pollution Research*, *24*(22), 18168–18178. https://doi.org/10.1007/s11356-017-9466-7

Wu, Z., Su, X., Lin, Z., Owens, G., & Chen, Z. (2019). Mechanism of As(V) removal by green synthesized iron nanoparticles. *Journal of Hazardous Materials*, *379*(June), 120811. https://doi.org/10.1016/j.jhazmat.2019.120811

Yoon, J., Amy, G., Chung, J., Sohn, J., & Yoon, Y. (2009). Removal of toxic ions (chromate, arsenate, and perchlorate) using reverse osmosis, nanofiltration, and ultrafiltration membranes. *Chemosphere*, *77*(2), 228–235. https://doi.org/https://doi.org/10.1016/j.chemosphere.2009.07.028

Zhou, Y., Zeng, Y., Zhou, J., Guo, H., Li, Q., Jia, R., Chen, Y., & Zhao, J. (2017). Distribution of groundwater arsenic in Xinjiang, P.R. China. *Applied Geochemistry*, *77*, 116–125. https://doi.org/10.1016/J.APGEOCHEM.2016.09.005

Zouboulis, A., & Katsoyiannis, I. (2002). REMOVAL OF ARSENATES FROM CONTAMINATED WATER BY COAGULATION–DIRECT FILTRATION. *Separation Science and Technology*, *37*(12), 2859–2873. https://doi.org/10.1081/SS-120005470

Werzer, O., Kowarik, S., Gasser, F., Jiang, Z., Strzalka, J., Nicklin, C., & Resel, R. (2024). X-ray diffraction under grazing incidence conditions. Nature Reviews Methods Primers, 4(1), 15.

Lee, B. D., Lee, J. W., Ahn, J., Kim, S., Park, W. B., & Sohn, K. S. (2023). A Deep Learning Approach to Powder X-Ray Diffraction Pattern Analysis: Addressing Generalizability and Perturbation Issues Simultaneously. Advanced Intelligent Systems, 5(9), 2300140.

Scandellari, F., Attou, T., Barbeta, A., Bernhard, F., D'Amato, C., Dimitrova-Petrova, K., ... & Sprenger, M. (2024). Using stable isotopes to inform water resource management in forested and agricultural ecosystems. Journal of environmental management, 365, 121381.

Majzlan, J., Plášil, J., Dachs, E., Benisek, A., Mangold, S., Škoda, R., & Abrosimova, N. (2021). Prediction and observation of formation of Ca–Mg arsenates in acidic and alkaline fluids: Thermodynamic properties and mineral assemblages at Jáchymov, Czech Republic and Rotgülden, Austria. Chemical Geology, 559, 119922.

Jafari, T., Kiem, A. S., Javadi, S., Nakamura, T., & Nishida, K. (2021). Using insights from water isotopes to improve simulation of surface water-groundwater interactions. Science of The Total Environment, 798, 149253.

Wang, H. Y., Byrne, J. M., Perez, J. P. H., Thomas, A. N., Göttlicher, J., Höfer, H. E., ... & Norra, S. (2020). Arsenic sequestration in pyrite and greigite in the buried peat of As-contaminated aquifers. Geochimica et Cosmochimica Acta, 284, 107-119.

Kumar, A., Ali, M., Kumar, R., Kumar, M., Sagar, P., Pandey, R. K., ... & Ghosh, A. K. (2021). Arsenic exposure in Indo Gangetic plains of Bihar causing increased cancer risk. Scientific reports, 11(1), 2376.

Shaji, E., Santosh, M., Sarath, K. V., Prakash, P., Deepchand, V., & Divya, B. V. (2021). Arsenic contamination of groundwater: A global synopsis with focus on the Indian Peninsula. Geoscience frontiers, 12(3), 101079.

Garcia-Sanchez, A., & Alvarez-Ayuso, E. (2003). Arsenic in soils and waters and its relation to geology and mining activities (Salamanca Province, Spain). Journal of Geochemical Exploration, 80(1), 69-79.

Taylor, S. R., & McLennan, S. M. (1985). The continental crust: its composition and evolution.

Parviainen, A., Loukola-Ruskeeniemi, K., Tarvainen, T., Hatakka, T., Härmä, P., Backman, B., ... & Luoma, S. (2015). Arsenic in bedrock, soil and groundwater—The first arsenic guidelines for aggregate production established in Finland. Earth-Science Reviews, 150, 709-723.

Neumann, R. B., Ashfaque, K. N., Badruzzaman, A. B. M., Ashraf Ali, M., Shoemaker, J. K., & Harvey, C. F. (2010). Anthropogenic influences on groundwater arsenic concentrations in Bangladesh. Nature geoscience, 3(1), 46-52.

Khan, I., Khan, M. U., Umar, R., & Rai, N. (2023). Occurrence, speciation, and controls on arsenic mobilization in the alluvial aquifer system of the Ghaghara basin, India. Environmental Geochemistry and Health, 45(11), 7933-7956.

Nickson, R. T., McArthur, J. M., Ravenscroft, P., Burgess, W. G., & Ahmed, K. M. (1998). Arsenic poisoning of Bangladesh groundwater. Nature, 395, 338.

Sharma, N., Liang, M. C., Laskar, A. H., Huang, K. F., Maurya, N. S., Singh, V., ... & Maurya, A. S. (2023). Basin-scale geochemical assessment of water quality in the Ganges River during the dry season. Water, 15(11), 2026.

Sharma, N., Liang, M.-C., Laskar, A. H., Huang, K.-F., Maurya, N. S., Singh, V., Ranjan, R., & Maurya, A. S. (2023). Basin-Scale Geochemical Assessment of Water Quality in the Ganges River during the Dry Season. Water, 15(11), 2026.

Gautam, A., Rai, S. C., Rai, S. P., & Ram, K. (2022). Impact of anthropogenic and geological factors on groundwater hydrochemistry in the unconfined aquifers of Indo-Gangetic plain. Physics and Chemistry of the Earth, Parts A/B/C, 126, 103109.

Field Photographs